UNIVERSITY OF CALIFORNIA SAN DIEGO

Biogenic Carbonate Dissolution in Shallow Marine Environments

A dissertation submitted in partial satisfaction of the requirements for the degree Doctor of Philosophy

in

Oceanography

by

Alyssa Jean Griffin

Committee in charge:

Professor Andreas J. Andersson, Chair
Professor Andrew Dickson
Professor Olivia Graeve
Professor Vicki Grassian
Professor Todd Martz

2020

The Dissertation of Alyssa Jean Griffin is approved, and it is acceptable in quality and form for publication on microfilm and electronically:

_____

_____

_____

_____

_____

Chair

University of California San Diego

2020

DEDICATION

TO MY DAUGHTER –

May your curiosity be deeper than the oceans,

Your aspirations higher than the mountains,

And your heart as unbounded as the cosmos.

EPIGRAPH

"For small creatures such as we the vastness is bearable only through love."

-Carl Sagan, *Contact*

TABLE OF CONTENTS

LIST OF TABLES

Chapter 1

Chapter 2

Chapter 3

LIST OF FIGURES

Chapter 1

Chapter 2

Chapter 3

Chapter 4

ACKNOWLEDGMENTS

This work was only possible through the guidance and support of so many mentors, colleagues, friends and family, to whom I am eternally grateful.

First, thank you to my advisor Dr. Andreas Andersson, for providing me with the opportunity to pursue a doctoral degree, supporting my research interests and allowing me the freedom to take my scientific inquiries in unexpected directions. Since day one, Andreas has challenged me to always do my best work and to become a better scientist with every endeavor. I have greatly appreciated his advice on navigating a career in academia as well as how to celebrate the wins and take the losses in stride. I have grown a great deal personally and professionally thanks to my time in his group (the Scripps Coastal and Open Ocean BiogeochemistrY, a.k.a. SCOOBY, Lab).

I would also like to thank and acknowledge my committee members for their time and feedback, which was integral to this work. First, I would like to recognize Dr. Joanna McKittrick, who is no longer with us and thank her for broadening my perspective of biological materials. Although I am deeply saddened that she is not here to see this work come to fruition, I am grateful for her contributions. I would also like to thank Dr. Olivia Graeve for agreeing to serve on my committee at the twilight of my dissertation work and for her contributions. Thank you to Dr. Andrew Dickson for always being available to meet with me to discuss anything and everything related to oceanic carbonate system measurements. Seeing that these types of measurements are the backbone of this work, his feedback was immensely beneficial to their quality and many of the resulting interpretations. I am deeply grateful to Dr. Vicki Grassian for graciously giving me so much of her time and access to the analytical capabilities of her laboratory as well as her willingness to submit a grant with

Andreas to support much of my work in Chapter 3. The measurements contained in Chapter 4 of this dissertation simply would not have been possible without the guidance and support of Dr. Todd Martz. I have thoroughly enjoyed being an honorary member of the Martz Lab over the years and cannot thank him enough for his extraordinary patience with me as I plunged into the unfamiliar and often times, maddening world of instrument development.

The SCOOBY Lab has been such a great home for the duration of my PhD. Everyone that has been a part of our lab has always been willing to help support one another in both our common and independent research goals. There are far too many past and present members to thank individually, but I would like to thank Morgan Goodrich for her immense help with tending to several dissolution experiments and improving many of my experimental protocols. I'd also like to thank Dr. Sydney D'Angelo for her extensive help when I first arrived at Scripps to troubleshoot my experimental system, training me on laboratory instruments and for being a friend as I adjusted to a new chapter in my life. I would especially like to thank Dr. Tyler Cyronak for his selfless support, feedback and willingness to always "talk shop" since our first weeks at Scripps together. I am truly grateful to have him as a colleague and friend.

I would also like to thank the many members of several other labs for their scientific support and friendship. The Martz and Dickson Labs, in particular, have served as second "homes" and I've enjoyed the many hours spent both inside and outside of work in the company of their members. Members of the Grassian group and Environmental and Complex Analysis Laboratory have also provided significant amounts of their time and assistance with several analyses related to this work and for this I am deeply grateful.

Becoming a scientific diver was one of the highlights of my PhD and I would like to thank Christian McDonald, Richard Walsh, Ashleigh Palinkas, Melissa Torres and Brett Pickering for their support and patience throughout my dive training and beyond.

Progressing through my PhD would not have been possible without the Scripps graduate office staff. Thank you to Gilbert Bertado, Denise Darling, Maureen McGreevy, Maureen McCormick, Josh Reeves, Shelley Weisel, Olivia Padilla and Tim DeBold for your tireless work to support students throughout their time at Scripps.

In 2017, I was fortunate enough to become an inaugural Scripps Community Engagement Diversity and Inclusion (EDI) Fellow under the supervision of Ms. Keiara Auzenne. This position has been one of the most rewarding experiences of my PhD and I have learned so much from Keiara and my other EDI team members. I would like to thank Keiara for sharing her knowledge and experiences with me, supporting me through some of the toughest moments of my PhD journey and training me to be an effective advocate for those most in need. I'd also like to thank Lynn Waterhouse, Osinachi Ajoku and the members of Women and Minorities and Science (WMIS) for your work to bring a greater sense of community and equity to Scripps as well as your friendship. It's an honor to fight the fight alongside you all.

This journey would have been much harder and much less enjoyable without my friends at Scripps. The 2014 Marine Chemistry and Geochemistry cohort and their partners, in particular, has been with me every step of the way and I truly cherish their friendships. Special thanks to Margot White for dealing with me as an officemate, Sara Rivera for being my "accountabilibuddy" and to them both for always listening.

Finally, I would like to thank my family and friends for their constant support throughout my life and especially during the past six years. They have always been there with encouragement, care, and love, but even more so through the many ups and downs of PhD life. Special thanks to Dr. Bill Lukens for navigating academia alongside me since we were just naïve undergraduates and for being a big part of my decision to become a geoscientist. Of course, none of this would be possible without my parents who have always whole-heartedly supported my aspirations and done everything they can to help me achieve my goals.

The greatest joy and honor in my life is sharing it with my husband Ted Griffin. He has selflessly and continuously supported me since we first met, commiserated with each disappointment, celebrated every success and helped me to always keep things in perspective. Our many adventures continue to keep me grounded and I have to thank him for always knowing when it's time to "take a break". With the forthcoming arrival of our daughter, I cannot wait to embark on our greatest adventure yet and could not imagine a better partner to have by my side. In all of this, he's the real PhD.

This work would not have been possible without support from various funding sources. The majority of this work was funded by the U.S. National Science Foundation (NSF) OCE 14-16518 (AJA, RJ) and OCE 12-55042 (AJA). In addition, student support and research funding was provided by the University of California, San Diego Frontiers of Innovation Scholars Program, Reagents Fellowship and the Scripps Institution of Oceanography department.

Chapter 1, in part, is currently being prepared for submission for publication of the material. Griffin, A. J.; Andersson, A. J.. The dissertation author was the primary investigator and author of this material.

Chapter 2, in part, is currently being prepared for submission for publication of the material. Griffin, A. J.; Cyronak, T.; Eyre, B.; Stoltenberg, L.; Andersson, A. J.. The dissertation author was the primary investigator and author of this material.

Chapter 3, in part, is currently being prepared for submission for publication of the material. Griffin, A. J.; Cyronak, T.; Eyre, B.; Andersson, A. J.. The dissertation author was the primary investigator and author of this material.

Chapter 4, in part, is currently being prepared for submission for publication of the material. Griffin, A. J.; Anderson, Z.; Ballard, J.; Bates, N.; Garley, R.; Johnson, R.; Martz, T.; Pacheco, F.; Takeshita, Y.; Andersson, A. J.. The dissertation author was the primary investigator and author of this material.

VITA

2010	Bachelor of Science, Geology, Religion, Temple University
2012	Master of Science, Geology, Temple University
2020	Doctor of Philosophy, Oceanography, Scripps Institution of Oceanography, University of California San Diego

ABSTRACT OF THE DISSERTATION

Biogenic Carbonate Dissolution in Shallow Marine Environments

by

Alyssa Jean Griffin

Doctor of Philosophy in Oceanography

University of California San Diego, 2020

Professor Andreas J. Andersson, Chair

Ocean acidification (OA), the decrease in surface ocean pH and seawater saturation state with respect to carbonate minerals (Ω), is expected to increase carbonate mineral dissolution. However, the influence of OA on carbonate dissolution has been largely neglected despite evidence that it is more sensitive to OA than calcification. Increases in the rate of carbonate dissolution could have severe impacts for ecosystems such as coral reefs, which rely on the

accumulation of carbonate structures and substrates to exist. At present, dissolution rates of bulk shallow biogenic carbonate sediments are largely unknown and laboratory dissolution rates exceed *in situ* rates by orders of magnitude. The goal of this study was to develop a better understanding of the drivers and controls of bulk carbonate sediment dissolution in coral reef environments.

Based on results from *in situ* benthic chambers and laboratory free-drift experiments of bulk biogenic carbonate sediments from global locations, dissolution rates were found to be primarily controlled by organic matter decomposition, but significantly influenced by the overlying seawater carbonate chemistry and the solubility of the most soluble mineral phase in the sediments. Shallow carbonate dissolution will therefore be enhanced via ocean acidification, increased respiration, or a combination of these processes. The sensitivity of bulk sediment dissolution rates to changes in Ω was not related to median grain size or mineralogy, but may be attributed to organic coatings on sediment grains. Dissolution rates in bulk sediments increased ~2-3-fold when these coatings were removed, suggesting that they act as a protective barrier that limits direct interaction of seawater with the mineral surface, thus inhibiting dissolution. On the ecosystem scale, carbonate dissolution was inferred from calcium anomalies measured using a novel spectrophotometric titration system and confirms seasonal and inter-annual trends in reef biogeochemical processes based on parallel alkalinity measurements. However, calcium measurements may be best employed in environments where multiple processes significantly influence alkalinity or Mg-calcites are precipitating and dissolving.

Although many questions remain, this work has elucidated certain key drivers and controls of shallow carbonate sediment dissolution and how they may respond to a rapidly changing ocean.

Chapter 1: Disparities between biogenic carbonate dissolution rates in laboratory and shallow marine settings: A review

Alyssa J. Griffin and Andreas J. Andersson

ABSTRACT

A significant amount of carbonate minerals accumulates in shallow marine environments. Even though the water column is typically supersaturated with respect to commonly occurring calcium carbonate mineral phases, carbonate dissolution is known to be a significant process in these shallow carbonate deposits. However, the relative importance of physical and chemical processes and properties that influence shallow carbonate dissolution rates or how they will be impacted by changing ocean chemistry is not fully understood. There is an extensive body of literature dedicated to the dissolution of carbonate minerals, however, the applicability of many studies to shallow marine carbonates is often limited due to significant differences in environment, experimental conditions and/or substrates.

Here, we review biogenic carbonate dissolution studies with direct application to shallow marine environments. A synthesis of dissolution rates and principal findings from laboratory, mesocosm and *in situ* field studies of shallow marine biogenic carbonate substrates are reported. Across these studies, the range of reported in situ dissolution rates are found to be orders of magnitude slower than laboratory dissolution rates. This significant disparity between dissolution rates measured in the laboratory versus those observed in the natural environment is consistent with dissolution rates in other marine environments and possible explanations are discussed. To address this disparity and improve our understanding

of dissolution in shallow biogenic carbonates, it is evident that a combination of field and laboratory approaches as well as concerted efforts to make experimental conditions more comparable between these settings will be necessary. Although dissolution in shallow marine environments is expected to increase in the future due to changing ocean chemistry (i.e. ocean acidification), parsing apart the true controls of dissolution in shallow marine environments will be critical to predicting the magnitude, rate and specific mechanisms for such increases in shallow marine environments.

INTRODUCTION

Calcium carbonate minerals ($CaCO_3$) are fundamental components of both marine and terrestrial environments on Earth's surface. Carbonate rocks are one of the largest carbon reservoirs on the planet and reactions involving carbonate minerals and natural waters can influence the chemistry of the atmosphere and oceans on various spatial and temporal scales (Morse and Mackenzie, 1990). Studying these reactions not only improves our understanding of these processes, but also has broad applications in both industry and science, spanning from petroleum reservoirs to paleoclimatology (Ries et al., 2016). For this reason, the formation and dissolution of carbonate minerals has been extensively studied for nearly half a century in both the laboratory and field (see Morse and Arvidson, 2002; Morse et al., 2007 for detailed reviews).

In recent decades, carbonate mineral formation and dissolution has received increased attention as anthropogenic activities, such as the burning of fossil fuels and land-use changes, have led to a perturbation in the global carbon cycle. Anthropogenic carbon dioxide (CO_2) emissions have caused an increase of CO_2 in the atmosphere, which directly exchanges CO_2

with the ocean. The ocean has taken up approximately 27% of anthropogenic CO_2 emissions released in recent decades (Le Quéré et al., 2018) leading to a global decrease in open ocean pH and the seawater saturation state with respect to carbonate minerals (Ω) (Bates et al., 2014; Doney et al., 2009). These changes in marine carbonate chemistry are collectively referred to as ocean acidification (OA). As the Ω decreases due to OA, it is expected that calcification in marine organisms will decrease (Kleypas et al., 1999; Langdon, 2002) and carbonate mineral dissolution will increase (Andersson and Gledhill, 2013; Andersson et al., 2009; Andersson et al., 2005; Andersson et al., 2003; Eyre et al., 2018; Morse et al., 2006; Tynan and Opdyke, 2011).

The dissolution of carbonate minerals can be represented with the following reaction:

$$CaCO_3 + H_2O + CO_2 = Ca^{2+} + 2HCO_3^- \qquad \text{Eq. (1)}$$

This reaction results in the addition of alkalinity to the surrounding seawater, which increases its ability to take up CO_2. Therefore, changes in the rate of carbonate mineral dissolution in various environments could have important influences on the carbonate chemistry of coastal and open ocean marine ecosystems, local and large-scale oceanic biogeochemical cycles, the global carbonate budget and ultimately, the global carbon cycle (Archer and Maier-Reimer, 1994; Mackenzie et al., 1980).

The formation of marine carbonate minerals is primarily facilitated by organisms making shells, tests, spicules, exo- and endoskeletons made of $CaCO_3$ (Morse et al., 2007). The presence, composition, and abundance of calcifying taxa vary across marine environments (Morse et al., 2007).When the formation of carbonate minerals exceeds

dissolution and other destructive processes (e.g., mechanical erosion, bioerosion, and export) in a given environment, they accumulate as biogenic carbonate structures and/or sediments. More than half of global carbonate sediments accumulate in shallow environments such as reefs, banks, and tropical shelves, while the remaining sediments accumulate in deep-sea environments (Andersson et al., 2013; Milliman, 1993; Milliman and Droxler, 1995).

Carbonate mineral dissolution is unequivocally associated with deep ocean environments where seawater is undersaturated with respect to carbonate minerals. This has led to a significant body of work investigating carbonate mineral dissolution in the context of settling particles in the water column and deep-sea benthic dissolution (Berelson et al., 1990; Berger, 1967; Cao and Dai, 2011; Chen, 1990; Chen et al., 2004; Feely et al., 2002; Friis et al., 2006; Gehlen et al., 2007; Keir, 1983; Kennish et al., 1993; Milliman et al., 1999; Oxburgh and Broecker, 1993; Peterson, 1966; Sabine and Mackenzie, 1995; Thunell et al., 1981; Troy et al., 1997). However, numerous studies have identified extensive dissolution in the water column above the saturation horizon (Berelson et al., 2007; Feely et al., 2004; Milliman et al., 1999). This has been attributed to dissolution within microenvironments in marine snow, fecal pellets, or zooplankton guts (Jansen and Wolf-Gladrow, 2001), or dissolution of highly soluble minerals excreted from fish guts (Wilson et al., 2009), but these remain working hypotheses. Furthermore, many studies have shown that carbonate mineral dissolution is a significant process in shallow marine deposits, even though bottom waters in these environments are typically supersaturated with respect to carbonate minerals (Aller, 1982; Andersson et al., 2007; Balzer and Wefer, 1981; Cyronak et al., 2013a; Cyronak et al., 2013b; Walter et al., 1990; Walter et al., 1993). Carbonate mineral dissolution in these environments occurs most notably in carbonate sediments where interstitial pore waters and

microenvironments become undersaturated with respect to carbonate minerals. This is due in part to the microbial remineralization of organic matter, a process that is referred to as metabolic dissolution (Andersson et al., 2007; Balzer and Wefer, 1981; Burdige and Zimmerman, 2002; Morse et al., 2006; Walter and Burton, 1990) as well as through the reoxidation of reduced compounds via oxygen delivery from bioturbation (Aller, 1982) or seagrass roots and rhizomes (Burdige and Zimmerman, 2002). Considering a substantial amount of global carbonate sediments are located in shallow marine environments, dissolution in these environments is not trivial (Walter and Burton, 1990).

The dissolution of carbonate sediment is of particular importance in carbonate dominated ecosystems such as coral reefs. Coral reefs depend on the physical accumulation of carbonate in order to grow and sustain their complex reef structures. As a result of OA, increased carbonate mineral dissolution could prevent accumulation and cause these ecosystems to shift from a state of net accretion to net erosion by the end of the century (Andersson et al., 2009; Hoegh-Guldberg et al., 2007; Silverman et al., 2009; Yates and Halley, 2006a). Some studies have indicated that dissolution of shallow carbonate minerals may be more sensitive to OA than calcification (Andersson et al., 2009; Eyre et al., 2018), but the rates of dissolution in shallow carbonate environments and the mechanisms that most strongly influence them are not well constrained (Andersson and Gledhill, 2013). Quantifying the relative importance of various biological, physical and chemical drivers of dissolution in shallow carbonate sediments is critical in predicting how future changes in ocean chemistry will affect carbonate mineral dissolution and in turn, shallow carbonate-dominated ecosystems.

Although carbonate dissolution has been extensively studied in both the field and laboratory, a significant disparity still exists between carbonate dissolution rates measured in the laboratory versus those measured in shallow marine environments (Morse et al., 2007). In the seminal review by Morse et al. (2007), the authors expressed the need for better conceptual bridging between carbonate mineral dissolution results obtained under relatively simple and well controlled experimental conditions and what goes on in the "real" ocean. A better understanding of the laboratory-field disparity would vastly improve the way we approach carbonate mineral dissolution research and guide our interpretation of results from both laboratory and field experiments.

The objective of this work is to review and compare dissolution rates obtained from laboratory, mesocosm and *in situ* field studies of shallow marine biogenic carbonate substrates. These substrates are primarily produced by the mechanical breakdown of the calcareous materials of benthic organisms, including corals, echinoids, mollusks, benthic foraminifera, and calcifying algae, predominantly made of aragonite or Mg-calcites (Chave et al., 1962). Since comprehensive and detailed reviews of carbonate mineral dissolution kinetics and the formation and dissolution of marine carbonate minerals already exist (Morse and Arvidson, 2002; Morse et al., 2007, respectively), this review will focus solely on carbonate-rich sediments in shoal-to-shallow waters (0 to less than ~200m).

A literature review was conducted and studies that reported dissolution rates under the following conditions were included:

1) Laboratory experiments assessing dissolution rates of biogenic carbonate substrates in natural or artificial seawater under various chemical conditions,

2) Mesocosm and *in situ* carbonate dissolution studies of biogenic carbonate sediments and substrates.

The aim of this review is to serve as a foundation for improving our understanding of carbonate mineral dissolution in shallow marine environments. It is of particular relevance in the context of ongoing climate change and OA, but is also relevant to the role of the coastal carbon cycle for any time period and environmental condition.

BIOGENIC CARBONATE MINERALS

Carbonate mineral properties

Contemporary marine carbonate sediments are predominately comprised of three carbonate minerals: calcite, aragonite, and magnesian calcite (Mg-calcite). Calcite and aragonite are $CaCO_3$ polymorphs and the differences between their crystal structures make aragonite denser (2.93 g cm^{-3} vs. 2.71 g cm^{-3}) and more soluble in seawater than calcite. Mg^{2+} ions are more readily incorporated into the structure of calcite, leading to the occurrence of calcites that contain variable amounts (10 to <30 mol %) of $MgCO_3$, which are collectively known as Mg-calcites (Morse et al., 2007). Mg-calcites with Mg content greater than 8-12 mol% are generally more soluble than aragonite and Mg-calcites with lower Mg content (Bischoff et al., 1993; Busenberg and Plummer, 1986, 1989; Mackenzie et al., 1983; Morse et al., 2006; Plummer and Mackenzie, 1974).

The vast majority of modern sedimentary carbonate minerals is biogenic in origin. These minerals are actively precipitated from seawater by organisms to form skeletal hard parts and are posthumously deposited in marine environments as sediments. Biogenic carbonates differ significantly from their abiogenic counterparts in terms of basic physical

properties, composition, impurities, and structure (Morse et al., 2007). Consequently, although composed of the same carbonate mineral, biogenic carbonates can have radically different solubility and reaction rates compared to their abiotic counterparts. These differences can be so striking that some have even said biogenic carbonates, in many ways, form an entirely different class of materials (Morse et al., 2007). Because of the complexity and heterogeneity of biogenic carbonate substrates, reactivity can vary substantially between different depositional environments depending on the mineral composition, size distribution and the organismal origin.

Reaction rates and solubilities

In general, the rate of carbonate mineral dissolution can be represented by the following equation:

$$R = k(1 - \Omega_x)^n \qquad \text{Eq. (2)}$$

where R is the dissolution rate (normalized to surface area or substrate weight), k is a rate constant, Ω is the saturation state of the solution with respect to the carbonate mineral of interest (x), and n is the reaction order (Keir, 1980; Morse, 1978).

As seen in Equation 2, the saturation state (Ω) with respect to the dissolving mineral is integral to the calculation of a rate equation. The saturation state in a given solution will differ with respect to calcite, aragonite, and Mg-calcite due to their different mineral stabilities. Numerous studies have investigated the solubility of various carbonate minerals (for an extensive review see Morse and Arvidson, 2002). Morse et al. (1980) determined the apparent

solubility of calcite in seawater and found their values were in good agreement with those of previous studies (Ingle et al., 1973; MacIntyre, 1965; Plath, 1979). In addition, they found no significant difference between measured solubilities of synthetic, natural, and biogenic materials for calcite and aragonites of >99% purity. The apparent solubility of aragonite, however, was found to be significantly lower than previous studies (Berner, 1975; MacIntyre, 1965; Plath, 1979). Mucci et al. (1983) also measured the solubility of calcite and aragonite, but under a range of temperature (5 – 40°C) and salinity (5 – 44‰). The solubility measurements from this study are most often referenced for saturation state calculations with respect to aragonite and calcite in seawater.

The solubility of biogenic magnesian calcites, on the other hand, is not agreed upon as easily. The fact that Mg-calcite solubility increases with increasing mol % $MgCO_3$ is not disputed, but the exact relationship between solubility and composition can vary tremendously depending on the preparation of the mineral sample used for solubility experiments (Fig. 1.1; Bischoff et al., 1993; Morse et al., 2006). Based on previous studies, the solubility of biogenic Mg-calcite, expressed as a function of Mg content, can be calculated based on two different solubility curves as seen in Fig. 1.1:

Curve B) The "cleaned" biogenic best-fit solubility (Bischoff et al., 1987; Walter and Morse, 1984a) where samples were well cleaned and annealed or,

Curve C) The Plummer-Mackenzie solubility where "minimally prepared" biogenic carbonate samples were washed in an ultrasonic bath and then dried (Plummer and Mackenzie, 1974)

Depending on the experimental curve adopted, the approximate Mg-calcite composition with the same solubility as aragonite ranges from 8 – 12 mol% $MgCO_3$ (Andersson et al., 2007; Morse et al., 2006). It is still not fully understood which solubility curve most accurately reflects the behavior of these minerals in the natural environment, however results from some studies (Andersson et al., 2007; Bischoff et al., 1993; Tribble et al., 1995) suggest the use of the "minimally prepared" curve (Morse et al., 2006). These differences in Mg-calcite solubilities make the use of Eq. 2 to represent dissolution rates in shallow carbonate sediments impractical because they contain considerable amounts of Mg-calcite of varying compositions and solubilities that often are unknown. As a consequence, it is challenging or not possible to determine accurate seawater saturation states with respect to these Mg-calcite minerals. In addition, the presence of both aragonite and Mg-calcites makes using a single saturation state inappropriate.

A significant portion of carbonate mineral dissolution studies has focused on rates in the open water column or from deep-sea sediments (Archer et al., 1989; Berelson et al., 2007; Berelson et al., 1990; Berelson et al., 1987; Berelson et al., 1994; Cao and Dai, 2011; Chen, 1990; Chen et al., 2004; Feely et al., 2002; Friis et al., 2006; Gehlen et al., 2007; Honjo and Erez, 1978; Kennish and Lutz, 1999; Kennish et al., 1993; Oxburgh and Broecker, 1993; Peterson, 1966; Thunell et al., 1981; Wilson and Wallace, 1990), but these results are generally difficult to apply to shallow marine environments, because deep-sea sediments are typically composed of more uniform mineralogy and organisms..

For abiogenic substrates, observed dissolution rates fit to Eq. 2 are typically normalized to the surface area of the substrate. However, this method of normalization is often inappropriate when studying biogenic substrates. Walter and Morse (1984b) studied the

dissolution of biogenic Mg-calcites and observed that although dissolution rates generally increased with total (BET) surface area, the increases were not proportional. The complex microstructures of biogenic Mg-calcites prevent the surrounding solution from reacting with the entire surface of the substrate. Therefore, BET surface area is typically not representative of reactive surface area. This presents a significant issue because normalization is necessary to compare dissolution rates for substrates with differing grain sizes or other physical differences (increased porosity of grains, density of reactive surface sites, etc.) To circumvent this issue, dissolution rates are often normalized to other factors such as weight (Pickett and Andersson, 2015; Walter and Morse, 1984b, 1985) or approximate geometric surface area (Cubillas et al., 2005).

LABORATORY STUDIES

To date, there are a number of studies that have investigated the dissolution kinetics of biogenic carbonate minerals in laboratory settings (Busenberg and Plummer, 1986; Cubillas et al., 2005; Findlay et al., 2011; Gehlen et al., 2005; Keir, 1980, 1983; Morse, 1978; Morse and Berner, 1972; Morse et al., 1979; Pickett and Andersson, 2015; Ries et al., 2016; Subhas et al., 2018; Tsurushima et al., 2008; Waldbusser et al., 2011; Walter and Burton, 1986; Walter and Morse, 1984b, 1985; Yamamoto et al., 2012). However, it is important to note that of these studies, which is believed to be a fairly inclusive list of laboratory biogenic carbonate mineral dissolution studies, only three studies conducted controlled dissolution rate experiments on bulk shallow marine sediments in natural seawater (Pickett and Andersson, 2015; Walter and Morse, 1985; Yamamoto et al., 2012). Biogenic carbonate mineral dissolution has been briefly reviewed in Morse and Arvidson (2002); Morse et al. (2007),

concluding that the understanding of how particular properties of biogenic carbonates influence dissolution remains limited.

Although experiments on whole tests and/or the calcareous hard parts of a single species may be useful in identifying properties that most influence dissolution and responses of particular substrates or organisms, their applicability to bulk sediment dissolution in the natural environment are limited. It is understood that several of these studies were designed to address very different research questions, but the end result is that there are few investigations on bulk shallow carbonate sediments. Extrapolation of laboratory dissolution rates into models of current conditions or future projections from substrates that are not representative of natural bulk sediments can lead to spurious projections and conclusions.

Early studies

The work of Chave (1954a, b; 1962) and others (Stehli and Hower, 1961) was seminal in defining the distribution of different mineralogies and the bulk mineralogy of shallow marine carbonate sediments. In particular, this work established the importance of Mg-calcites in shallow marine environments. Some of the earliest laboratory experiments related to carbonate mineral dissolution were conducted to determine the stability of assorted carbonate mineral phases in various mediums (Garrels et al., 1960; Greenwald, 1941). However, like many of the laboratory studies on carbonate mineral dissolution kinetics, these early studies investigated the dissolution of abiogenic carbonate mineral phases or lithified carbonate samples (e.g., limestone, magnesite, dolomite rocks), thus making comparison between reported solubilities problematic (see *Carbonate mineral properties* above). The earliest

experiments on the stability of biogenic shallow substrates were conducted by Chave and colleagues (Chave et al., 1962) using the saturometer technique (Weyl, 1961).

Shortly thereafter, the seminal *in situ* experiments of Peterson (1966) and Berger (1967) were conducted, where smoothed calcite spheres and foraminiferal oozes, were hung at different depths in the Pacific and Atlantic Oceans, respectively. These experiments revealed that the extent of calcite dissolution in seawater is not simply proportional to saturation state (Morse and Arvidson, 2002).

These field experiments gave rise to extensive work on carbonate mineral dissolution published in a series of papers by Berner, Morse and others to better understand carbonate deposition rates in deep-sea sediments (Berner and Morse, 1974; Berner and Wilde, 1972; Morse, 1974a, b; Morse and Berner, 1972). However, only one of these experiments (Berner and Wilde, 1972) used biogenic carbonate minerals (deep-sea carbonate sediments). In this study, they found that changes in dissolution rates as a function of seawater undersaturation were similar in both laboratory and open ocean experiments, but the absolute rates of dissolution were much greater in the laboratory than in the open ocean experiments. This led (Morse, 1978) to undertake another study to investigate carbonate-rich deep-sea sediments from the Indian, Pacific, and Atlantic Oceans. His results indicated that the dissolution kinetics of deep-sea carbonate sediments is complex and that sediments from various areas showed significantly different reaction orders and rate constants (Table 1.2). He mainly attributed these differences to different grain size distributions and different surface histories (Morse, 1978).

The field experiments of Berger (1967), specifically, led to dissolution experiments conducted on aragonitic substrates by Morse and others (1979), which showed good

agreement with the rate of pteropod dissolution in the laboratory and the field experiments (Berger, 1967). The study found that pteropod dissolution was less than an order of magnitude greater than that of the calcitic fraction of deep-sea sediments (Morse, 1978). However, the results of this study were significantly higher and in poor agreement with previous field experiments (Honjo and Erez, 1978; Milliman, 1977). The differences were attributed to the larger size fractions used in the field experiments or the potential "ponding" of the pteropods at the bottom of the experimental field chambers.

Later on, significant work was also conducted by Keir (1980, 1983) to understand biogenic carbonate dissolution. Keir (1980) investigated several foraminifera, coccoliths, deep-sea sediments and a pteropod assemblage in addition to synthetic calcite and aragonite analogs in artificial seawater. He found that all the synthetic and biogenic calcite appeared to conform to the rate law:

$$R_{\%} = k_{\%}(1 - \Omega)^n \qquad \text{Eq. (3)}$$

where $R_{\%}$ is the rate of dissolution normalized to the mass of calcium carbonate sample and expressed as percentage, $k_{\%}$ is the rate constant, Ω is the saturation state, and n is the order of the reaction. In the coccoliths and forams, n was 4.5 ± 0.7 and the synthetic aragonite and pteropods had an $n \approx 4.2$. The $k_{\%}$ widely varied for the different carbonate samples used.

However, Keir (1983) demonstrated in later experiments that fluxes from unsuspended grains (more representative of deposited sediments) resulted in a rate constant that was approximately two orders of magnitude lower than values measured in previous kinetic

experiments on suspended substrates (Keir, 1980). Even though Keir's studies focused mainly on open ocean and deep-sea sediment dissolution, the values for kinetic dependence (n) from his 1980 study are still widely used to model dissolution in various systems. This reaction order may be inappropriate, even for deep sea foraminifera, where a reaction of order of 2.6 was obtained under high pressure (>100 kg/cm^2) and high pCO_2 (1,000 – 15,000 ppm) conditions (Tsurushima et al., 2008). In addition, reaction orders in shallow biogenic carbonates differ significantly from these values. For example, although shallow carbonates on single-species substrates also fit the empirical kinetic expression (Eq. 2), reaction orders are near 2.9 for low-Mg calcites, 2.5 for aragonites and 3.4 for Mg-calcites and rate constants vary by nearly a factor of ten for different carbonate samples in a study by Walter and Morse (1985).

Surface area and grain size

Differences in rate constants, such as those observed in Walter and Morse (1985), can be explained by differences in reactive surface areas. Unlike their abiogenic counterparts, biogenic carbonate minerals exhibit complex microstructures and for this reason, the total (BET) surface area may greatly overestimate the amount of surface area available for reaction during dissolution. (see *Reaction rates and solubilities* above). Since the reactive surface area cannot be directly measured, it has been estimated by an empirical "roughness factor" which compares the BET surface area of a biogenic carbonate substrate to the geometric surface area of rhombic calcite of equivalent grain size (Walter and Morse, 1984b). Both microstructure and grain size can play important roles in controlling the dissolution rates of biogenic carbonates (Walter and Morse, 1984b) and in some cases, grain microstructural complexity

can "override" thermodynamic constraints and lead to the selective dissolution of a thermodynamically more stable phase (Walter and Morse, 1985). In general, the use of BET surface areas to normalize dissolution rates in shallow biogenic carbonates is not favored and geometric surface area is a much closer estimate of how much substrate surface is actually participating in dissolution reactions (Cubillas et al., 2005; Walter and Morse, 1984b).

Studies on inhibitors

To better understand the chemical behavior of carbonate minerals in natural waters, several studies have investigated potential inorganic and organic inhibitors of carbonate precipitation and dissolution (see Morse, 1986 and Morse et al., 2007 for reviews). It is difficult, however, to draw overall conclusions about the role of specific inhibitors from these various studies because of the differences in saturation state and major ion composition for each experiment (Morse et al., 2007). There is substantial evidence from this body of work that dissolved organic and inorganic phosphate species inhibit carbonate precipitation and dissolution in seawater (Morse et al., 2007). Studies have shown that various organic and inorganic phosphate species are effective inhibitors at even micromolar concentrations (Walter and Burton, 1986). However, many of these studies were conducted on synthetic calcite or aragonite (Berner and Morse, 1974; Keir, 1980; Morse, 1974b; Morse et al., 1979; Pesret, 1972; Sjöberg, 1978) and for this reason, their application to the natural environment may be limited. Walter and Burton (1986) investigated the influence of phosphate on biogenic carbonate substrates and found that that phosphate inhibits the dissolution rates of calcites, Mg-calcites and aragonites to similar degrees. The magnitude of the rate reductions they observed were less than a factor of 5 under their experimental conditions. Their work was also

in good agreement with the earlier work of Walter and Hanor (1979) on the influence of orthophosphate on biogenic Mg-calcite dissolution kinetics.

Organic coatings have also been invoked as a potential inhibitor of dissolution (Suess, 1970, 1973). Organic matter can be associated with biogenic carbonates in two primary ways: incorporation into the mineral lattice via the calcifying organism and/or adsorbed or adhered to the mineral surfaces (Ingalls et al., 2004). When adsorbed to carbonate substrates, organic matter may inhibit direct interaction of mineral surfaces with surrounding seawater, thus limiting dissolution. The removal of organic coatings via surficial oxidation has shown to increase rates of dissolution in deep sea biogenic carbonates, namely coccoliths and foraminifera (Honjo and Erez, 1978; Keir, 1980), but a more recent study has contested these findings (Subhas et al., 2018). The role of organic coatings remains open-ended and has yet to be explicitly investigated in shallow carbonate substrates or sediments.

Studies in the context of ocean acidification

In response to time-series evidence of recent changes in global surface seawater carbonate chemistry (Bates, 2001; Bates et al., 2014; Dore et al., 2009; Olafsson et al., 2009; Santana‐Casiano et al., 2007), research efforts relating to OA have increased in the last couple of decades (Gattuso and Hansson, 2011). Of the various areas of OA research, the biological response of marine organisms has been most heavily studied (Gattuso and Hansson, 2011). Countless experimental studies have investigated the responses of calcification and other biological processes to OA in many species of marine calcifiers. The results of these studies vary and are well-summarized in multiple review articles (Doney et al., 2009; Fabry et al., 2008; Hendriks et al., 2010; Kleypas et al., 2005; Kroeker et al., 2010). Even though

dissolution processes may be more sensitive to OA than biological processes, there is a clear publication bias between measurements or estimates of calcification compared with dissolution from shallow marine environments (Eyre et al., 2014). For example, Eyre et al. (2014) found that of 370 studies that had 'ocean acidification' and 'coral' in the title, abstract and keywords, only 4.1% measured or estimated net carbonate dissolution.

The concern regarding organismal responses to OA, however, has led to several dissolution experiments on whole tests or shells of various marine organisms. The range of organisms studied is broad and includes various species of gastropods, bivalves, echinoderms, barnacles, corals, bryozoa and coralline algae. Dissolution has been measured both in shells isolated from their various calcifying organisms (Findlay et al., 2011; Ries et al., 2016; Waldbusser et al., 2011) as well as when associated with the living calcifying organism (Findlay et al., 2011). Dissolution rates of isolated shells decreased with increased exposure to natural weathering processes (Waldbusser et al., 2011) and when associated with their living calcifying organism (Findlay et al., 2011). However, the response of net calcification in living organisms is complex (Kroeker et al., 2010; Ries et al., 2009) and it is important to note that although net calcification may remain constant in some species, enhanced dissolution may exert a cost, physically or energetically on the organisms (Findlay et al., 2011).

Dissolution rates of isolated whole tests were shown to increase with decreasing Ω (ocean acidification) and increasing temperature (ocean warming) and that shells/skeletons composed of the more soluble polymorphs of carbonate will be the most vulnerable to these stressors (Ries et al., 2016). For example, dolomite-rich crustose coralline algae (CCA) dissolved 6–10 times slower than predominantly Mg-calcite CCA in both high-CO_2 (~ 700 ppm) and control (~ 380 ppm) environments (Nash et al., 2013). However, this was

shown to be a result of both selective dissolution of more soluble carbonate minerals and reduced porosity due to dolomite infilling (Nash et al., 2013), which further demonstrates the complex relationship between mineral solubility and microarchitecture in shallow biogenic carbonates. In addition, due to fundamental differences between the dissolution kinetics of whole-shell biogenic carbonate and inorganic carbonate, modelling gross dissolution of biogenic carbonates by applying stoichiometric solubility products derived for inorganic carbonate may substantially underestimate the impacts of ocean acidification on net calcification (Ries et al., 2016).

Dissolution rates have also been measured for size fractions of single carbonate species (Pickett and Andersson, 2015; Walter and Morse, 1984b, 1985; Yamamoto et al., 2012). Despite the broad range of conditions and experimental approaches (Tables 1.1 and 1.2), all substrates showed increased dissolution with lower Ω. However, due to their higher solubilities relative to aragonite and calcite, some high Mg-calcite substrates were found to dissolve at aragonite saturation states (Ω_{Ar}) as high as 3.2 (Yamamoto et al., 2012). For a given Ω, studies suggest that different single-species substrates show a consistent relative ranking of dissolution rates (Pickett and Andersson, 2015; Yamamoto et al., 2012) which suggests that substrates may undergo sequential dissolution in bulk sediments and that some substrates may be more vulnerable to OA than others (Pickett and Andersson, 2015). The relative ranking appears to be most closely related to Mg-content of the Mg-calcite substrates (Pickett and Andersson, 2015) and grain microarchitecture (Pickett and Andersson, 2015; Walter and Morse, 1985). In addition, the calculated solubilities of substrates with minimal preparation (ultrasonic cleaning and drying only) were similar to those reported by Plummer and Mackenzie (1974) (see *Reaction rates and solubilities* above) and are more comparable to

solubilities obtained from field data (Yamamoto et al., 2012). This supports that conducting dissolution experiments using the minimal preparation method for biogenic carbonate substrates may be more representative of dissolution in the natural environment.

To date, only a few experiments have conducted laboratory dissolution experiments on natural, bulk carbonate sediments from shallow marine environment (Pickett and Andersson, 2015; Walter and Morse, 1985; Yamamoto et al., 2012). As with single-species experiments, sediments from these experiments show that dissolution rates increase with decreasing $[CO_3^{2-}]$ and Ω (Pickett and Andersson, 2015; Walter and Morse, 1985; Yamamoto et al., 2012). Bulk sediment samples were found to dissolve at Ω_{Ar} as high as 3.8 (Yamamoto et al., 2012) and although dissolution rates were higher for sediments than some single-species substrates, they typically fell on the lower end of relative rankings (Pickett and Andersson, 2015; Yamamoto et al., 2012). In addition, carbonate sands with smaller median grain sizes were also shown to dissolve faster than the sand with a larger median grain size even though mineralogies of the bulk sediments differed (Walter, 1985). However, it is important to note that all the experiments mentioned here were conducted on bulk sediment separated into known grain size fractions which does not reflect dissolution of the complete (and often broad) grain size distributions found in natural sediments.

Comparison of laboratory biogenic carbonate dissolution studies

Although the studies discussed above offer considerable insight to the drivers of biogenic carbonate mineral dissolution, differences in bulk mineralogy, solution parameters, physical substrate properties (grain size, surface are, etc.), experimental design and calculation methods make inter-comparisons of laboratory dissolution data challenging.

One difficulty is that although many studies have shown the kinetic behavior of carbonate dissolution follows various iterations of Eq. 2, some studies do not report a fit to this equation. This is often due to difficulties associated with the determination of the saturation state with respect to the dissolving phase, particularly when analyzing Mg-calcites of varying %mol content or sediments that contain multiple phases with poorly defined solubilities (see *Carbonate mineral properties* above). In other cases, the research question simply isn't concerned with kinetic behavior and therefore it is not necessary to fit experimental data to a rate equation. Another difficulty stems from differences in Ω between studies, which can result from the use of different carbonic acid dissociation constants used to calculate the speciation of the carbonate system and stoichiometric solubility products for the various carbonate mineral phases (Gehlen et al., 2005). Using different values for these parameters can lead to significant differences in the saturation states reported and make inter-comparison impossible if certain experimental parameters are not reported.

For example, although Keir's values for kinetic dependence (n) has been widely used, they have been challenged by various investigators that claim lower order reactions best describe dissolution in the natural environment (Gehlen et al., 2005; Hales and Emerson, 1997). First order kinetics may be appropriate under certain conditions, (Boudreau, 2013; Cubillas et al., 2005); Hales and Emerson (1997), but several studies report non-linear relationships between dissolution rates and Ω. Some have suggested that Keir's high value for *n* could be attributed to uncertainties linked to the saturation state of the experimental seawater solution (Gehlen et al., 2005), however recent work has demonstrated that this alone cannot account for observed non-linear kinetics in both synthetic and biogenic calcites (Subhas et al., 2017; Subhas et al., 2015; Subhas et al., 2018). Regardless of this on-going

debate, the wide range of reported reaction orders can have significant impacts on models of calcite dissolution (Jansen et al., 2002).

The studies that do fit the data to a kinetic equation typically report the reaction orders (n) and rate constants (k) for the various substrates investigated (Cubillas et al., 2005; Keir, 1980; Morse, 1978; Walter and Morse, 1984b, 1985). Other studies may also expand Eq. 2 to include other variables such as temperature (Ries et al., 2016). However, even when fit to Eq. 2, observed dissolution rates can be reported in various units depending on how the data are normalized. Differences can easily be seen between studies that report in the same units, but it is very difficult to convert from one unit to another without certain experimental information.

Experimental methods can also complicate inter-comparison. There are several physical aspects of the experimental reactors and substrates that can significantly influence dissolution. These include, but are not limited to, whether the substrate is abiotic or biogenic in origin (see discussion above), how the substrate is oriented in the reactor (suspended or settled grains), how the substrate is treated prior to dissolution (sonicated to remove submicron particles or soaked in NaOH to remove organics) and the design of the reactor itself (pH-stat, flow-through, free-drift, etc.).

Several of these physical differences are related to the amount of surface area exposed to the surrounding medium. One of the greatest challenges of inter-comparison between laboratory studies is how measured dissolution rates are normalized to account for these differences. For example, many experiments have been done on whole shells of organisms, but one can imagine the difference in exposed surface area between whole shells and smaller grained substrates such as sediments. This issue is usually addressed for other substrates by normalizing observed dissolution rates to the total measured (BET) surface area of the

substrate. It has been established that the total surface area of biogenic carbonates is not available for interaction with the surrounding medium (Walter and Morse, 1984b) and therefore, normalizing to the total surface area results in artificially low dissolution rates. It has been suggested that geometric surface area (GSA) could be used instead (Cubillas et al., 2005), but this method is challenging for substrates with a wide range of grain sizes. In addition, (Walter and Morse, 1984b) found that biogenic aragonites can have a total:geometrically calculated surface area ratio of 5.4 (for 51 μm grains of coral) to 541.2 (for 513 μm grains of Halimeda). This indicates a wide range of microstructure in various biogenic carbonates which could significantly influence observed dissolution rates depending on the grain size used.

Experiments are also done under a wide range of experimental conditions (Table 1.2). For example, both the studies of Cubillas et al. (2005) and Busenberg and Plummer (1989) were conducted over a similar pH range, but the range of saturation states with respect to calcite differed significantly between the two studies (approximately 0-1.5 and near zero only, respectively). These subtle differences in experimental conditions can lead to false confirmation between data sets regarding the dissolution rates of a given substrate.

MESOCOSM AND IN SITU STUDIES

Although laboratory measurements can provide significant insight into the mechanisms of carbonate dissolution, findings from these experiments must be placed in the broader context of dynamic marine environments. There are numerous *in situ* carbonate sediment dissolution studies both in the deep-sea (>200 m; Berelson et al., 1990; Berelson et al., 1987; Berelson et al., 1994; Berger, 1967; Boudreau, 2013; Cai et al., 1995; Hales and

Emerson, 1996; Honjo and Erez, 1978; Jahnke and Jahnke, 2004; Kennish and Lutz, 1999; Kennish et al., 1993; Lutz et al., 1988; Lutz et al., 1994; Martin and Sayles, 1996; Wilson and Wallace, 1990) and in shallow marine environments (Aller, 1982; Anthony et al., 2013; Balzer and Wefer, 1981; Berner, 1966; Boucher et al., 1998; Burdige and Zimmerman, 2002; Burdige et al., 2008; Cyronak et al., 2013a; Cyronak et al., 2013b; Leclercq et al., 2002; Rao et al., 2012; Rude and Aller, 1991; Silverman et al., 2007; Walter et al., 1993; Walter and Burton, 1990; Yates and Halley, 2003; Yates and Halley, 2006a). These studies vary in their methods from pore water sampling (Aller, 1982; Berner, 1966; Burdige and Zimmerman, 2002; Burdige et al., 2008; Rao et al., 2012; Rude and Aller, 1991; Walter et al., 1993; Walter and Burton, 1990), sediment core incubations (Rude and Aller, 1991), and *in situ* benthic chambers (Boucher et al., 1998; Cyronak et al., 2013a; Cyronak et al., 2013b; Leclercq et al., 2002; Rao et al., 2012; Stoltenberg et al., 2019; Yates and Halley, 2003; Yates and Halley, 2006a). In addition, carbonate dissolution has also been characterized in experimental mesocosms or flumes (Anthony et al., 2013; Comeau et al., 2015; Lantz et al., 2019). These dissolution studies have demonstrated that dissolution is a significant process in shallow marine environments despite surface seawater Ω with respect to the commonly occurring mineral phases. However, the relative importance of various properties and processes on dissolution rates in the natural environment remain elusive.

Early studies on carbonate diagenesis

As previously stated, the earliest in situ studies on carbonate dissolution occurred in environments where the seawater was undersaturated with respect to carbonate minerals, such as on the seafloor or water column below the saturation horizon. However, early shallow

marine studies documented carbonate dissolution in terrigenous muds (Aller, 1982; McNichol et al., 1988; Reaves, 1986) and tropical carbonate sediments (Berner, 1966; Morse et al., 1985; Walter et al., 1993; Walter and Burton, 1990). Pore water undersaturation with respect to carbonate mineral phases in these environments were attributed to various processes including oxygenic organic matter oxidation (Berner, 1966; Morse et al., 1985) and the initial stages of microbial sulfate reduction (Morse and Mackenzie, 1990; Walter et al., 1993; Walter and Burton, 1990).

These early field studies of shallow marine carbonate dissolution were often motivated by attempts to understand early diagenesis in carbonate sediments (e.g., Berner, 1966; Hatcher et al., 1982; Lyons et al., 1979; Rosenfeld, 1979). Early diagenetic processes are of particular interest in carbonate sediments because many geochemical paleo-proxies rely on the underlying assumption that the chemical composition of marine carbonate sediments accurately preserve a record ancient open-ocean seawater chemistry and conditions (Higgins et al., 2018). However, this assumption is still widely debated because the extent to which the original geochemistry of the sediments is altered during diagenesis and subsequent lithification is not well understood (Higgins et al., 2018). For example, measured rates of recrystallization have been found to cause significant mineralogical and chemical changes on rapid timescales (Rude and Aller, 1991). Some researchers have suggested that due to these perceived rates of recrystallization, ancient shelf carbonates may record the geochemical signature of pore waters rather than the overlying water column (Walter et al., 1993). These early studies provided insight to the dissolution process itself because it is an integral component of early diagenesis and set the foundation for future research of shallow marine carbonate sediment dissolution.

Studies in the context of ocean acidification

The motivation for studying *in situ* carbonate dissolution has increased in recent decades because of increasing concerns associated with OA. Researchers have been particularly interested in the response of coral reefs, both on the organismal and the ecosystem scale (Andersson et al., 2015). Numerous studies have measured the organic carbon productivity and net calcification rates on reefs to determine overall ecosystem function and how OA may influence these processes (e.g., Albright et al., 2016; Albright et al., 2018; Boucher et al., 1998; Langdon et al., 2000; Shamberger et al., 2011; Silverman et al., 2007). From these studies, useful information has been derived on the rates of dissolution across various reef environments and benthic communities. Although many studies related to the effects of OA on coral reefs have reported net dissolution (or negative net community calcification) in shallow marine environments, the full breadth of these studies is beyond the scope of this review.

In order to understand how OA will impact coral reefs, the controls of dissolution must be considered alongside changes in reef biogeochemical processes on different spatial and temporal scales. Several studies set out to investigate what drives these changes and how these changes will influence the dissolution of reef structures and foundational sediments. We focus here on studies that investigate dissolution in carbonate sediments or substrates where the inclusion of actively calcifying organisms is as limited as possible (i.e., sediment-only mesocosms or flumes and in situ benthic measurements within sediments/bare substrates).

Mesocosm and flume studies

Mesocosms are a useful way to more closely mimic the natural environment, while still maintaining control over the manipulation of certain variables. Experimental mesocosm studies have tried to determine the contribution of various benthic organisms and communities to overall productivity and calcification in the natural environment. These types of experiments have historically yielded somewhat varying results in regards to the role of sediment dissolution.

Some mesocosm experiments with sand only-communities show that net community calcification, under certain conditions, decrease with decreasing Ω_{Ar} (Anthony et al., 2013; Comeau et al., 2015; Leclercq et al., 2002). Leclercq et al. (2002) found this relationship during the day, but no correlation with Ω_{Ar} existed at night, suggesting that nighttime dissolution was more likely a function of pore water conditions with elevated CO_2 and low Ω_{Ar} owing to bacterial respiration in the sediments with little influence from the overlying seawater. A study on the effects of warming showed a greater increase in dissolution during the day, which was attributed to increased metabolic activity under the warmer conditions (Lantz et al., 2019). Net sediment dissolution was also observed during the day by (Anthony et al., 2013) in sand-only communities exposed to high flow and acidified conditions. These communities showed stronger variation in net community calcification across different regimes of flow and acidification treatments compared to other experimental communities (Anthony et al., 2013). Sand communities that undergo net dissolution may contribute positive changes in Ω to overlying seawater, and partially counteract reductions in Ω by calcifiers. Depending on the extent of sand cover in an area, the residence time of water over the area, and the relative upstream–downstream arrangement of the various habitats, this

influence may be more or less pronounced (Anthony et al., 2013; Murillo et al., 2014). Page et al. (2016) found that seawater pH and Ω_{Ar} of a sand-only community were relatively static, which they attributed to the counteracting effects of net calcification and autotrophy during the day and net dissolution and heterotrophy during the night (Andersson and Gledhill, 2013).

Although the findings and rates from these experiments differ (Table 1.3), they demonstrate that carbonate dissolution may be more sensitive to changes in ocean conditions (such as OA, flow regime and/or warming) than calcification by benthic organisms (Andersson et al., 2009; Anthony et al., 2013; Comeau et al., 2015; Lantz et al., 2019). For example, in a mesocosm study by (Comeau et al., 2015), enhanced sediment dissolution under high pCO_2 conditions could account for 50% of the decrease observed in net community calcification, and in a study by Andersson et al. (2009), carbonate dissolution increased by more than 200% under elevated CO_2 conditions. Clearly, the role of sediment dissolution is important to consider when interpreting changes in net community calcification of mixed mesocosm communities.

In situ studies of carbonate dissolution in sediments and substrates

It is well established that dissolution occurs in shallow marine carbonate sediments, but the physical and chemical controls of dissolution in these environments or how they will change due to changing ocean conditions is still not fully understood. Several studies have directly attempted to not only constrain in situ dissolution rates, but to answer some of the fundamental questions regarding how various physical and chemical characteristics or processes influence dissolution in the natural environment (see Eyre et al., 2014 for a review).

Mineralogy

It has been hypothesized that metastable carbonate phases such as high Mg-calcite of variable Mg content are the first phases to dissolve because they are more soluble than both calcite and aragonite (see *Reaction rates and solubilities* above). Some field studies have demonstrated this preferential dissolution of high Mg-calcite in the natural environment (Andersson et al., 2007; Balzer and Wefer, 1981; Schmalz, 1967; Walter and Burton, 1990).

Berner (1966) found that the interstitial waters of fine-grained carbonate sediments were generally in equilibrium with low-Mg calcite in both south Florida and Bermuda. However, Morse (1985) suggested that this conclusion was the result of the carbonate system constants and activity coefficients (see *Surface area and grain size* above) used by Berner and that the interstitial waters were actually in equilibrium with high-Mg calcites.

Both Balzer and Wefer (1981) and Andersson et al. (2007) demonstrated significant dissolution in Harrington Sound, Bermuda, which exhibits large differences in environmental conditions and CO_2 content within the 25m depth profile of Devil's Hole due to seasonal stratification. Balzer and Wefer (1981) calculated a significant flux of TA from the sediment-water interface and upper sediments into the water column using bell jar incubations whereas Andersson et al. (2007) inferred dissolution from vertical TA gradients. Both studies showed that the conditions in the subthermocline layer of the sound favor Mg-calcite dissolution during the time of stratification. Andersson et al. (2007) also demonstrated based on calcium to TA ratios that the average dissolving mineral contained significant mol% $MgCO_3$.

Using a large portable and transparent incubation chamber deployed in different habitats on the Molokai reef flat, Yates and Halley (2003) found the highest rates of dissolution for coral rubble and sand substrates. They suggested that this may result from a

high content of high Mg-calcite in these substrates (Yates and Halley, 2003). Preferential dissolution of high-Mg calcite has also been observed in seagrass sediments (Burdige et al., 2010).

Advection and bioturbation

Physical processes such as advection, bioturbation and bioirrigation have been shown to influence dissolution in shallow marine carbonate sediments as inferred from benthic alkalinity fluxes (Aller, 1982; Cyronak et al., 2013a; Rao et al., 2012). For example, Cyronak et al. (2013a) found that pore water advection under high pCO_2 conditions could more than double dissolution rates measured under diffusive conditions. Advective flow has also been shown to increase the influence of organic processes (i.e., photosynthesis and respiration) in permeable carbonate sands (Cyronak et al., 2013a; Rao et al., 2012), which influences carbonate chemistry in sediment pore waters and in turn, dissolution.

Bioturbation and bioirrigation can also enhance pore water exchange and influence the chemistry of interstitial waters (Aller, 1982). These processes can introduce oxygen to otherwise anoxic sediment layers and stimulate aerobic respiration, which can generate carbonic acid and drive dissolution (Walter and Burton, 1990). Dissolution within the uppermost sediment layers of terrigenous muds has also been partly attributed to the oxidation of iron sulfide particles reworked by bioturbation (Aller, 1982).

Seagrasses

Much like bioturbation, it has been suggested that seagrasses can introduce oxygen (O_2) into otherwise anoxic sedimentary environments via transport through their roots and

rhizomes (Ku et al., 1999). Early shallow carbonate dissolution studies demonstrated that acid generation via aerobic respiration or oxidation of reduced iron and sulfur species in Fe-poor shallow carbonates could not account for the total amount of carbonate dissolution inferred from excess Ca^{2+} in pore waters (Ku et al., 1999; Walter et al., 1993; Walter and Burton, 1990). It has been suggested that O_2 transport from seagrasses could potentially account for this discrepancy and balance the carbonate dissolution budgets observed (Burdige and Zimmerman, 2002; Ku et al., 1999). In addition, sea grass productivity can be an important source of sediment organic matter, which produces carbonic acid when respired and drives dissolution (Hu and Burdige, 2007). The relative importance of belowground input by seagrasses to carbonate dissolution depends on both seagrass density and on how bottom water flow interacts with the seagrass canopy, however, rates of dissolution appear to increase linearly with increasing seagrass density (Burdige et al., 2010).

Environmental dissolution

The carbonate chemistry of the overlying water column has been shown to influence the rates of dissolution in shallow carbonate sediments, a process referred to as environmental dissolution (Eyre et al., 2014). A recent study even suggests that carbonate sediment dissolution is 10-fold more sensitive to these changes in overlying seawater chemistry than coral calcification (Eyre et al., 2018).

Rates of net calcification and dissolution on bare sand and coral rubble have been shown to linearly correlate with both $[CO_3^{2-}]$ and pCO_2 of overlying water (Yates and Halley, 2006a). A shift from net precipitating to net dissolving over diel cycles under elevated pCO_2 (~800 μatm) and advective conditions has also been observed (Cyronak et al., 2013a). Most

recently, a negative correlation between carbonate dissolution in reef sediments across five globally distributed sites and Ω_{Ar} of overlying seawater was reported and suggested that reef sediments could transition to net dissolution by the end of the century (Eyre et al., 2018).

Metabolic dissolution

Unlike in deeper sediments, light reaches the surface of shallow marine carbonates and allows for photosynthesis and respiration to occur on a diel cycle. Metabolic carbonate dissolution occurs when aerobic respiration generates CO_2 that drives dissolution in the sediment pore water or other microenvironments (Ku et al., 1999; Werner et al., 2008; Yates and Halley, 2006b). To the contrary, when organisms photosynthesis during the day, the consumption of CO_2 reduces the production of carbonic acid and associated net dissolution, potentially leading to net calcification (Cyronak et al., 2013b; Rao et al., 2012; Yates and Halley, 2006b). These biological processes, rather than the chemistry of the overlying water column have a stronger influence on carbonate dissolution in shallow marine environments (Cyronak et al., 2013b; Morse and Mackenzie, 1990; Tribble, 1990).

Although microbial metabolism is the primary driver of carbonate dissolution dynamics in shallow environments (Morse and Mackenzie, 1990), a combination of factors including the overlying water chemistry, the biological activity in sediment microenvironments, mineral composition and properties, and physical processes such as bioturbation and advection influence in situ dissolution rates. For example, Rao et al. (2012) found that under highly energetic conditions, increased pore water exchange reduced the efficiency of respiration-driven dissolution in carbonate sands. This observation was explained by the enhanced influx of supersaturated bottom water and/or loss of metabolic

acidity under increased pore water exchange. These changes can limit the effect of aerobic respiration and sulfide oxidation on lowering pore water saturation state and promoting carbonate dissolution (Rao et al., 2012).

It has also been hypothesized that metabolic and environmental dissolution act in tandem to enhance dissolution. The hypothesis is that if overlying seawater with a lower Ω_{Ar} value is advected into the sediments, less respiration need to occur to initiate dissolution, and more respiratory CO_2 will be available to drive additional dissolution (Andersson, 2015). Recent analyses of sediment incubation experiments from around the world support this hypothesis (Griffin et al., in prep.)

Comparison of biogenic carbonate dissolution rates from the field

Dissolution rates obtained from various studies of carbonate sediments in shallow tropical and subtropical marine environments fall within a consistent, albeit large, range considering the differences in environment, experimental approaches and sediment characteristics. Almost all the studies observed net dissolution occurring at night and many over 24-hour period. A comparison of many shallow carbonate mineral dissolution studies by Andersson et al. (2007), found that 80% of the data from existing field studies report rates in the range of 0.1 – 1.5 mmol $CaCO_3$ m^{-2} h^{-1}. Net shallow carbonate sediment dissolution rates (0.1 to 0.8 mmol $CaCO_3$ m^{-2} h^{-1}) in a later comparison of benthic chamber incubations by Eyre et al. (2014) also fell within this range. It is important to note, however, that some studies are cited in both references.

This range of in situ dissolution rates covers an order of magnitude difference in the measured rates. This broad range could be due to various factors including the natural or

experimental conditions under which these results were observed, environmental differences between habitats and/or large variations in the physical and chemical make-up of the sediments investigated. These differences between field locations and the complexity of the natural environment make it difficult to isolate the primary controls of dissolution in the field.

THE DISPARITY BETWEEN LABORATORY AND *IN SITU* STUDIES

Comparing *in situ* and laboratory dissolution rates

Significant disparities have been demonstrated between dissolution rates measured in the laboratory and those observed in the field in open ocean and deep-sea sediments (Morse et al., 2007). However, this has yet to be demonstrated in shallow carbonate environments.

Normalization (see *Surface area and grain size* above) of dissolution rates makes comparison between the laboratory and the field challenging. The units used in field studies represent a flux across a benthic boundary (unit of planar area) rather than the surface area of the sediments interacting with overlying or pore waters. This is mostly due to the fact that measuring or even closely estimating the latter is currently near impossible, because the amount of sediment contributing to dissolution is unknown. However, by making certain assumptions we have attempted to compare the ranges of laboratory and field reported in this review.

Assuming a density of aragonite (D_A) of 2830 kg m^{-3}, a porosity range of coral reef sediment (P_C) of 0.40 – 0.90 and that anywhere from the uppermost 0.01 – 0.5 m depth of sediment is responsible for dissolution (d_d), R_F, the observed range of field dissolution rates (0.1 to 1.5 mmol $CaCO_3$ m^{-2} h^{-1}), can be converted to μmol $CaCO_3$ g^{-1} h^{-1}, a common unit for laboratory dissolution rates, as follows:

$$R\ (\mu mol\ CaCO_3\ g^{-1}h^{-1}) = \frac{R_F(1 - P_C)}{D_A d_d} \qquad \text{Eq. (4)}$$

This simple calculation provides a rough estimate that allows for comparison between field and laboratory data. The lower limit for R, where $R_F = 0.1$, $P_C = 0.9$ and $d_d = 0.5$ m, is approximately 7×10^{-6} µmol $CaCO_3$ g^{-1} h^{-1} and the upper limit for R, where $R_F = 1.5$, $P_C = 0.45$ and $d_d = 0.01$ m, is approximately 3×10^{-2} µmol $CaCO_3$ g^{-1} h^{-1} (Table 1.4). These values are two to several orders of magnitudes lower than rates reported in the same units from laboratory measurements on bulk sediment which range from ~3 – 152 µmol g^{-1} hr^{-1} (Pickett and Andersson, 2015; Walter and Morse, 1985). Direct comparison of studies that use different methods of normalization (e.g., surface area versus weight) is much more daunting, but may be feasible. Table 1.4 shows a comparison of field rates converted via this method using reasonable assumptions for porosity and depth of dissolution in reef carbonate sediments.

The reason laboratory measurements are significantly higher than observed dissolution rates in the field has not been explicitly demonstrated, but has also been reported for dissolution rates of deep-sea sediments and carbonate substrates in the water column (Morse et al., 2007). One possible explanation could be that the solid:solution ratio is much higher in sediments than those in the laboratory (Table 1.2). For this reason, interstitial seawater that is in direct contact with the sediments may become buffered leading to lowered dissolution rates or even precipitation in some cases. This idea is supported by the fact that some rate equations determined from laboratory experiments drastically decrease when extrapolated closer to Ω =

1. These slower dissolution rates are closer to observed field rates (when converted as in Table 1.4) and may be occurring in buffered pore waters that are approaching saturation with respect to a given phase. However, for the rates to overlap based on our calculations in Table 1.4, the sediments would need to have relatively low porosity (40-50%) and the uppermost millimeters would be responsible for the majority of dissolution occurring. This suggests that although pore water buffering could partially explain the disparity between laboratory and field measurements, it is likely not the only factor in need of consideration.

Related to this, *in situ* flushing rates in sediments may differ drastically when compared to fluid exchange in laboratory experiments. For example, as discussed above, dissolution rates in suspended substrates using a vigorously stirred reactor resulted in significantly higher dissolution rates than in a settled, uniform layer (Kier, 1983). This is likely due to the ability for fluid to more readily and rapidly exchange with suspended sediments when compared to settled substrates, where fluid may or may not interact with sediments deeper in the settled layer. Seeing that advection can play an important role for in situ dissolution rates (see *Advection and bioturbation* above), the ability for surrounding seawater to exchange with mineral grains must be considered in both the laboratory and the field.

In general, field experiments often do not report physical and chemical characteristics of the sediments investigated. For this reason, it is nearly impossible to determine if rates in the laboratory and field differ due to differences in the physical and chemical characteristics. However, since few laboratory experiments have measured dissolution rates of bulk sediment samples of a fully representative grain size distribution, differences in substrates may be a significant source of the disparity observed between laboratory and field rates. In addition to

this, natural sediments clearly demonstrate different solubilities than prepared biogenic or abiotic carbonate substrates (see *Reaction rates and solubilities* above). One potential explanation for this difference is the presence of organic coatings which in inhibit direct interaction of the mineral surface with surrounding seawater, which are partially or fully removed during various preparation processes (Suess, 1968) Although the reason for these differences are not fully known, they could lead to significant differences between laboratory and field rates if laboratory substrates undergo additional preparation beyond sonication and drying (Plummer and Mackenzie, 1974; Yamamoto et al., 2012).

FUTURE DIRECTIONS

Although critical information can be drawn from both laboratory and field carbonate dissolution studies, it is still uncertain how various physical and chemical properties of biogenic carbonates and their surrounding environments influence dissolution in shallow marine settings. As in most complex natural environments, a myriad of biological, physical and chemical processes are interacting in various ways with numerous sediment properties. It is no small task to parse apart these interactions and how they will be influenced by changing ocean conditions, but the following suggestions may help design experiments that can better address these questions.

Laboratory experiments should aim to recreate the natural environment as much as possible. For example, using natural, minimally or unprepared sediments and natural seawater may yield more representative results (Yamamoto et al., 2012). Due to the difficulty of comparing even laboratory studies to one another due to normalization, the community should agree on the most appropriate units for reporting measured dissolution rates in both the lab

and the field moving forward. Knowing that physical processes such as advection can influence dissolution, studies could be conducted in reactors that more closely mimic the natural hydrodynamics in sediments, such as flow-through mesocosms, flumes or bed reactors. All experimental conditions and constants used in calculations should also be reported to insure comparisons can be made more readily in the future.

Mesocosm and in situ studies often do not report the physical and chemical data of the substrates investigated. The relevant physical and chemical properties of sediments or substrates, including mineralogy, grain size, origin (i.e. biogenic calcifier), and organic content, should be reported for all studies. In addition, knowing that various inhibitors influence dissolution, it may be pertinent to analyze overlying and/or pore waters for potential dissolved and particulate organic content and/or species of known inhibitors, such as phosphate.

Clearly, there is much work to be done to determine how various physical and chemical processes interact with differing properties of sediments to influence dissolution in the natural environment. This can be achieved through a combination of field and laboratory approaches if concerted efforts are made to make experimental conditions and reporting as comparable as possible. It is important to note that laboratory approaches that do not mimic the natural environment will still be necessary to answer more detailed, mechanistic questions regarding controls of carbonate dissolution. Regardless of approach, continued efforts to parse apart the true controls of dissolution in shallow marine systems will be critical to predicting how these important environments will fare in a rapidly changing ocean.

ACKNOWLEDGEMENTS

Chapter 1, in part, is currently being prepared for submission for publication of the material. Griffin, A. J.; Andersson, A. J.. The dissertation author was the primary investigator and author of this material.

FIGURES AND TABLES

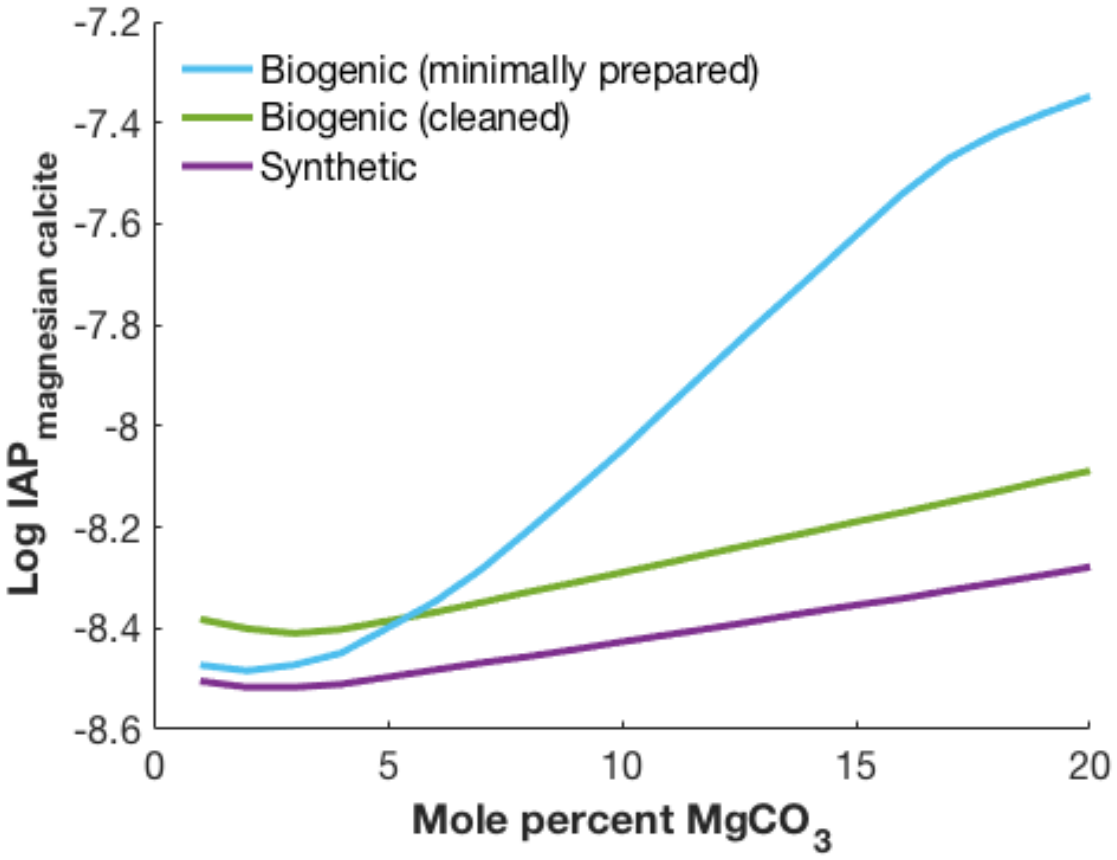

Figure 1.1: Mg-calcite solubility curves for synthetic pure phases (Bischoff et al., 1987; Busenberg and Plummer, 1989) biogenic (cleaned; Bischoff et al., 1987; Busenberg and Plummer, 1989; Walter and Morse, 1984a), and biogenic (minimally prepared; Plummer and Mackenzie, 1974).

Table 1.1: Summary of substrates, preparation steps and reactor types from laboratory studies.

Reference	Substrate				Solution	Reactor Type/Method (manipulation)
	Material	Grain Size (µm)	Surface Area ($m^2 g^{-1}$)	Preparation		
Morse and Berner, 1972	Atlantic deep-sea sediment (86% $CaCO_3$)	---	---	---	Filtered seawater	pH-stat (HCl addition)
Morse, 1978	Indian deep-sea sediment (98% $CaCO_3$)	Whole sediment	3.60	---	Deep Atlantic seawater	pH-stat (HCl addition)
		>62	0.877			
	Pacific deep-sea sediment (82% $CaCO_3$)	Whole sediment	---			
		125-500	---			
Kier, 1980	Foraminifera, *G. sacculifer*	700	3.44	Sonicated	Undersaturated artificial seawater	Suspended stirred-flow reactor
	Foraminifera, *B. bulloides*	250	2.67	Sonicated		
	Foraminifera, *G. pachyderma*	150	1.41	Sonicated		
	Coccolith, *E. huxleyi*	---	10.4	Untreated		
				2.5% NaOCl for 24 hours		
	Coccolith, *C. neohelis*	---	9.86	Rinsed with artificial seawater and ethanol		
	Rio Grande Rise sediment	125-250	1.70	---		
		"coarse" extract of <62				
	Pteropods	> 830	2.17	---		
		(% of Total Mass)				
	Ontong-Java Plateau Sediment	> 300 (26%)	---	---		
		125-300 (18.7%)				

Table 1.1, Continued

Kier, 1980 cont'd.	Ontong-Java Plateau Sediment	62-125 (15.0%) < 62 (39.5%) Bulk sediment	---	---	Undersaturated artificial seawater	Suspended stirred-flow reactor
		% $CaCO_3$	% Fragments	Benthic: Planktonic Formanifera		
Kier, 1983 (flux issues)	Top 6cm of sediment cores taken from the southern Brazil Basin	57	---	---	Bicarbonate-free artificial seawater	Not suspended stirred flow-through reactor ($NaHCO_3$)
		37	37	0.018		
		21	64	0.050		
		3	---	---		
		85	8	0		
		68	40	0.027		
		60	54	0.055		
		32	65	0.105		
		23	57	0.190		
		3	---	---		

		Median Grain Size	BET	Geo-metric			
Walter and Morse, 1984	Green algae, *Halimeda*	81	0.14	5.7	Crushed, sieved, ultrasonically clean in distilled water, soaked for 12 hrs in cold 30% H_2O_2, rinsed in distilled water, dried at 50°C, annealed at 170°C for 6 hrs	Filtered low-phosphate (<0.1 µm) Gulf stream seawater (diluted for consistent salinity)	Suspended stirred pH-stat (dilute HCl)
		153	---	---			
		215	---	---			
		275	0.14	12.4			
		513	0.09	20.5			
	Coral, *Fungia*	51	0.23	5.9			
		81	0.22	8.9			
		153	---	---			
		240	0.17	23.4			
		513	0.12	30.8			
	Echinoid, *Clypeaster*	81	2.04	82.6			
		153	---	---			
		215	2.10	225.8			
		275	---	---			

Table 1.1, Continued

Walter and Morse, 1985 cont'd.	Echinoid, *Clypeaster*	513	2.11	541.2		Filtered low-phosphate (<0.1 µm) Gulf stream seawater (diluted for consistent salinity)	pH-stat (dilute HCl)
	Barnacle, *Balanus*	37-125	0.19		Crushed and wet sieved, ultra-sonically cleaned, soaked overnight in 30% hydrogen peroxide, rinsed with distilled water, dried at 50°C, annealed at 170°C for 6 hrs (A) or unannealed (U)		
					A		
					U		
	Coral, *Fungia*		0.22		A		
					U		
	Coral, *Acropora*		0.48		A		
	Green algae, *Halimeda*		2.04		A		
					U		
	Gastropod, *Strombus*		0.20		A		
					U		
	Pelecypod, *Hippopus*		0.19		A		
					U		
	Echinoid, *Echinus*		---		A		
	Echinoid, *Clypeaster*		0.14		A		
					U		
	Echinoid, *Tripneustes*		0.15		A		
	Foraminifera, *Peneroplis*		2.50		A		
	Red algae, *Goniolithon*		24.00		A		
	Red algae, *Neogoniolithon*		16.50		A		
	Beach carbonate sand	180-300	---		Wet sieved, one split treated with 30% H_2O_2, other split left untreated, all dried at 50°C		
	Subtidal carbonate sand	125-180	---				
	Reefal carbonate sand						
Gehlen et al. 2005	Sediment cores from Sierra Leone Rise and Cape Verde Plateau in the eastern equatorial Atlantic	>150	---		Wet-sieved, sonicated, rinsed with distilled water, oven-dried	Artificial seawater	Suspended free-drift (N_2-CO_2 gas mixture)
Tsurushima et al., 2008	Foraminifera, *G. sacculifer*, from subtropical N. Pacific deep sea sediments	125-250; 425-500	---		Sieved; Broken then sieved for smaller grain size	Filtered surface sea water	Lined batch reactor with circulating seawater and five in-line cells (CO_2)

Table 1.1, Continued

Waldbussler et al., 2011 cont'd.	Oyster, *Crassostrea virginica*	Full shells; Approx. 10 cm	---	**Fresh:** Shucked, meat removed, used within 24 hrs **Weathered:** Shucked, placed on sandy beach for 2 yrs **Dredged:** Sifted from dredge spoils, 3,000 to several hundred yrs. old	Patuxent River water from mesohaline tributary of Chesapeake Bay Patuxent River water from mesohaline tributary of Chesapeake Bay	Flow-through, feedback-control (CO_2)
Yamamoto et al., 2012	Bulk Sediment	1-2 mm	---	Sonicated and dried at 40ºC for about 12 h	Filtered, UV-sterilized seawater	Flow-through reactor (CO_2 gas)
	Coralline Algae	---				
	Foraminifera	---				
	Coral	---				
Pickett and Andersssson, 2014	Benthic forminifera	850-1000	0.25	Soaked in bleach for 12h, crushed and ground using ethanol (mixed sediment not crushed), wet sieved, sonicated in ethanol, dried at 60°C for 12h	Filtered, UV-sterilized seawater	Not suspended, stirred batch reactor (N_2- CO_2 gas mixture);
	Goose barnacle		1.90			
	Sea urchin		0.15			
	Bryozoan		0.59			
	Coralline algae		0.69			
	Coralline algae (Porolithon)		2.70			
	Mixed sediment		0.50			
Ries, 2016	*Mytilus edulis* (blue mussel)	Whole-shell samples	---	Euthanized in 95% ethanol, gently cleaned of living tissue, rinsed in 95% ethanol to remove salts, and air-dried for 14 days	*Instant Ocean Sea Salt* mixed with deionized water and sterilized with addition of $HgCl_2$	Flow through aquaria (CO_2 mixed with compressed air)
	Crassostrea virginica (oyster)					
	Balanus eburneus (ivory barnacle)					
	Schizoporella errata (branching bryozoan)					
	Strombus alatus (conch)					
	Neogoniolithon sp. (red algae)					

Table 1.1, Continued

Ries, 2016 cont'd.	*Mercenaria mercenaria* (hard clam)	Whole-shell samples	---	Euthanized in 95% ethanol, gently cleaned of living tissue, rinsed in 95% ethanol to remove salts, and air-dried for 14 days	*Instant Ocean Sea Salt* mixed with deionized water and sterilized with addition of $HgCl_2$	Flow through aquaria (CO_2 mixed with compressed air)
	Mya arenaria (soft clam)					
	Oculina arbuscula (temperate coral)					
	Siderastrea siderea (tropical coral)					
Subhas et al., 2018	Soft coral, *Rhythismia fulvum*	mixed	0.69	Bleached: treated with unbuffered 2% sodium hypochlorite to remove organic matter; Unbleached: no treatment	Filtered, UV-sterilized, undersaturated natural seawater, poisoned with $HgCl_2$	Batch reactor bags, continuously shaken to suspend grains (0.1N HCl)
	E. huxleyi, bleached	mixed	10.4			
	E. huxleyi, unbleached	mixed	10.4			
	Planktic Foraminifera	mixed	4.3			
	Benthic Foraminifera	710-1000	0.11			
		300-500	---			
		125-300	---			

Table 1.2: Summary of experimental conditions and rates from laboratory studies

Reference	Substrate		Conditions							Rate
	Material	Grain Size	T (°C)	S	Dura-tion	Soln: Solid	$\Omega_{mineral}$	pH (Scale)	pCO_2	
Morse and Berner, 1972	Atlantic deep-sea sediment (86% $CaCO_3$)	---	25	30‰	---	300 mL: 400 mg	---	---	$10^{-3.5}$ atm	$10^{3.1}(1-\Omega)^{4.5}$ (% d^{-1})
Morse, 1978	Indian deep-sea sediment (98% $CaCO_3$)	Whole sediment	25	34.6‰	---	300 mL: 1-5g	0.62-0.91	7.32-7.405	$10^{-2.35}$ atm	$10^{4.3}(1-\Omega)^{5.2}$ (% d^{-1})
		>62					0.54-0.74	7.29-7.36		~3% of whole sediment
	Pacific deep-sea sediment (82% $CaCO_3$)	Whole sediment					0.54-0.85	7.29-7.39		$10^{2.7}(1-\Omega)^{3.0}$ (% d^{-1})
		125-500					0.43-0.62	7.24-7.32		~1.5x rates reported in Berger (1967)
Kier, 1980							Ω_c			
	Foraminifera, *G. sacculifer*	700	20	18.60 – 19.08 (Chlo-rinity ‰)	---	---	0.481-0.557	---	---	$31.4(1-\Omega)^{4.5}$ (% d^{-1})
	Foraminifera, *G. bulloides*	250					0.521-0.699			$70.4(1-\Omega)^{4.5}$ (% d^{-1})
	Foraminifera, *G. pachyderma*	150					0.513-0.649			$72.7(1-\Omega)^{4.5}$ (% d^{-1})
	Coccolith, *E. huxleyi* (untreated)	---					0.587-0.733			$330(1-\Omega)^{4.5}$ (% d^{-1})
	Coccolith, *E. huxleyi* (bleached)	---					0.539-0.730			$753(1-\Omega)^{4.5}$ (% d^{-1})
	Coccolith, *C. neohelis*	---					0.569-0.681			$293(1-\Omega)^{4.5}$ (% d^{-1})

Table 1.2., Continued

Kier, 1980 cont'd.	Rio Grande Rise sediment	125-250	20	18.60 – 19.08 (Chlo-rinity ‰)	---	---	0.626-0.690		---	---	$549(1-\Omega)^{4.5}$ ($\%\ d^{-1}$)
		"coarse" extract of <62					0.542-0.728				$151(1-\Omega)^{4.5}$ ($\%\ d^{-1}$)
							Ω_a				
	Pteropods	>830					0.582-0.740				$318(1-\Omega)^{4.2}$ ($\%\ d^{-1}$)
	Ontong-Java Plateau Sediment	Grain Size (% of Total Mass)					Ω_c	Ω_a			Calcite: $R\%=k_c\%(1-\Omega)^{4.5}$ Aragonite: $R\%=k_a\%(1-\Omega)^{4.2}$
											k_c / k_a
		>300 (26%)					0.549 - 0.766	0.320 - 0.447			58.1 / 4.5
		125-300 (18.7%)					0.581 - 0.818	0.338 - 0.477			87.2 / 14.0
		62-125 (15.0%)					0.689 - 0.900	0.401 - 0.524			375 / 13.7
		<62 (39.5%)					0.739 - 0.980	0.430 - 0.571			2780 / 70.5
		Bulk sediment					0.721 - 0.876	0.420 - 0.510			2990 / 41.1

Table 1.2, Continued

		%$CaCO_3$				$S_{0c} = 1-\Omega_c$			$\gamma\left\|f_c\left(CO_3^{2-}\right)k_c \ldots + f_a\left(CO_3^{2-}\right)k_a\right\|^{1/2}$	
									k_c (d^{-1})	k_a (d^{-1})
Kier, 1983	Top 6cm of sediment cores taken from the southern Brazil Basin	57	20 (±1)	18.86-19.13 (Chlo-rinity x 10^3)	2-3 d	---	0.032 -0.566	Day 1: 7.2 Day 2-3: 7.7	---	0.093
		37					0.313-0.688		0.162	0.015
		21					0.361-0.726		0.082	0.008
		3					0.550-0.712		0.002	0
		85					0.244-0.858		0.164	0.006
		68					0.295-0.576		0.252	0.014
		60					0.265-0.457		0.232	0.018
		32					0.300-0.646		0.034	0.011
		23					0.329-0.617		0.295	0.006
		3					0.517-0.617		0.0004	0
									$R=k(1-\Omega)^n$, where n≈3	
						$\sim\Omega_A$			k (µmol g^{-1} h^{-1})	
Walter and Morse, 1984	Green algae, *Halimeda*	81	25 (±0.05)	35‰	Up to 6 h	---	0.17-0.67	---	$10^{-2.5}$ atm	1,288
		153					0.17-0.56			741
		215					0.19			426
		275					0.19			389
		513					0.20-0.36			229
						$\sim\Omega_A$				
	Coral, *Fungia*	51					0.21			871
		81					0.13-0.68			537
		153					0.15-0.55			288
		240					0.13-0.44			177
		513					0.09-0.29			83
						$\sim\Omega_{12\%MgCO3}$				
	Echinoid, *Clypeaster*	81					0.15-0.61			224
		153					0.17-052			145
		215					0.045			120
		275					0.045			79
		513					0.045			48

Table 1.2, Continued

		GS	P								$R=k(1-\Omega)^n$ ($\mu mol\ g^{-1}\ h^{-1}$)	
											n	log k
Walter and Morse, 1985	Barnacle, *Balanus*	37-125	A	25 (±0.05)	35‰	1.5-5 h	0.03-6.0 g/L	0.05-0.80	---	$10^{-2.5}$ atm	2.74	2.66
			U								1.82 x annealed	
	Coral, *Fungia*		A								2.45	2.73
			U								1.28 x annealed	
	Coral, *Acropora*		A								2.50	2.67
	Green algae, *Halimeda*		A								2.43	3.10
			U								1.26 x annealed	
	Gastropod, *Strombus*		A								2.54	3.00
			U								1.06 x annealed	
	Pelecypod, *Hippopus*		A								2.50	2.96
			U								1.82 x annealed	
	Echinoid, *Echinus*	37-125	A								---	---
	Echinoid, *Clypeaster*		A								3.30	2.32
			U								1.20 x annealed	
	Echinoid, *Tripneustes*		A								---	---
	Foraminifera, *Peneroplis*		A								3.51	2.82
	Red algae, *Goniolithon*		A								3.20	2.73
	Red algae, *Neo-goniolithon*		A								---	---
											Rate ($\mu mol\ g^{-1}\ h^{-1}$)	
	Beach carbonate sand	180-300									39.3491	
											20.3226	
											10.5293	

Table 1.2, Continued

Walter and Morse, 1985 cont'd.	Subtidal carbonate sand	125-180	25 (±0.05)	35‰	1.5-5 h	0.03-6.0 g/L	0.05-0.80	---	$10^{-2.5}$ atm	152.3575
										73.0781
										32.6878
	Reefal carbonate sand									128.3202
										58.2594
										30.8235
Gehlen et al. 2005	Sediment cores from Sierra Leone Rise and Cape Verde Plateau in the eastern equatorial Atlantic	>150	20	32.66 (±0.82)	50 h	1-100	---	~7.05 – 7.35	~3100 ppm	$\log R_S = n \log (1-\Omega) + \log k_S$; where n = 1.4 – 2.8, k_S = 0.9 – 0.48
Tsurushima et al., 2008	Foraminifera, *G. sacculifer*,	125-250	9-9.6	---	10 d	5L:20 mg	---	---	1,000-15,000 ppm	$R = 24(1-\Omega)^{2.6}$ (% d^{-1}); Normalized to weight of sample
Waldbussler et al., 2011	Oyster, *Crassostrea virginica*	Full shells; Approx. 10 cm	27.28 (±0.48)	13-14 psu	2 wk	20L:15 shells Flow rate: 5.7L/h	2.17 = control; 1.33 = high; 0.73 = mid; 0.47 = low	Control 7.90; high 7.67; mid 7.38; low 7.17 (NBS)	---	Dredged: -0.005 to -0.097 (% d^{-1}) Weathered: -0.0519 to -0.1525 (% d^{-1}) Fresh: -.0911 to -0.1828 (% d^{-1})
Yamamoto et al., 2012							Ω_a		ppm	R (% h^{-1})
	Bulk Sediment	1-2 mm	26	---	~3-14 h	310:1	1.2-3.5	---	420-2030	$R=-0.0015 \times \Omega_a + 0.0056$
	Coralline Algae	---					1.2-2.9		570-2000	$R=-0.0045 \times \Omega_a + 0.0143$

Table 1.2, continued

Yamamoto et al., 2012, cont'd.	Foraminifera	---	26	---	~3-14 h	310:1	1.1-3.2	---	510-2210	$R=-0.0027 \times \Omega_a + 0.0081$
	Coral	---					1.1-1.9		1070-2100	---
Pickett and Andersson, 2014	Benthic forminifera	850-1000	25 (±1)	33.64 (± 0.07)	2 h	1.5 g: 245 g	---	6.95-7.24	~3053-5560 µatm	4.956 - 8.564 umol g^{-1} h^{-1}
	Goose barnacle									2.465 - 4.575 umol g^{-1} h^{-1}
	Sea urchin									3.664 - 6.510 umol g^{-1} h^{-1}
	Bryozoan									7.085 - 11.860 umol g^{-1} hr^{1}
	Coralline algae									11.613 - 18.655 umol g^{-1} h^{-1}
	Coralline algae (Porolithon)									6.907 - 8.913 umol g^{-1} h^{-1}
	Mixed sediment									2.974 - 4.836 umol g^{-1} h^{-1}
Ries, 2016							Ω_a			Average dissolution rate (% d^{-1})
										10°C / 25°C
	Mytilus edulis (blue mussel)	Whole-shell samples	10.0 (±0.2)-25.0 (±0.2)	32.0 (±0.1)	47 d	---	0.2 – 5.0	6.96-8.08	497, 535, 4144, 4870, 5841, 9212	-0.0279 / -0.0492
	Crassostrea virginica (oyster)									-0.0461 / -0.0690
	Balanus eburneus (ivory barnacle)									-0.0456 / -0.0673

Table 1.2, Continued

Ries, 2016 cont'd.	*Crassostrea virginica* (oyster)	Whole-shell samples	10.0 (±0.2)-25.0 (±0.2)	32.0 (±0.1)	47 d	---	0.2 – 5.0	6.96-8.08	497, 535, 4144, 4870, 5841, 9212	-0.0461	-0.0690
	Balanus eburneus (ivory barnacle)									-0.0456	-0.0673
	Schizoporella errata (branching bryozoan)									-0.1023	-0.1631
	Strombus alatus (conch)									-0.0422	-0.0649
	Neo-goniolithon (red algae)									-0.0754	-0.1228
	Mercenaria mercenaria (hard clam)									-0.0388	-0.0611
	Mya arenaria (soft clam)									-0.0538	-0.0867
	Oculina arbuscula (temperate coral)									-0.0949	-0.1209
	Siderastrea siderea (tropical coral)									-0.0746	-0.0987

Table 1.2, Continued

										$R=k(1-\Omega)^n$ k_{mass} ($g\ g^{-1}\ d^{-1}$) k_{SA} ($g\ cm^{-2}\ d^{-1}$)			
										n		-log k_{mass} -log k_{SA}	
										$\Omega<$ 0.85	$\Omega>$ 0.85	$\Omega<$ 0.85	$\Omega>$ 0.85
Subhas et al., 2018	Soft coral, *Rhythismia fulvum*	mixed	20-22	33.2-33.6	1-10 d	300g: 1-5mg	0.2-0.99	---	---	1.7	---	0.99	---
												4.83	---
	E. huxleyi, bleached	mixed								1.7	---	0.35	---
												5.0	---
	E. huxleyi, unbleached	mixed								1.8	0.19	1.1	2.7
												4.1	5.6
	Planktic Foraminifera	mixed								1.8	---	1.2	---
												n/a	---
	Benthic Foraminifera	710-1000								1.8	---	1.8	---
												4.3	---
		300-500								2.3	0.33	0.31	0.33
												5.44	1.8
		125-300								2.1	---	0.3	---
												5.5	---

Table 1.3: Summary of substrates, conditions and rates from *in situ* and mesocosm studies

Reference	Location	Environment	Method	Substrate			Conditions				Rate (mmol m^{-2} h^{-1})
				Sediment Type	Grain Size	Depth (m)	T (°C)	S	pH (Scale)	pCO_2 (µatm)	
Balzer and Wefer, 1981	Devil's Hole, Bermuda	Tidal Sounds	Saturometry technique with dive operated bell jars and in situ pore water sampling	Aragonite from ground coral *Porites porites*; Ground Atlantic oyster *Ostrea edulis*	<63 um	1-24	23.0-28.2	36.04 - 36.24	7.741-8.219	---	0.3
Aller, 1982	Long Island Sound, U.S.A	Tidal Channel	Coring, pore water profiles	Terrigenous muds; ~2 – 25% carbonate	Silt-clay	8, 15, 34	2-22	24-28‰	---	---	~0.01-0.08
Barnes and Devereux, 1984	Great Barrier Reef	Reef Flat	pH and oxygen electrodes	---	---	---	27.87-28.82	---	---	---	4
Walter and Burton, 1990	Florida Bay	Cores collected from various zones: Mudbank, Offbank, Island flank, Coralalgal, Mangrove, Inner grass, Outer grass	Sediment core incubations; In-situ substrate samples	See ref Fig. 2	See ref Fig. 2	0.5-4	20-32	---	---	---	0.4-0.8

Table 1.3, Continued

Rude and Aller, 1991	Bob Allen Key Bank, Florida Bay, USA	Carbonate mud bank	Pore water sampling, Sediment core incubation	Biogenic aragonite and calcite	---	0.5-1	29-30	---	6.78-7.55 (core); 8.29-8.48 (water)	---	~0.25-0.3 (based on mass balance model)
Walter et al., 1993	South Florida and Bahamas	Carbonate platform	Pore water via centrifugation of boxcores	Aragonite (60%), HMC (40%), minor low-Mg calcite	---	<4	---	---	---	---	0.2-0.4
Conand et al., 1997	Reunion Island	Back Reef Zone	Water samples	---	---	< 1.35	---	---	---	---	7
Boucher et al., 1998	Moorea	Tiahura barrier reef	Incubation chambers; alkalinity anomaly technique	---	Fine to med. Sand	0-3	---	---	---	---	0.5-0.9
Burdige and Zimmerman, 2002	Lee Stocking Island, Exuma Islands, Bahamas	oolitic sands, sea grass meadows, grapestone deposits, bioturbated sediments with extensive shrimp mounds	Pore water samples (20 cm max depth)	Aragonite (80%) and HMC (20%). Biogenic skeletal debris (mollusks, coral, red and green algae, calcareous sponges, and foraminifera), ooids, peloids, and grapestones	~200-800 μm	2-20	---	---	~7.4-8.25	---	0.04 (dense grasses), 0.008 (sparse grasses), 0.0004 (no grasses)
Leclercq et al., 2002	Monaco	Sand community	Open top mesocosm	---	---	---	25.6-26	38	7.919-7.995	393-641	0.8

Table 1.3, Continued

Yates and Halley, 2003	Molokai, HI and Biscayne National Park, FL, USA	Sand bottom substrates on reef flats	SHARQ incubation chamber	High content of HMC in Molokai carbonate sand (40%) relative to Biscayne Bay carbonate sand (24%)	---	1.2-2 (HI); 3-10 (FL)	24.0-28.1 (HI); 27.3-30.2 (FL)	33.2-35.6 (HI); 33.6-35.4 (FL)	---	---	Night-time dissolu-tion: ~0.3 (both HI and FL)
Yates and Halley, 2006	Molokai reef flat, HI, USA	Sand bottom on reef flat	SHARQ incubation chamber	40% HMC with a mol% of $MgCO_3$ 20-24%	Med to coarse sand	1-2	23.6-29.3	33.7-34.3	7.84-8.12 (free)	429-802	0.05-0.6
Andersson et al., 2007	Devil's Hole, Bermuda	Tidal Sound	Alkalinity anomaly, Ca^{2+} measure-ments	Aragonite (65 wt%); calcite and LMC (<8 mol% $MgCO_3$, 26 wt%); HMC (>8 mol% $MgCO_3$, 9 wt%)	---	24	29-30 (de-crease of 5-6 below thermo-cline	~36.4-36.9	Upper layer >8; ~7.5 to 7.7 at 23m depth	380-2000	0.2-0.8
Silverman et al., 2007	Nature Reserve Reef in the northern Gulf of Eilat (Aqaba), Northern Red Sea	High-latitude fringing reef	Water sampling; alkalinity anomaly	---	---	1.5-1.8	27.8-20.8	40.47-40.88	8.175-8.269	---	0.08-1.42
Burdige et al, 2008	Bahamas Bank	Sandy sea grass bed	Pore water samples (20 cm max	Aragonite (70–90 wt%) and HMC (10–30	~200-800 μm	~2-10	---	---	~6.9-7.6 (typical	---	0.01-10.75 (depth-

Table 1.3 Continued

Burdige et al, 2008, cont'd.	Bahamas Bank	Sandy sea grass bed	depth)	wt%) with a mol% $MgCO_3$ of 11–13%; small amount of LMC (~ 3 wt%) Sediment porosities range from , 50% to 80%	~200-800 µm	~2-10	---	---	pore water profile	---	inte-grated rates based on pore water calculations)
Burdige et al., 2010	Great Bahamas Bank	fine-grained and pellet muds; coarse-grained oolitic	Pore water samples (20 cm max depth)	Aragonite (~80-90%) and HMC (~10-20%), with a with a mol% $MgCO_3$ of ~12%	~238-1319 µm	4-10	---	---	~7.4-8.13	---	0.0008-3.35
Burdige et al., 2010 cont'd.		carbonate sands, grape-stones; seagrass beds									
Rao et al., 2012	Heron Reef, Australia	Lagoonal platform reef system	In situ benthic flux chambers; planar optodes, microsensors, sediment cores, pore water samples	Coarse Site / Fine Site Aragonite (wt%) 70 ± 3 / 74 ± 3 LMC (<4 mol % Mg, wt %) 3.7 / 3.9	Coarse Site 897±53 µm; Fine Site 590± 35 µm	0.2-2	22-30	35.24-35.87	7.68-8.44	---	0.5-1.1

Table 1.3, Continued

Rao et al., 2012, cont'd.	Heron Reef, Australia	Lagoonal platform reef system	In situ benthic flux chambers; planar optodes, microsensors, sediment cores, pore water	HMC (>4 mol % Mg, wt %)		Coarse Site 897±53 µm; Fine Site 590± 35 µm	0.2-2	22-30	35.24 - 35.87	7.68-8.44	---	0.5-1.1
				26 ± 3	22 ± 3							
Anthony et al., 2013	Heron Reef, Great Barrier Reef, Australia	Lagoonal Reef System	Laboratory flume experiments	---		0.5 -2 mm	0.1	26-27	---	---	Ambient (350-450); Acidified (560-700)	2.6-5.7
Cyronak et al., 2013a	Heron Island, Australia	Coral cay; High permeability and porosity sands, free from macro-phytes and macrofauna burrows	In situ, advective chamber incubations	Aragonite (65%) and HMC (32%) with with a mol% $MgCO_3$ of 15.2%		---	1.7	---	---	7.94-8.18	**Control:** 418 ±48 (diffusive) 427 ±20 (advective) **High pCO_2 treatment:** 803 ±98 (diffusive) 839 ±90 (advective)	0.5 (advective) 0.2 (diffusive)
Cyronak et al., 2013b	Heron Island, Australia	Coral cay/Sand patch	In situ, advective chamber incubations	1% quartz, 33.1% calcite, and 65.4% aragonite; calcite fraction		Med. To very coarse sand	1.7	---	---	~7.8-8.4	---	2.1-3.7

Table 1.3, Continued

Cyronak et al., 2013b	Heron Island, Australia	Coral cay/Sand patch	In situ, advective chamber incubations	was composed of 2% LMC (2.3 ± 1 mol% $MgCO_3$) and 98% HMC (15.2 ± 1 mol% $MgCO_3$); low in organic carbon content (0.24%)		Med. To very coarse sand	1.7	---	---	~7.8-8.4	---	2.1-3.7
Cyronak and Eyre, 2016										Ω_a		
	Heron Island, Australia	Reef flat	In situ, advective chamber incubations under ambient, low light, high CO_2, and low light + high CO_2 conditions	aragonite (65%); HMC (33%) with a mol% $MgCO_3$ of 15.2%		0.83 mm	0.2-2.2	21.0-24.3	34.3-34.5	3.0±0.1	457±13	−1.38±0.1
										2.4±0.2	632±70	0.38±0.18
										2.0±0.1	949±111	0.28±0.06
										1.5±0.1	1239±118	0.65±0.18
Eyre et al., 2018				Ara-gonite	HMC	mm				Ω_a		
	Bermuda	Seagrass bed; Patch reef	In situ, advective chamber incubations	61.5-75.5	21.4-33.5	0.37	1.0	---	---	2.23-3.89	---	-21.06-32.39
						0.69	3.0					
	Cook Islands	---		42.7	55.7	0.18	3.0			2.60-3.80		-4.51-4.98
	Heron Island	Reefal lagoon		65.4	32.6	0.83	1.0			1.65-3.45		-9.92-13.64

Table 1.3, Continued

Eyre et al., 2018, cont'd.	Hawaii, USA	Reefal lagoon		56.5	42.2	0.28	0.5			1.34-2.37		2.67-18.53
	Tetiaroa, Tahiti	Reef Flat: Reefal lagoon		60.0	38.8	0.03	7.5			2.46-4.07		-17.26-6.12
				51.3	48.2	0.16	3.5					
				71.9	26.3	0.41	1.0					
Lantz et al., 2019	Mo'orea, French Poly-nesia	Simulated back reef	Laboratory flume experiments under control and warmed conditions	---		See ref. Table 5	---	27.4 ±0.7	35.7 ±0.1	---	---	0.06 ± 0.2
								27.5 ±1.0	35.8 ±0.1			
								30.5 ±0.8	35.8 ±0.1			-1.11 ± 0.5
								30.3 ±0.7	35.7 ±0.1			
Stoltenberg et al., 2019										Ω_a		
	Heron Island, Australia	Reef flat	In situ, advective chamber incubations conducted seasonally	Aragonite (50.6±0.2%); HMC (46.2%±0.2%) with a mol% $MgCO_3$ of 16.4%±0.5%		---	0.3-2.5	24.4 ±1.6	---	4.88 ±0.34	---	average: 0.11±0.2
								26.1 ±0.7		4.22 ±0.28		
								25.8 ±1.2		4.66 ±0.04		
								21.3 ±0.7		4.71 ±0.05		
								22.8		4.44 ±0.31		

Table 1.4: Comparison of field rates for a given depth and porosity over the range of observedfield dissolution rates (nmol/ $CaCO_3$ g^{-1} h^{-1}) in carbonate sediments.

		Porosity Range (%)					
		40	**50**	**60**	**70**	**80**	**90**
Depth (m)	**0.01**	2 – 30	2 – 30	1 – 20	1 – 20	0.7 – 10	0.4 – 5
	0.05	0.4 – 6	0.4 – 5	0.3 – 4	0.2 – 3	0.1 – 2	0.07 – 1
	0.1	0.2 – 3	0.2 – 3	0.1 – 2	0.1 – 2	0.07 – 1	0.04 – 0.5
	0.2	0.1 – 2	0.09 – 1	0.07 – 1	0.05 – 0.8	0.04 – 0.5	0.02 – 0.3
	0.5	0.04 – 0.6	0.04 – 0.5	0.03 – 0.4	0.02 – 0.3	0.01 – 0.2	0.007 – 0.1

REFERENCES

Albright, R., Caldeira, L., Hosfelt, J., Kwiatkowski, L., Maclaren, J.K., Mason, B.B., Nebuchina, Y., Ninokawa, A., Pongratz, J., Ricke, K.L., Rivlin, T., Schneider, K., Sesboüé, M., Shamberger, K., Silverman, J., Wolfe, K., Zhu, K. and Caldeira, K. (2016) Reversal of ocean acidification enhances net coral reef calcification. Nature 531, 1-4.

Albright, R., Takeshita, Y., Koweek, D.A., Ninokawa, A., Wolfe, K., Rivlin, T., Nebuchina, Y., Young, J. and Caldeira, K. (2018) Carbon dioxide addition to coral reef waters suppresses net community calcification. Nature 555, 516-519.

Aller, R.C. (1982) Carbonate dissolution nearshore terrigenous muds; the role of physical and biological reworking. Journal of Geology 90, 79-95.

Andersson, A.J. (2015) A fundamental paradigm for coral reef carbonate sediment dissolution. Frontiers in Marine Science 2.

Andersson, A.J., Bates, N.R., Jeffries, M.A., Freeman, K., Davidson, C., Stringer, S., Betzler, E. and Mackenzie, F.T. (2013) Clues from current high CO_2 environments on the effects of ocean acidification on $CaCO_3$ preservation. Aquatic geochemistry 19, 353-369.

Andersson, A.J., Bates, N.R. and Mackenzie, F.T. (2007) Dissolution of Carbonate Sediments Under Rising pCO_2 and Ocean Acidification: Observations from Devil's Hole, Bermuda. Aquatic Geochemistry 13, 237-264.

Andersson, A.J. and Gledhill, D. (2013) Ocean acidification and coral reefs: effects on breakdown, dissolution, and net ecosystem calcification. Annual Review of Marine Science 5, 321-348.

Andersson, A.J., Kline, D.I., Edmunds, P.J., Archer, S.D., Bednaršek, N., Carpenter, R.C., Chadsey, M., Goldstein, P., Grottoli, A.G. and Hurst, T.P. (2015) Understanding ocean acidification impacts on organismal to ecological scales. Oceanography 28, 16-27.

Andersson, A.J., Kuffner, I.B., Mackenzie, F.T., Jokiel, P.L., Rodgers, K.S. and Tan, A. (2009) Net Loss of $CaCO_3$ from a subtropical calcifying community due to seawater acidification; mesocosm-scale experimental evidence. Biogeosciences 6, 1811-1823.

Andersson, A.J., MacKenzie, F.T. and Lerman, A. (2005) Coastal ocean and carbonate systems in the high CO_2 world of the Anthropocene. American Journal of Science 305, 875-918.

Andersson, A.J., Mackenzie, F.T. and Ver, L.M. (2003) Solution of shallow-water carbonates: An insignificant buffer against rising atmospheric CO_2. Abstracts with Programs - Geological Society of America 35, 507.

Anthony, K.R.N., Diaz-Pulido, G., Verlinden, N., Tilbrook, B. and Andersson, A.J. (2013) Benthic buffers and boosters of ocean acidification on coral reefs. Biogeosciences 10, 4897-4909.

Archer, D., Emerson, S. and Reimers, C. (1989) Dissolution of calcite in deep-sea sediments: pH and O_2 microelectrode results. Geochimica et Cosmochimica Acta 53, 2831-2845.

Archer, D. and Maier-Reimer, E. (1994) Effect of deep-sea sedimentary calcite preservation on atmospheric CO_2 concentration. Nature 367, 260.

Balzer, W. and Wefer, G. (1981) Dissolution of carbonate minerals in a subtropical shallow marine environment. Marine Chemistry 10, 545-558.

Bates, N.R. (2001) Interannual variability of oceanic CO_2 and biogeochemical properties in the Western North Atlantic subtropical gyre. Deep Sea Research Part II: Topical Studies in Oceanography 48, 1507-1528.

Bates, N.R., Astor, Y.M., Church, M.J., Currie, K., Dore, J.E., Gonzalez-Davila, M., Lorenzoni, L., Muller-Karger, F., Olafsson, J. and Santana-Casiano, J.M. (2014) A Time-Series View of Changing Surface Ocean Chemistry Due to Ocean Uptake of Anthropogenic CO_2 and Ocean Acidification. Oceanography 27, 126-141.

Berelson, W.M., Balch, W.M., Najjar, R., Feeley, R.A., Sabine, C. and Lee, K. (2007) Relating estimates of $CaCO_3$ production, export, and dissolution in the water column to measurements of $CaCO_3$ rain into sediment traps and dissolution on the sea floor: A revised global carbonate budget. Global Biogeochemical Cycles 21, GB1024.

Berelson, W.M., Hammond, D.E. and Cutter, G.A. (1990) In situ measurements of calcium carbonate dissolution rates in deep-sea sediments. Geochimica et Cosmochimica Acta 54, 3013-3020.

Berelson, W.M., Hammond, D.E. and Johnson, K.S. (1987) Benthic fluxes and the cycling of biogenic silica and carbon in two southern California borderland basins. Geochimica et Cosmochimica Acta 51, 1345-1363.

Berelson, W.M., Hammond, D.E., McManus, J. and Kilgore, T.E. (1994) Dissolution kinetics of calcium carbonate in equatorial Pacific sediments. Global Biogeochemical Cycles 8, 219-235.

Berger, W.H. (1967) Foraminiferal Ooze: Solution at Depths. Science 156, 383-385.

Berner, R.A. (1966) Chemical diagenesis of some modern carbonate sediments. American Journal of Science 264, 1-36.

Berner, R.A. (1975) The role of magnesium in the crystal growth of calcite and aragonite from sea water. Geochimica et Cosmochimica Acta 39, 489-504.

Berner, R.A. and Morse, J.W. (1974) Dissolution kinetics of calcium carbonate in sea water IV. Theory of calcite dissolution. American Journal of Science 274, 108-134.

Berner, R.A. and Wilde, P. (1972) Dissolution kinetics of calcium carbonate in sea water I. Saturation state parameters for kinetic calculations. American Journal of Science 272, 826-839.

Bischoff, W.D., Bertram, M.A., Mackenzie, F.T. and Bishop, F.C. (1993) Diagenetic stabilization pathways of magnesian calcites. Carbonates and Evaporites 8, 82-89.

Bischoff, W.D., Mackenzie, F.T. and Bishop, F.C. (1987) Stabilities of synthetic magnesian calcites in aqueous solution: Comparison with biogenic materials. Geochimica et Cosmochimica Acta 51, 1413-1423.

Boucher, G., Clavier, J., Hily, C. and Gattuso, J.-P. (1998) Contribution of soft-bottoms to the community metabolism (primary production and calcification) of a barrier reef flat (Moorea, French Polynesia). Journal of Experimental Marine Biology and Ecology 225, 269-283.

Boudreau, B.P. (2013) Carbonate dissolution rates at the deep ocean floor. Geophysical Research Letters 40, 744-748.

Burdige, D.J., Hu, X. and Zimmerman, R.C. (2010) The widespread occurrence of coupled carbonate dissolution/reprecipitation in surface sediments on the Bahamas Bank. American Journal of Science 310, 492-521.

Burdige, D.J. and Zimmerman, R.C. (2002) Impact of sea grass density on carbonate dissolution in Bahamian sediments. Limnology and Oceanography 47, 1751-1763.

Burdige, D.J., Zimmerman, R.C. and Hu, X. (2008) Rates of carbonate dissolution in permeable sediments estimated from pore-water profiles: The role of sea grasses. Limnology and Oceanography 53, 549-565.

Busenberg, E. and Plummer, L.N. (1986) A Comparative Study of the Dissolution and Crystal Growth Kinetics of Calcite and Aragonite. U. S. Geological Survey Bulletin, 139-168.

Busenberg, E. and Plummer, L.N. (1989) Thermodynamics of magnesian calcite solid-solutions at 25˚C and 1 atm total pressure. Geochimica et Cosmochimica Acta 53, 1189-1208.

Cai, W.-J., Reimers, C.E. and Shaw, T. (1995) Microelectrode studies of organic carbon degradation and calcite dissolution at a California Continental rise site. Geochimica et Cosmochimica Acta 59, 497-511.

Cao, Z. and Dai, M. (2011) Shallow-depth $CaCO_3$ dissolution: Evidence from excess calcium in the South China Sea and its export to the Pacific Ocean. Global Biogeochemical Cycles 25, Citation GB2019.

Chave, K.E. (1954a) Aspects of the Biogeochemistry of Magnesium 1. Calcareous Marine Organisms. The Journal of Geology 62, 266-283.

Chave, K.E. (1954b) Aspects of the Biogeochemistry of Magnesium 2. Calcareous Sediments and Rocks. The Journal of Geology 62, 587-599.

Chave, K.E., Deffeyes, K.S., Weyl, P.K., Garrels, R.M. and Thompson, M.E. (1962) Observations on the Solubility of Skeletal Carbonates in Aqueous Solutions. Science 137, 33-34.

Chen, C.-T.A. (1990) Rates of Calcium Carbonate Dissolution and Organic Carbon Decomposition in the North Pacific Ocean. Journal of the Oceanographical Society of Japan 46, 201-210.

Chen, C.-T.A., Andreev, A., Kim, K.-R. and Yamamoto, M. (2004) Roles of Continental Shelves and Marginal Seas in the Biogeochemical Cycles of the North Pacific Ocean. Journal of Oceanography 60, 17-44.

Comeau, S., Carpenter, R.C., Lantz, C.A. and Edmunds, P.J. (2015) Ocean acidification accelerates dissolution of experimental coral reef communities. Biogeosciences 12, 365-372.

Cubillas, P., Köehler, S., Prieto, M., Chaïrat, C. and Oelkers, E.H. (2005) Experimental determination of the dissolution rates of calcite, aragonite, and bivalves. Chemical Geology 216, 59-77.

Cyronak, T., Santos, I.R. and Eyre, B.D. (2013a) Permeable coral reef sediment dissolution driven by elevated pCO_2 and pore water advection. Geophysical Research Letters 40, 4876-4881.

Cyronak, T., Santos, I.R., McMahon, A. and Eyre, B.D. (2013b) Carbon cycling hysteresis in permeable carbonate sands over a diel cycle: Implications for ocean acidification. Limnology and Oceanography 58, 131-143.

Doney, S.C., Fabry, V.J., Feely, R.A. and Kleypas, J.A. (2009) Ocean Acidification: The Other CO_2 Problem. Annual Review of Marine Science 1, 169-192.

Dore, J.E., Lukas, R., Sadler, D.W., Church, M.J. and Karl, D.M. (2009) Physical and biogeochemical modulation of ocean acidification in the central North Pacific. Proceedings of the National Academy of Sciences 106, 12235-12240.

Eyre, B.D., Andersson, A.J. and Cyronak, T. (2014) Benthic coral reef calcium carbonate dissolution in an acidifying ocean. Nature Climate Change 4, 969-976.

Eyre, B.D., Cyronak, T., Drupp, P., De Carlo, E.H., Sachs, J.P. and Andersson, A.J. (2018) Coral reefs will transition to net dissolving before end of century. Science 359, 908-911.

Fabry, V.J., Seibel, B.A., Feely, R.A. and Orr, J.C. (2008) Impacts of ocean acidification on marine fauna and ecosystem processes. ICES Journal of Marine Science 65, 414-432.

Feely, R.A., Sabine, C.L., Lee, K., Berelson, W., Kleypas, J., Fabry, V.J. and Millero, F.J. (2004) Impact of Anthropogenic CO_2 on the $CaCO_3$ System in the Oceans. Science 305, 362-366.

Feely, R.A., Sabine, C.L., Lee, K., Millero, F.J., Lamb, M.F., Greeley, D., Bullister, J.L., Key, R.M., Peng, T.-H., Kozyr, A., Ono, T. and Wong, C.S. (2002) In situ calcium carbonate dissolution in the Pacific Ocean. Global Biogeochemical Cycles 16, 12.

Findlay, H.S., Wood, H.L., Kendall, M.A., Spicer, J.I., Twitchett, R.J. and Widdicombe, S. (2011) Comparing the impact of high CO_2 on calcium carbonate structures in different marine organisms. Marine Biology Research 7, 565-575.

Friis, K., Najjar, R.G., Follows, M.J. and Dutkiewicz, S. (2006) Possible overestimation of shallow-depth calcium carbonate dissolution in the ocean. Global Biogeochemical Cycles 20, GB4019.

Garrels, R.M., Thompson, M.E. and Siever, R. (1960) Stability of some carbonates at 25˚C and one atmosphere total pressure. American Journal of Science 258, 402-418.

Gattuso, J.-P. and Hansson, L. (2011) Ocean acidification. Oxford University Press.

Gehlen, M., Bassinot, F.C., Chou, L. and McCorkle, D. (2005) Reassessing the dissolution of marine carbonates: II. Reaction kinetics. Deep Sea Research Part I: Oceanographic Research Papers 52, 1461-1476.

Gehlen, M., Gangstø, R., Schneider, B., Bopp, L., Aumont, O. and Ethe, C. (2007) The fate of pelagic $CaCO_3$ production in a high CO_2 ocean: a model study. Biogeosciences 4, 505-519.

Greenwald, I. (1941) The dissociation of calcium and magnesium carbonates and bicarbonates. Journal of Biological Chemistry 141, 789-796.

Griffin, A.J., Andersson, A., Cyronak, T., Eyre, B.D. and Stoltenberg, L. (in prep.) Seawater carbonate chemistry and organic matter decomposition control calcium carbonate dissolution in coral reefs sediments.

Hales, B. and Emerson, S. (1996) Calcite dissolution in sediments of the Ontong-Java Plateau: In situ measurements of pore water O_2 and *p*H. Global Biogeochemical Cycles 10, 527-541.

Hales, B. and Emerson, S. (1997) Evidence in support of first-order dissolution kinetics of calcite in seawater. Earth and Planetary Science Letters 148, 317-327.

Hatcher, P.G., Simoneit, B.R., Mackenzie, F.T., Neumann, A.C., Thorstenson, D.C. and Gerchakov, S.M. (1982) Organic geochemistry and pore water chemistry of sediments from Mangrove Lake, Bermuda. Organic Geochemistry 4, 93-112.

Hendriks, I.E., Duarte, C.M. and Álvarez, M. (2010) Vulnerability of marine biodiversity to ocean acidification: A meta-analysis. Estuarine, Coastal and Shelf Science 86, 157-164.

Higgins, J.A., Blättler, C., Lundstrom, E., Santiago-Ramos, D., Akhtar, A., Ahm, A.C., Bialik, O., Holmden, C., Bradbury, H. and Murray, S. (2018) Mineralogy, early marine diagenesis, and the chemistry of shallow-water carbonate sediments. Geochimica et Cosmochimica Acta 220, 512-534.

Hoegh-Guldberg, O., Mumby, P.J., Hooten, A.J., Steneck, R.S., Greenfield, P., Gomez, E., Harvell, C.D., Sale, P.F., Edwards, A.J., Caldeira, K., Knowlton, N., Eakin, C.M., Iglesias-Prieto, R., Muthiga, N., Bradbury, R.H., Dubi, A. and Hatziolos, M.E. (2007) Coral Reefs Under Rapid Climate Change and Ocean Acidification. Science 318, 1737-1742.

Honjo, S. and Erez, J. (1978) Dissolution rates of calcium carbonate in the deep ocean; an in-situ experiment in the North Atlantic Ocean. Earth and Planetary Science Letters 40, 287-300.

Hu, X. and Burdige, D.J. (2007) Enriched stable carbon isotopes in the pore waters of carbonate sediments dominated by sea grasses: Evidence for coupled carbonate dissolution and reprecipitation. Geochimica et Cosmochimica Acta 71, 129-144.

Ingalls, A.E., Aller, R.C., Lee, C. and Wakeham, S.G. (2004) Organic matter diagenesis in shallow water carbonate sediments. Geochimica et Cosmochimica Acta 68, 4363-4379.

Ingle, S.E., Culberson, C.H., Hawley, J.E. and Pytkowicz, R.M. (1973) The solubility of calcite in seawater at atmospheric pressure and 35%permil; salinity. Marine Chemistry 1, 295-307.

Jahnke, R.A. and Jahnke, D.B. (2004) Calcium carbonate dissolution in deep sea sediments: Reconciling microelectrode, pore water and benthic flux chamber results. Geochimica et Cosmochimica Acta 68, 47-59.

Jansen, H. and Wolf-Gladrow, D.A. (2001) Carbonate dissolution in copepod guts: a numerical model. Marine Ecology Progress Series 221, 199-207.

Jansen, H., Zeebe, R.E. and Wolf-Gladrow, D.A. (2002) Modeling the dissolution of settling $CaCO_3$ in the ocean. Global Biogeochemical Cycles 16, 16.

Keir, R.S. (1980) The dissolution kinetics of biogenic calcium carbonates in seawater. Geochimica et Cosmochimica Acta 44, 241-252.

Keir, R.S. (1983) Variation in the carbonate reactivity of deep-sea sediments: determination from flux experiments. Deep-Sea Research. Part A: Oceanographic Research Papers 30, 279-296.

Kennish, M.J. and Lutz, R.A. (1999) Calcium carbonate dissolution rates in deep-sea bivalve shells on the East Pacific Rise at 21˚N: results of an 8-year in-situ experiment. Palaeogeography, Palaeoclimatology, Palaeoecology 154, 293-299.

Kennish, M.J., Lutz, R.A. and Anonymous (1993) Calcium carbonate dissolution rates in hydrothermal vent fields of the Guaymas Basin. Eos, Transactions, American Geophysical Union 74, 179.

Kleypas, J.A., Buddemeier, R.W., Archer, D., Gattuso, J.-P., Langdon, C. and Opdyke, B.N. (1999) Geochemical Consequences of Increased Atmospheric Carbon Dioxide on Coral Reefs. Science 284, 118-120.

Kleypas, J.A., Feely, R.A., Fabry, V.J., Langdon, C., Sabine, C.L. and Robbins, L.L. (2005) Impacts of Ocean Acidification on Coral Reefs and Other Marine Calcifiers: A Guide for Future Research, report of a workshop held 18-20 April 2005, St. Petersburg, FL, p. 20.

Kroeker, K.J., Kordas, R.L., Crim, R.N. and Singh, G.G. (2010) Meta-analysis reveals negative yet variable effects of ocean acidification on marine organisms. Ecology Letters 13, 1419-1434.

Ku, T.C.W., Walter, L.M., Coleman, M.L., Blake, R.E. and Martini, A.M. (1999) Coupling between sulfur recycling and syndepositional carbonate dissolution: Evidence from oxygen and sulfur isotope composition of pore water sulfate, South Florida Platform, U.S.A. Geochimica et Cosmochimica Acta 63, 2529-2546.

Langdon, C. (2002) Review of Experimental Evidence for Effects of CO_2 on Calcification of Reef builders, Proceedings of the 9th International Coral Reef Symposium, pp. 1091-1098.

Langdon, C., Takahashi, T., Sweeney, C., Chipman, D., Goddard, J., Marubini, F., Aceves, H., Barnett, H. and Atkinson, M.J. (2000) Effect of calcium carbonate saturation state on the calcification rate of an experimental coral reef. Global Biogeochemical Cycles 14, 639-654.

Lantz, C.A., Schulz, K.G. and Eyre, B.D. (2019) The effect of warming and benthic community acclimation on coral reef carbonate sediment metabolism and dissolution. Coral Reefs 38, 149-163.

Le Quéré, C., Andrew, R.M., Friedlingstein, P., Sitch, S., Hauck, J., Pongratz, J., Pickers, P.A., Korsbakken, J.I., Peters, G.P. and Canadell, J.G. (2018) Global carbon budget 2018. Earth System Science Data 10, 2141-2194.

Leclercq, N., Gattuso, J.-P. and Jaubert, J. (2002) Primary production, respiration, and calcification of a coral reef mesocosm under increased CO_2 partial pressure. Limnology and Oceanography 47, 558-564.

Lutz, R.A., Fritz, L.W. and Cerrato, R.M. (1988) A comparison of bivalve (*Calyptogena magnifica*) growth at two deep-sea hydrothermal vents in the eastern Pacific. Deep Sea Research Part A. Oceanographic Research Papers 35, 1793-1810.

Lutz, R.A., Kennish, M.J., Pooley, A.S. and Fritz, L.W. (1994) Calcium carbonate dissolution rates in hydrothermal vent fields of the Guaymas Basin. Journal of Marine Research 52, 969-982.

Lyons, W.B., Gaudette, H.E. and Hewitt, A.D. (1979) Dissolved organic matter in pore water of carbonate sediments from Bermuda. Geochimica et Cosmochimica Acta 43, 433-437.

MacIntyre, W.G. (1965) The temperature variation of the solubility product of calcium carbonate in sea water. Dalhousie University.

Mackenzie, F.T., Bischoff, W.D., Bishop, F.C., Loijens, M., Schoonmaker, J. and Wollast, R. (1983) Magnesian calcites; low-temperature occurrence, solubility and solid-solution behavior. Reviews in Mineralogy 11, 97-144.

Mackenzie, F.T., Lerman, A. and LM, B.V. (1980) Global Carbon Cycle. Carbon Dioxide Effects Research and Assessment Program, 360.

Martin, W.R. and Sayles, F.L. (1996) $CaCO_3$ dissolution in sediments of the Ceara Rise, western Equatorial Atlantic. Geochimica et Cosmochimica Acta 60, 243-263.

McNichol, A.P., Lee, C. and Druffel, E.R. (1988) Carbon cycling in coastal sediments: 1. A quantitative estimate of the remineralization of organic carbon in the sediments of Buzzards Bay, MA. Geochimica et Cosmochimica Acta 52, 1531-1543.

Milliman, J.D. (1977) in: Neil R. Andersen, A.M. (Ed.), The fate of fossil fuel CO2 in the oceans. Plenum Press, New York.

Milliman, J.D. (1993) Production and accumulation of calcium carbonate in the ocean: Budget of a nonsteady state. Global Biogeochemical Cycles 7, 927-957.

Milliman, J.D. and Droxler, A.W. (1995) Calcium carbonate sedimentation in the global ocean: linkages between the neritic and pelagic environments. Oceanography 8, 92-94.

Milliman, J.D., Troy, P.J., Balch, W.M., Adams, A.K., Li, Y.-H. and Mackenzie, F.T. (1999) Biologically mediated dissolution of calcium carbonate above the chemical lysocline? Deep-Sea Research. Part I: Oceanographic Research Papers 46, 1653-1669.

Morse, J.W. (1974a) Dissolution kinetics of calcium carbonate in sea water. III: A new method for the study of carbonate reaction kinetics. American Journal of Science 274, 97-107.

Morse, J.W. (1974b) Dissolution kinetics of calcium carbonate in sea water. V. Effects of natural inhibitors and the position of the chemical lysocline. American Journal of Science 274, 638-647.

Morse, J.W. (1978) Dissolution kinetics of calcium carbonate in sea water: VI. The near-equilibrium dissolution kinetics of calcium carbonate-rich deep sea sediments. American Journal of Science 278, 344-353.

Morse, J.W. (1986) The surface chemistry of calcium carbonate minerals in natural waters: An overview. Marine Chemistry 20, 91-112.

Morse, J.W., Andersson, A.J., Mackenzie, F.T., Canfield, D.E. and Lyons, T.W. (2006) Initial responses of carbonate-rich shelf sediments to rising atmospheric pCO_2 and "ocean acidification": Role of high Mg calcites. Geochimica et Cosmochimica Acta 70, 5814-5830.

Morse, J.W. and Arvidson, R.S. (2002) The dissolution kinetics of major sedimentary carbonate minerals. Earth-Science Reviews 58, 51-84.

Morse, J.W., Arvidson, R.S. and Lüttge, A. (2007) Calcium Carbonate Formation and Dissolution. Chemical Reviews 107, 342-381.

Morse, J.W. and Berner, R.A. (1972) Dissolution kinetics of calcium carbonate in sea water: II. A kinetic origin for the lysocline. American Journal of Science 272, 840-851.

Morse, J.W., de Kanel, J. and Harris, K. (1979) Dissolution kinetics of calcium carbonate in seawater: VII. The dissolution kinetics of synthetic aragonite and pteropod tests. American Journal of Science 279, 488-502.

Morse, J.W. and Mackenzie, F.T. (1990) Geochemistry of Sedimentary Carbonates. Elsevier, Amsterdam-Oxford-New York.

Morse, J.W., Mucci, A. and Millero, F.J. (1980) The solubility of calcite and aragonite in seawater of 35‰ salinity at 25˚C and atmospheric pressure. Geochimica et Cosmochimica Acta 44, 85-94.

Morse, J.W., Zullig, J.J., Bernstein, L.D., Millero, F.J., Milne, P., Mucci, A. and Choppin, G.R. (1985) Chemistry of calcium carbonate-rich shallow water sediments in the Bahamas. American Journal of Science 285, 147-185.

Mucci, A. (1983) The solubility of calcite and aragonite in seawater at various salinities, temperatures, and one atmosphere total pressure. American Journal of Science 283, 780-799.

Murillo, L.J.A., Jokiel, P.L. and Atkinson, M.J. (2014) Alkalinity to calcium flux ratios for corals and coral reef communities: variances between isolated and community conditions. PeerJ 2, e249.

Nash, M.C., Opdyke, B.N., Troitzsch, U., Russell, B.D., Adey, W.H., Kato, A., Diaz-Pulido, G., Brent, C., Gardner, M., Prichard, J. and Kline, D.I. (2013) Dolomite-rich coralline algae in reefs resist dissolution in acidified conditions. Nature Climate Change 3, 268.

Olafsson, J., Olafsdottir, S.R., Benoit-Cattin, A., Danielsen, M., Arnarson, T.S. and Takahashi, T. (2009) Rate of Iceland Sea acidification from time series measurements. Biogeosciences 6, 2661-2668.

Oxburgh, R. and Broecker, W.S. (1993) Pacific carbonate dissolution revisited. Palaeogeography, Palaeoclimatology, Palaeoecology 103, 31-40.

Page, H.N., Andersson, A.J., Jokiel, P.L., Rodgers, K.u.S., Lebrato, M., Yeakel, K., Davidson, C., D'Angelo, S. and Bahr, K.D. (2016) Differential modification of seawater carbonate chemistry by major coral reef benthic communities. Coral Reefs 35, 1311-1325.

Pesret, F. (1972) Kinetics of carbonate-seawater interactions. University of Hawaii Institute of Gephysics and Planetology.

Peterson, M.N.A. (1966) Calcite; rates of dissolution in a vertical profile in the central Pacific. Science 154, 1542-1544.

Pickett, M. and Andersson, A.J. (2015) Dissolution Rates of Biogenic Carbonates in Natural Seawater at Different pCO_2 Conditions: A Laboratory Study. Aquatic Geochemistry 21, 459-485.

Plath, D. (1979) The Solubility of $CaCO_3$ in Seawater and the Determination of Activity Coefficients in Electrolyte Solutions. MS Thesis, Oregon State Universlty, Corvallis.

Plummer, L.N. and Mackenzie, F.T. (1974) Predicting mineral solubility from rate data; application to the dissolution of magnesian calcites. American Journal of Science 274, 61-83.

Rao, A.M.F., Polerecky, L., Ionescu, D., Meysman, F.J.R. and de Beer, D. (2012) The influence of pore-water advection, benthic photosynthesis, and respiration on calcium carbonate dynamics in reef sands. Limnology and Oceanography 57, 809-825.

Reaves, C.M. (1986) Organic matter metabolizability andd calcium carbonate dissolution in nearshore marine muds. Journal of Sedimentary Research 56, 486-494.

Ries, J.B., Cohen, A.L. and McCorkle, D.C. (2009) Marine calcifiers exhibit mixed responses to CO2-induced ocean acidification. Geology 37, 1131-1134.

Ries, J.B., Ghazaleh, M.N., Connolly, B., Westfield, I. and Castillo, K.D. (2016) Impacts of seawater saturation state (Ω_A = 0.4–4.6) and temperature (10, 25 °C) on the dissolution kinetics of whole-shell biogenic carbonates. Geochimica et Cosmochimica Acta 192, 318-337.

Rosenfeld, J.K. (1979) Interstitial water and sediment chemistry of two cores from Florida Bay. Journal of Sedimentary Research 49, 989-994.

Rude, P.D. and Aller, R.C. (1991) Fluorine mobility during early diagenesis of carbonate sediment; an indicator of mineral transformations. Geochimica et Cosmochimica Acta 55, 2491-2509.

Sabine, C.L. and Mackenzie, F.T. (1995) Bank-derived carbonate sediment transport and dissolution in the Hawaiian Archipelago. Aquatic Geochemistry 1, 189-230.

Santana-Casiano, J.M., González-Dávila, M., Rueda, M.J., Llinás, O. and González-Dávila, E.F. (2007) The interannual variability of oceanic CO_2 parameters in the northeast Atlantic subtropical gyre at the ESTOC site. Global Biogeochemical Cycles 21.

Schmalz, R.F. (1967) Kinetics and diagenesis of carbonate sediments. Journal of Sedimentary Research 37.

Shamberger, K., Feely, R., Sabine, C., Atkinson, M., DeCarlo, E., Mackenzie, F., Drupp, P. and Butterfield, D. (2011) Calcification and organic production on a Hawaiian coral reef. Marine Chemistry 127, 64-75.

Silverman, J., Lazar, B., Cao, L., Caldeira, K. and Erez, J. (2009) Coral reefs may start dissolving when atmospheric CO_2 doubles. Geophysical Research Letters 36, L05606.

Silverman, J., Lazar, B. and Erez, J. (2007) Effect of aragonite saturation, temperature, and nutrients on the community calcification rate of a coral reef. Journal of Geophysical Research 112, C05004.

Sjöberg, E.L. (1978) Kinetics and mechanism of calcite dissolution in aqueous solutions at low temperatures. Almqvist & Wiksell.

Stehli, F.G. and Hower, J., Jr. (1961) Mineralogy and early diagenesis of carbonate sediments. Journal of Sedimentary Petrology 31, 358-371.

Stoltenberg, L., Schulz, K.G., Cyronak, T. and Eyre, B.D. (2019) Seasonal variability of calcium carbonate precipitation and dissolution in shallow coral reef sediments. Limnology and Oceanography.

Subhas, A.V., Adkins, J.F., Rollins, N.E., Naviaux, J., Erez, J. and Berelson, W.M. (2017) Catalysis and chemical mechanisms of calcite dissolution in seawater. Proceedings of the National Academy of Sciences 114, 8175-8180.

Subhas, A.V., Rollins, N.E., Berelson, W.M., Dong, S., Erez, J. and Adkins, J.F. (2015) A novel determination of calcite dissolution kinetics in seawater. Geochimica et Cosmochimica Acta 170, 51-68.

Subhas, A.V., Rollins, N.E., Berelson, W.M., Erez, J., Ziveri, P., Langer, G. and Adkins, J.F. (2018) The dissolution behavior of biogenic calcites in seawater and a possible role for magnesium and organic carbon. Marine Chemistry 205, 100-112.

Suess, E. (1968) Calcium carbonate interaction with organic compounds. Lehigh University.

Suess, E. (1970) Interaction of organic compounds with calcium carbonate—I. Association phenomena and geochemical implications. Geochimica et Cosmochimica Acta 34, 157-168.

Suess, E. (1973) Interaction of organic compounds with calcium carbonate-II. Organo-carbonate association in Recent sediments. Geochimica et Cosmochimica Acta 37, 2435-2447.

Thunell, R.C., Keir, R.S. and Honjo, S. (1981) Calcite dissolution; an in situ study in the Panama Basin. Science 212, 659-661.

Tribble, G.W. (1990) Early diagenesis in a coral reef framework, p. 247.

Tribble, J.S., Arvidson, R.S., Lane, M. and Mackenzie, F.T. (1995) Crystal chemistry, and thermodynamic and kinetic properties of calcite, dolomite, apatite, and biogenic silica: applications to petrologic problems. Sedimentary Geology 95, 11-37.

Troy, P.J., Li, Y.-H. and Mackenzie, F.T. (1997) Changes in surface morphology of calcite exposed to the oceanic water column. Aquatic Geochemistry 3, 1-20.

Tsurushima, N., Suzumura, M., Yamada, N. and Harada, K. (2008) Dissolution rate of calcium carbonate in high pCO_2 seawater under high pressure, OCEANS 2008-MTS/IEEE Kobe Techno-Ocean. IEEE, pp. 1-3.

Tynan, S. and Opdyke, B.N. (2011) Effects of lower surface ocean pH upon the stability of shallow water carbonate sediments. Science of the Total Environment 409, 1082-1086.

Waldbusser, G.G., Steenson, R.A. and Green, M.A. (2011) Oyster shell dissolution rates in estuarine waters: effects of pH and shell legacy. Journal of Shellfish Research 30, 659-669.

Walter, L., Bonnell, L. and Patterson, W. (1990) Syndepositional dissolution of shallow marine carbonates: American Association of Petroleum Geologists. Bulletin 74, 787.

Walter, L.M. (1985) Relative reactivity of skeletal carbonates during dissolution: implications for diagenesis.

Walter, L.M., Bischof, S.A., Patterson, W.P. and Lyons, T.W. (1993) Dissolution and recrystallization in modern shelf carbonates; evidence from pore water and solid phase chemistry. Philosophical Transactions - Royal Society of London, Physical Sciences and Engineering 344, 27-36.

Walter, L.M. and Burton, E.A. (1986) The effect of orthophosphate on carbonate mineral dissolution rates in seawater. Chemical Geology 56, 313-323.

Walter, L.M. and Burton, E.A. (1990) Dissolution of Recent platform carbonate sediments in marine pore fluids. American Journal of Science 290, 601-643.

Walter, L.M. and Hanor, J.S. (1979) Effect of orthophosphate on the dissolution kinetics of biogenic magnesian calcites. Geochimica et Cosmochimica Acta 43, 1377-1385.

Walter, L.M. and Morse, J.W. (1984a) Magnesian calcite stabilities: A reevaluation. Geochimica et Cosmochimica Acta 48, 1059-1069.

Walter, L.M. and Morse, J.W. (1984b) Reactive surface area of skeletal carbonates during dissolution; effect of grain size. Journal of Sedimentary Petrology 54, 1081-1090.

Walter, L.M. and Morse, J.W. (1985) The dissolution kinetics of shallow marine carbonates in seawater: A laboratory study. Geochimica et Cosmochimica Acta 49, 1503-1513.

Werner, U., Blazejak, A., Bird, P., Eickert, G., Schoon, R., Abed, R.M., Bissett, A. and de Beer, D. (2008) Microbial photosynthesis in coral reef sediments (Heron Reef, Australia). Estuarine, Coastal and Shelf Science 76, 876-888.

Weyl, P.K. (1961) The carbonate saturometer. The Journal of Geology 69, 32-44.

Wilson, R., Millero, F.J., Taylor, J., Walsh, P., Christensen, V., Jennings, S. and Grosell, M. (2009) Contribution of fish to the marine inorganic carbon cycle. Science 323, 359-362.

Wilson, T.R.S. and Wallace, H.E. (1990) The rate of dissolution of calcium carbonate from the surface of deep-ocean turbidite sediments. Philosophical Transactions of the Royal Society of London, Series A: Mathematical and Physical Sciences 331, 41-49.

Yamamoto, S., Kayanne, H., Terai, M., Watanabe, A., Kato, K., Negishi, A. and Nozaki, K. (2012) Threshold of carbonate saturation state determined by CO_2 control experiment. Biogeosciences 9, 1441-1450.

Yates, K. and Halley, R. (2003) Measuring coral reef community metabolism using new benthic chamber technology. Coral reefs 22, 247-255.

Yates, K.K. and Halley, R.B. (2006a) CO_3^{2-} concentration and pCO_2 thresholds for calcification and dissolution on the Molokai reef flat, Hawaii. Biogeosciences 3, 357-369.

Yates, K.K. and Halley, R.B. (2006b) Diurnal variation in rates of calcification and carbonate sediment dissolution in Florida Bay. Estuaries and Coasts 29, 24-39.

Chapter 2: Seawater carbonate chemistry and organic matter decomposition control carbonate sediment dissolution rates in coral reefs

Alyssa J. Griffin, Tyler Cyronak, Bradley D. Eyre, Laura Stoltenberg, and Andreas J. Andersson

ABSTRACT

Ocean acidification threatens the capacity of coral reefs to build calcium carbonate ($CaCO_3$) structures and many studies have shown strong correlation between reef net community calcification (NCC) and seawater carbonate chemistry. However, it is currently unknown whether this relationship is due to changes in calcification and/or $CaCO_3$ dissolution. Here, we demonstrate the underlying mechanisms of how and why carbonate sediment dissolution increases in response to ocean acidification, even though seawater will remain supersaturated with respect to the most common carbonate mineral phases. Through laboratory and field experiments, we show that the extent of $CaCO_3$ dissolution in reef sediments is controlled by organic matter decomposition, but significantly influenced by the overlying seawater carbonate chemistry and the solubility of the most soluble mineral phase in the sediments. As seawater acidifies, less carbon dioxide (CO_2) is needed to reach undersaturation with respect to this mineral phase, leaving more CO_2 available to drive dissolution.

INTRODUCTION

Coral reefs are among the most biologically diverse ecosystems on Earth and provide habitat for up to 35% of known marine species (Reaka-Kudla, 1997). They also provide food,

economic resources and physical protection along shorelines to millions of people around the world (Moberg and Folke, 1999). The accretion of coral reefs requires that rates of calcium carbonate ($CaCO_3$) production outpace rates of $CaCO_3$ dissolution and export (Eyre et al., 2014). Ocean acidification (OA), the lowering of seawater pH and aragonite saturation state (Ω_{Ar}) due to oceanic uptake of anthropogenic carbon dioxide (CO_2), could alter this balance and potentially cease coral reef accretion (Eyre et al., 2018; Hoegh-Guldberg et al., 2007). OA is expected to reduce biological calcification rates (Kroeker et al., 2010) while also increasing bioerosion (Schönberg et al., 2017) and geochemical dissolution rates (Eyre et al., 2014), which could ultimately lead to shifts from net reef growth to net erosion (Silverman et al., 2009).

This is supported by recent field studies showing that net community calcification (NCC = gross calcification – gross $CaCO_3$ dissolution) in coral reef communities and sediments respond directly to changes in surface seawater pH and Ω_{Ar} (Albright et al., 2016; Albright et al., 2018; Eyre et al., 2018). This response in NCC could be attributed to either a decrease in gross calcification and/or an increase in $CaCO_3$ dissolution. However, it has yet to be resolved which process is primarily responsible for the observed changes in NCC, or whether it is a combination of changes in both calcification and dissolution.

Several lines of evidence suggest that the observed changes in NCC may primarily arise from changes in $CaCO_3$ dissolution rates rather than changes in biological calcification rates (Albright et al., 2016; Albright et al., 2018; Andersson et al., 2009; Eyre et al., 2018). For example, some experimental results suggest that community scale NCC is more sensitive to OA than individual calcifiers, which has been attributed to increased $CaCO_3$ dissolution (Pandolfi et al., 2011). Furthermore, many calcifiers appear relatively insensitive to OA under

natural conditions of high light, flow and nutrition (Towle et al., 2015), and some experimental studies have explicitly demonstrated that geochemical dissolution is more strongly affected by OA than biological calcification (Andersson et al., 2009; Comeau et al., 2015; Eyre et al., 2018). Nonetheless, it is not clear why $CaCO_3$ dissolution on coral reefs should increase in response to OA because surface seawater will remain supersaturated with respect to the most commonly occurring mineral phases (i.e., aragonite and Mg-calcite) even under the worst-case CO_2 emission scenario (Hoegh-Guldberg et al., 2007).

A significant body of work has been dedicated to the understanding of carbonate mineral dissolution in both the laboratory and the field, but has mainly focused on the open-ocean, deep-sea sediments, and calcite mineral phases (see (Morse et al., 2007) and references therein) whereas less focus has been dedicated to shallow water environments and biogenic mineral phases of aragonite and Mg-calcite (e.g., Morse et al., 1985a; Plummer and Mackenzie, 1974; Walter and Morse, 1984b, 1985). Increased attention has recently been given to shallow water environments because of the hypothesized negative effect of OA on shallow carbonate substrates (Cyronak et al., 2013a; Pickett and Andersson, 2015; Ries et al., 2016; Yamamoto et al., 2012). Still, relatively little is known about the control of natural properties and processes, such as grain size, microstructure, mineralogy, organic matter, and advective flow rates, on shallow carbonate dissolution rates or how they might interact with decreasing seawater pH and Ω_{Ar} (Andersson and Gledhill, 2013). Furthermore, there is a large disparity between laboratory and field observations, and reconciling this disparity remains a challenging task (e.g., Morse et al., 2007; Pickett and Andersson, 2015). Carefully controlled laboratory studies of specific mineralogy and grain size classes strive to provide a mechanistic understanding of $CaCO_3$ dissolution (Subhas et al., 2018; Walter and Morse, 1984b), but the

results are challenging to extrapolate to natural environments because of the complexity of environmental factors as well as inherently large variability in the physical and chemical properties of biogenic carbonate substrates. This variability in properties is particularly pronounced in shallow carbonate sediments and few laboratory studies have characterized dissolution rates for such substrates (Pickett and Andersson, 2015; Walter and Morse, 1985; Yamamoto et al., 2012). Field studies, on the other hand, can provide insight into net dissolution rates of bulk carbonate sediments, but it is difficult to attribute these rates to specific substrates and parse apart the actual factors that drive the dissolution process (Andersson and Gledhill, 2013). Bridging the gap between laboratory and field experiments is critical to accurately predicting future consequences of OA on coral reef ecosystems (Andersson, 2015).

In this study, we measured and evaluated dissolution rates of bulk biogenic carbonate sediments from differing reef environments in both field (Eyre et al., 2018) and laboratory settings. This was done in an attempt to more directly compare results from these different approaches, identify the main parameters affecting in situ dissolution rates, interpret observed changes in reef and sediment NCC as a function of Ω_{Ar} (Albright et al., 2016; Albright et al., 2018; Eyre et al., 2018) and to better understand the potential effect of OA on future coral reef accretion. Field incubations of permeable carbonate sediments were evaluated from contrasting reef environments at eleven sites in Tetiaroa, Tahiti, Kaneohe Bay, Hawaii, Heron Island, Australia and the North Lagoon of Bermuda (Eyre et al., 2018, See Table 2.1). Chamber incubations with a fixed stirring rate (Fig. 2.1A and Supplemental Fig. 2.1; Eyre et al., 2018) were used to measure sediment dissolution rates over complete diel cycles under both ambient and high partial pressure of CO_2 (pCO_2)/low pH conditions to mimic future OA

scenarios expected during this century (ΔpH≈ -0.10, -0.24 and -0.33) (Hoegh-Guldberg et al., 2007). The different field sites covered a range of initial water column Ω_{Ar} (Supplemental Table 2.1) as well as different sediment properties including grain size distribution (Supplemental Fig. 2.2) and carbonate mineralogy (Table 2.1). Sediments were collected from each incubation site and used in carefully controlled laboratory free-drift dissolution experiments under a range of seawater pCO_2 conditions (Pickett and Andersson, 2015); Fig. 2.1B).

RESULTS

Laboratory and field dissolution rates

In general, bulk carbonate sediment dissolution rates increased as a function of decreasing Ω_{Ar} in both laboratory and field incubations (Fig. 2.1C; Supplemental Table 2.2). The only exceptions were field incubations in Shark's Bay (Australia) and at Hog Reef (Bermuda), which showed no significant effect of seawater Ω_{Ar} on dissolution rates. The reason for this deviation from the general trend is unclear for Shark's Bay but at Hog Reef was most likely due to the small range in experimental Ω_{Ar}. All laboratory experiments were conducted in seawater undersaturated with respect to aragonite (Ω_{Ar} = 0.25-0.59) whereas field incubations experienced average surface seawater Ω_{Ar} ranging from 1.32 to 4.80, but pore water Ω_{Ar} was most likely lower than this range (Morse et al., 1985a).

In the laboratory, the majority of sediments had similar negative linear responses in dissolution rates to changes in seawater Ω_{Ar} (i.e. similar slopes; Fig. 2.1C, Supplemental Fig. 2.5, Supplemental Table 2.3). Tahiti 2, however, had a statistically significantly greater response to decreases in Ω_{Ar} than all other sites except for Crescent (Bermuda) and Heron 7

(Australia) (Fig. 2.1C, Supplemental Table 2.3). Bulk sediments from Tahiti 2 and Crescent had the highest absolute rates of $CaCO_3$ dissolution in the laboratory with the former exceeding the latter (Fig. 2.1C). No correlation was observed between dissolution rates in the laboratory and bulk mineralogy. However, the high dissolution rates and sensitivity to changes in Ω_{Ar} observed for Tahiti 2 appeared correlated with a higher proportion of sediment grains smaller than 63 μm (>65%), which was substantially greater than the proportion observed for any other site (<8%) (Supplemental Fig. 2.3).

Similar to laboratory experiments, field incubations showed that daily net dissolution rates at Tahiti 2 had the strongest response to decreasing Ω_{Ar}, but, because of a large standard error, they were not significantly different from any other location (Fig. 2.1C, inset). In fact, the majority of field incubations revealed no significantly different relationships between dissolution rate and Ω_{Ar} (Supplemental Table 2.3). Some field sites experienced daily net $CaCO_3$ precipitation under both control and acidified conditions, where others transitioned from daily net calcification to daily net dissolution at different values of Ω_{Ar} (1.27 to 3.28; Fig. 2.1C). Unlike in the laboratory experiments, daily net dissolution rates from field incubations were correlated with bulk sediment mineralogy and increased with increasing high magnesian calcite to aragonite ratio ($F_{1,76} = 7.74$, $p<0.01$; Supplemental Fig. 2.4).

Due to the limitations of uniformly normalizing laboratory and field rates, (see Supplementary Materials for discussion) the ranking of the relative sensitivity of dissolution rates to changes in Ω_{Ar} for each experiment was used to compare rates from both settings (Fig. 2.1D). If the response of dissolution rates to changes in Ω_{Ar} were primarily controlled by physical properties of the bulk sediment, the relative rank of the response (i.e., the slope of the dissolution rate vs. Ω_{Ar}) was expected to be the same for a given sediment in both the

laboratory and the field. This was not the case and the ranking was different for every experiment except for Tahiti 2, which had the highest sensitivity to changes in Ω_{Ar} in both the laboratory and the field experiments (Fig. 2.1D).

One critical difference between the laboratory and field experiments was the low Ω_{Ar} conditions experienced from the onset of and throughout the laboratory experiments. As a result, multiple mineral phases with different stabilities (e.g., mineral phases more soluble than aragonite; Table 2.1) most likely dissolved simultaneously and potentially masked the effect of mineralogical differences between sites in the laboratory. In contrast, mineral phases in the field may have dissolved sequentially according to mineral stability, developing a metastable equilibrium between the dissolving mineral phase and the surrounding pore waters due to the greater substrate to water volume ratio in natural sediments (Schmalz and Chave, 1963). Since high magnesian calcite can be more soluble than aragonite depending on the amount of Mg substituting for Ca in the mineral lattice (Bischoff et al., 1987; Plummer and Mackenzie, 1974), these differences could partly explain the observed correlation between dissolution rates and wt% high magnesian calcite in the field and the lack of correlation between these parameters in the laboratory. However, it is clear that factors other than physical properties of the sediments need to be considered to explain the discrepancy between the field and the laboratory results and any potential drivers of the observed dissolution rates.

Metabolic activity and dissolution

Another major difference between the laboratory and the field experiments was the influence of metabolic activity (i.e. respiration and photosynthesis), which was absent in the laboratory. Organic metabolism has been well documented as a driver of $CaCO_3$ sediment

dissolution under aerobic conditions and is typically referred to as metabolic dissolution (see (Eyre et al., 2014) and references therein). Evaluating net flux in seawater alkalinity owing to calcification and dissolution processes (F_{NCC}) as a function of net flux in dissolved inorganic carbon owing to net organic carbon community production (F_{NCP}, where NCP = gross primary production – total respiration) in the field experiments, revealed a strong positive correlation ($R^2 = 0.86$) with mostly net production and calcification during the day and net respiration and $CaCO_3$ dissolution during the night (Figs. 1.2A-B). The initial Ω_{Ar} of the incubations during the daytime (i.e. dawn conditions) were low with no clear relation to F_{NCC} or F_{NCP} rates (Fig. 2.2A) whereas the largest changes in $\Delta\Omega_{Ar}$ were associated with the highest rates of F_{NCP} (Fig. 2.2B). The magnitude of $\Delta\Omega_{Ar}$ was gradually tempered as F_{NCC} increased (Fig. 2.2B), which can be attributed to the counteracting effects of positive NCP and NCC on seawater Ω_{Ar} (Andersson and Gledhill, 2013). In contrast to daytime, nighttime results revealed trends in dissolution rates ($-F_{NCC}$) as a function of respiration ($-F_{NCP}$) that were associated with distinct combinations of initial Ω_{Ar} and $\Delta\Omega_{Ar}$, such that incubations with high initial Ω_{Ar} (> 4) were associated with large decreases in $\Delta\Omega_{Ar}$ (> 1 units), and incubations with low initial Ω_{Ar} (< 2) were associated with small changes in $\Delta\Omega_{Ar}$ (± 0.5 units) (Figs. 1.2A-B).

These trends in Ω_{Ar} can be explained by the flux of alkalinity from the sediments owing to carbonate dissolution (F_{NCC}) relative to production of DIC from respiration (F_{NCP}) with additional influence from the initial seawater Ω_{Ar}, the solubility of the most reactive bulk mineral phase in the sediments, and the filtration rate of the pore water (Rao et al., 2012). If the initial Ω_{Ar} or the pore water filtration rate were high, more respiration would be required to lower pore water saturation state to initiate dissolution of the most soluble mineral phase compared to a condition where the initial Ω_{Ar} was lower or the pore water filtration rate was

slower. In such a scenario, the relative flux of alkalinity to DIC was low, and the $\Delta\Omega_{Ar}$ was large. In the opposite scenario (i.e., low initial Ω_{Ar} or low filtration rate), less respiration would be required to initiate dissolution and a larger flux of alkalinity relative to DIC would result in a greater buffer effect and thus, a smaller $\Delta\Omega_{Ar}$ (Fig. 2.3). Since the pore water saturation state required to initiate dissolution within the sediments or at the seawater-sediment interface is determined by the solubility of the most reactive mineral phase, this property also influences the observed changes in Ω_{Ar} similar to the initial seawater Ω_{Ar} condition (i.e., reaching undersaturation with respect to the most soluble mineral phase requires less respiration when this phase is more soluble).

Assuming that the pore water filtration rates were similar for all incubations (i.e., all experiments were conducted at a disc rotation of 40 rpm), the observed changes in seawater Ω_{Ar} were mainly a function of the initial Ω_{Ar}, the solubility of the most reactive mineral phase and the extent of respiration (Figs. 1.2C-D). However, Rao et al. (2012) showed that pore water filtration rates could vary between incubations despite constant rates of disc rotation, and thus, could affect the observed results. Consequently, to validate the hypothesized mechanisms controlling the chamber carbonate chemistry, we used a simple box model to investigate the influence of the initial seawater Ω_{Ar}, the solubility of the most soluble mineral phase, and also varying respiration rates. These results followed our interpretation of the experimental results closely (Supplemental Fig. 2.7) and also agreed with previous work by Morse et al. (2006), Rao et al. (2012), Andersson (2015), and Eyre et al. (2018).

Based on the field and model results, it can be concluded that the magnitude of dissolution in the field incubations was largely driven by the extent of respiration beyond seawater saturation with respect to the most soluble bulk mineral phase within the sediments

or at the seawater-sediment interface, which was significantly dependent on the initial seawater Ω_{Ar}, the apparent solubility of this mineral phase and possibly, also modified by uncharacterized variations in pore water filtration rates (Rao et al., 2012). In spite of the potential uncertainty associated with the latter, the field experiments showed consistent decreases in daily F_{NCC} rates under high pCO_2 treatments relative to control conditions while no clear trend was observed between the different treatments with respect to changes in F_{NCP} (Figs. 1.2C-D). These results lend strong support to the hypothesized link between dissolution rates, respiration (organic matter decomposition), seawater Ω_{Ar}, and mineral solubility.

In addition, evaluating the independent contributions from F_{NCP} and F_{NCC} to the observed net changes in dissolved inorganic carbon (DIC) and total alkalinity (TA) during the nighttime period of incubations by graphical vector analysis (Deffeyes, 1965), provide a rough approximation of the Ω_{Ar} that is in equilibrium with the most soluble mineral phase present in the sediments. That is, the higher the seawater Ω_{Ar} coinciding with the onset of the metabolic dissolution vector (Fig. 2.3), the higher the apparent solubility of the most soluble mineral phase present in the sediments. The highest seawater Ω_{Ar} coinciding with the metabolic dissolution vector was observed at Heron 7 on the Great Barrier Reef ($\Omega_{Ar} = 3.88$) while the lowest was observed at the CRIMP site in Hawaii ($\Omega_{Ar} = 1.62$) (Fig. 2.3). These results are also corroborated by the observed transition from daily net calcification to daily net dissolution at different values of Ω_{Ar} (Fig. 2.1), which followed a similar order. As expected for the high CO_2 treatments, there was no or little separation between the respiration and metabolic dissolution vectors because $CaCO_3$ dissolution was more or less instantaneous as the low initial Ω_{Ar} was already undersaturated with respect to the most soluble bulk mineral phase in these experiments (Fig. 2.3). However, some caution is advised in the interpretation

of these results as uncharacterized variations in the filtration rates could affect the results of the vector analysis. Furthermore, explicitly identifying the most soluble bulk mineral phase is challenging because of the immense spectrum of physical properties that may contribute to the solubility including mineralogy, microarchitecture, organic coatings, and grain size (Morse et al., 2007), and will require a substrate specific research approach which was beyond the scope of this study.

DISCUSSION

Implications to coral reef sediments in the context of ocean acidification

The results of this study show that the extent of $CaCO_3$ dissolution in the natural environment is a function of a combination of the initial seawater Ω_{Ar}, the solubility of the most soluble bulk mineral phase in the sediments, and the extent of CO_2 produced from respiration beyond the pore water Ω_{Ar} that corresponds to the apparent solubility of this mineral phase (Andersson, 2015), which is influenced by the pore water filtration rate (Rao et al., 2012). Furthermore, the results explicitly demonstrate why carbonate dissolution occurs in shallow near-shore environments despite seawater being highly supersaturated with respect to the most commonly occurring carbonate mineral phases and why dissolution rates/NCC will increase/decrease in response to OA and the associated changes in surface seawater Ω_{Ar}. Fundamentally, decreasing seawater Ω_{Ar} will lead to more dissolution because more CO_2 from decomposition of organic material will be available to fuel metabolic dissolution (assuming there is no change in aerobic respiration rates and pore water filtration rates). However, higher respiration rates due to ocean warming (Lantz et al., 2019) or increased deposition of organic

matter to the sediments could further enhance carbonate dissolution rates (Andersson, 2015; Eyre et al., 2018), although ocean deoxygenation could potentially counter this increase to some extent (Burdige and Zimmerman, 2002). On longer timescales, the onset of dissolution may shift as the sediment composition and most soluble bulk mineral phase could change owing to both selective dissolution (Morse et al., 2006; Schmalz and Chave, 1963) and alterations to the supply and mineralogy of carbonate sediments (Yates et al., 2017). However, these shifts are probably only relevant on timescales of several decades or longer (Morse et al., 2006; Yates et al., 2017).

The results reported here provide the mechanism underlying the inverse relationship between seawater Ω_{Ar} and carbonate sediment dissolution rates reported from global locations in Eyre et al. (2018) (i.e., lower Ω_{Ar}, higher dissolution rates). This same mechanism can operate in any shallow carbonate substrate, including the reef framework, however sulfate reduction may play a more important role in other microenvironments (Tribble, 1993). We also argue that the results offer a plausible explanation to changes in NCC as a result of seawater alkalinity or CO_2 manipulations at One Tree Island (Great Barrier Reef) reported by Albright et al. (2016; 2018), although they cannot eliminate that organismal calcification rates were also affected in these experiments. In fact, Albright et al. (2018) hypothesized that their results potentially stemmed from changes in carbonate dissolution rather than gross calcification because there was no connection between the magnitude change in NCC in response to CO_2 addition and the background rates of NCC. This conundrum could be addressed by conducting the same experiments from Albright et al. (2016; 2018) at nighttime.

Future changes in dissolution rates for any given coral reef environment will be a function of both local and global processes influencing local seawater Ω_{Ar}, the properties affecting the reactivity of carbonate sediment grains (e.g., mineralogy, size distribution, microarchitecture, and protective organic coatings), the advective flow rate and residence time of pore waters (Cyronak et al., 2013b; Rao et al., 2012), and the amount and reactivity of organic matter deposited and decomposed within the sediments. Recently, an increasing number of studies have reported observations of temporary reef scale net dissolution from multiple locations (e.g., Yeakel et al., 2015) and even on annual timescales from the Florida reef tract (Muehllehner et al., 2016). These observations are likely to increase in frequency, duration and magnitude as OA intensifies. Furthermore, reef accretion and structural complexity of many reef environments have already significantly declined due to drastic reductions in coral cover and changes in community composition resulting from poor water quality, ocean warming and disease (Perry and Alvarez-Filip, 2018). As a result, it has been proposed that few reefs will have the capacity to produce sufficient $CaCO_3$ to keep up with sea level rise under anticipated CO_2 emission scenarios (Perry and Alvarez-Filip, 2018). This projection is further supported by recent observations that seafloor accretion has declined and become net erosional in reef environments in the Florida Keys, US Virgin Islands, and Maui, Hawaii (Yates et al., 2017). It is currently unknown how different processes have contributed to this change, but irrespective of the mechanism(s), it is evident that future increases in carbonate dissolution rates (Andersson and Gledhill, 2013; Eyre et al., 2018; Silverman et al., 2009) as a result of OA will continue to accelerate these trends. Drastic interventions to reduce global anthropogenic carbon emissions are critical to preserve future coral reef accretion at both local and global scales.

MATERIALS AND METHODS

Site locations

A total of seventy in situ chamber incubation experiments were conducted at eleven sites in four different coral reef ecosystems in Australia, Tahiti, Bermuda and Hawaii (Supplemental Fig. 2.1). Incubations were conducted at four sites across the Heron Island lagoon, a platform reef located on the Great Barrier Reef off the eastern coast of Queensland, Australia (Jell and Webb, 2012). Incubations were conducted at three sites in Tetiaroa, an atoll north of Tahiti (Jeanson et al., 2014). One site was located on the reef flat and two within the lagoon in order to cover a variety of depths and sediment types. Incubations were also conducted at three sites across the Bermuda carbonate platform near Hog Reef (a rim reef), Crescent Reef (a patch reef), and within Bailey's Bay (a seagrass bed) (e.g., Takeshita et al., 2018; Yeakel et al., 2015). A single site was chosen to conduct incubations in the lagoon of the Kaneohe Bay barrier reef, located on the eastern side of Oahu, Hawaii.

Sediment collection and analysis

Bulk sediment samples were collected in close proximity to all eleven chamber incubation sites. The samples were oven-dried for at least 24 hours at 60ºC and stored for use in the laboratory free-drift experiments. Bulk mineralogy of each sample was determined by X-ray diffraction (XRD). XRD analysis was carried out with a PANalytical X'Pert Pro XRD diffractometer equipped with a X'Celerator detector, using Co K-α radiation. Samples were milled and spiked with 20% fluorite and then mounted on zero diffraction silicon XRD plates. Carbonate minerals were identified based on the d-spacings from the Joint Committee on Powder Diffraction Standards (JCPDS) database and weight percent was quantified using

relative peak areas. Mg-calcite composition was calculated from the shift in d-spacing of the calcite 104 reflection using the method described by Bischoff et al. (1983). All results were processed using MDI-Jade version 9.7.0 software. Grain size analysis was performed using the Wet Sieving Analysis method (Lewis and McConchie, 2012) and divided into the following grain size fractions: granule/gravel (>2mm), very coarse sand (1000-2000 μm), coarse sand (500-1000 μm), medium sand (250-500 μm), fine sand (125-250 μm), very fine sand (63-125 μm), and silt/clay (<63 μm).

Field chamber experiments

Incubation chambers identical to those described in Glud et al. (2008) were deployed at each study site to estimate *in situ* rates of $CaCO_3$ sediment dissolution, benthic respiration and benthic productivity under controlled advective flow. Seawater advection was controlled within the chambers by a spinning acrylic disk set to spin at 40 rotations per minute (RPM) (Glud et al., 2008). Dissolution rates were measured under control (ambient) conditions at all eleven sites as well as under elevated pCO_2 levels at all locations except for at Hog Reef in Bermuda using the methods described in Cyronak et al. (2013a). Seawater pCO_2 levels were manipulated in the chambers by pressurizing a closed loop of silicone tubing inside the chambers with 99.9% pure CO_2 , or by introducing low pH seawater into the chambers to reach the targeted treatment levels (medium treatments, $\Delta pH \approx -0.10$; high treatments, $\Delta pH \approx -0.24$; ultra-high treatments, $\Delta pH \approx -0.33$), before the start of the incubation (Eyre et al., 2018). Incubations started at either dawn or dusk and were conducted over a full diel cycle. The chambers were sampled at 0, 12 and 24 hours following the protocol outlined in (Eyre et al., 2018).

Rate calculations

Solute flux rates (F_{NCC} and F_{NCP}) were calculated using the following equation:

$$r_x = \frac{\Delta s_x \times \rho \times h}{\Delta t} \quad (1)$$

where Δs_x is the change in solute concentration (in μmol kg^{-1}), ρ is the density of the seawater (in kg/m^3), h is the average height of the water enclosed within the chamber (in meters), Δt is the change in time (in hours, or days for diel fluxes) and r_x is the flux rate of solute x (in mmol m^{-2} h^{-1}) (Cyronak et al., 2013b). Hourly fluxes were calculated by measuring the solute concentrations (s_x) at the start and end points of the light and dark periods and dividing by the total number of daylight or darkness, respectively (which varied by location). Daily fluxes were calculated by measuring the solute concentrations (s_x) at the start and end points of an entire diel cycle (Cyronak et al., 2013b). Changes in total alkalinity (divided by two according to reaction stoichiometry) were used to calculate flux rates due to $CaCO_3$ precipitation and dissolution (F_{NCC}). The flux rate of dissolved inorganic carbon due to respiration and photosynthesis (F_{NCP}) were then calculated by subtracting half of the TA flux rate from the overall DIC flux rate, which assumes that no other reactions are contributing or consuming alkalinity (Cyronak et al., 2013b).

The complete carbonic acid system was calculated based on in situ temperature, salinity, TA and measured pH or DIC values (Eyre et al., 2018) and using CO2SYS (Lewis et al., 1998) with CO_2 dissociation constants defined by Mehrbach et al. (1973) and refit by Dickson and Millero (1987).

Laboratory free-drift experiments

Reactor design

A duplicate free-drift reactor previously described and validated by Pickett and Andersson (2015) was used for all laboratory experiments in this study (Bischoff et al., 1987), barring the few differences described below. In brief, the reactor (Fig. 2.1A) is designed with two jacketed beakers (250mL) where dissolution occurs in seawater that can be manipulated to desired pCO_2 levels and temperature. Experiments on each substrate were conducted at four pCO_2 conditions (~3500, 5000, 6500, 8000 µatm). This range of pCO_2 values was chosen to represent pCO_2 conditions observed in sediments on representative carbonate platforms such as Bermuda (Pickett and Andersson, 2015) and the Bahamas (Morse et al., 1985b) as well as potentially higher conditions due to ocean acidification. The nitrogen flow rate was set to either 1.70 or 2.00 standard liters per minute (slpm), and the CO_2 flow rate was set to values between 11.09 and 15.00 standard cubic centimeters per minute (sccm) to obtain the desired pCO_2 values in the experimental seawater.

Materials

For all experiments, seawater from the Scripps Institution of Oceanography (SIO) flow-through system was vacuum filtered (0.47µm Millipore HVLP filters) and sterilized with UV light using a low-pressure mercury lamp. The UV-treated seawater batches were measured for salinity (33.71± 0.29, n = 44). Bulk sediments containing a wide range of grain sizes were divided into equal representative samples of 1.5 grams using a riffle-type sample splitter that was able to accommodate the full range of grain sizes found in all samples. The difference in sample weight between cells was never more than 0.01 grams and a solid to

solution ratio of ~6×10^{-3} ($\pm9.38\times10^{-5}$, n = 88) was used in all experiments. To assure that the sediment samples more closely represented conditions in the natural environment, the samples did not undergo any grinding, cleaning or sonicating prior to use in the dissolution experiments (Bischoff et al., 1987; Plummer and Mackenzie, 1974; Walter and Morse, 1984a).

Dissolution experiments

Integrated dissolution rates of sediments from each study site were measured over two hours of incubation in the laboratory. This duration allowed for measureable changes in total alkalinity, but was short enough to prevent significant increases in the experimental seawater carbonate saturation state. At the end of each experiment, the seawater and solid samples were recovered. After removing the gas pipette and stir probe from the first cell, a 200 mL syringe was first rinsed with the experimental seawater, then filled with the seawater sample. The seawater was then filtered through a 0.47 μm Millipore HVLP filter to remove smaller grains that could easily enter the sample during siphoning and syringed into a 200-mL Kimax screw-top bottle with a cone lid and Teflon-taped threads. This process was repeated once more to recover the maximum amount of experimental seawater from the cell. The gas pipette and stir probe was then removed from the second cell and the sampling process was repeated. The solid samples were also recovered, rinsed with deionized water, dried at 60 ºC for 24 hours, and stored. Due to the high pCO_2 conditions of the experimental seawater, significant degassing was observed during the sampling process. The use of a syringe to recover the seawater also induced gas exchange between the air and seawater samples. For these reasons, in situ pH measurements and TA samples taken following equilibration with CO_2 gas and at

the end of each dissolution run were used to calculate the range of the experimental seawater pCO_2 and Ω_{Ar} experienced during the experiments. The Nernstian behavior of the pH probes were carefully evaluated at the beginning of each experiment using low ionic strength NBS buffers 4.00, 7.00, and 10.00 at 25 °C. The electrodes were then calibrated on the total pH scale using a single point Tris buffer prepared in synthetic seawater (pH 8.11 at 25 °C) (Dickson, 1993) before each experiment (Pickett and Andersson, 2015). Electrode drift was found to be less than the analytical uncertainty of the electrodes (0.01 units) in all experiments. TA was determined via potentiometric acid titrations of a 15 g sample using an open titration cell system. The average (± 1 standard deviation) accuracy and precision of replicate certified reference materials (prepared by A. Dickson at SIO) was 0.49 ± 2.10 μmol kg^{-1} (n=17). Gas equilibration experiments (n=5) were also conducted to obtain an average rate of increase in total alkalinity (TA) due to evaporation. This average rate was 2.31 ± 1.44 μmol kg^{-1} (n=5) over the course of a 2-hr dissolution experiment.

Rate calculations

The measured TA values between initial and final samples were used to calculate the average rate of dissolution during the 2 h incubation as follows:

$$R = 0.5 \times W_{SW}\left(\frac{\Delta TA - TA_E}{\Delta t \times W_C}\right) \quad (2)$$

where W_{SW} designates the weight of the seawater (kg), ΔTA represents the final minus initial TA (μmol kg^{-1}), TA_E represents the correction for the increase in TA due to evaporation (2.31 ± 1.44 μmol kg^{-1}), t is the length of the experiment (h), and W_C is the weight of the carbonate substrate (g). The total value is multiplied by 0.5 because the dissolution of one mole of

$CaCO_3$ results in a two mole increase in TA.

The complete carbonic acid system was calculated based on reactor temperature, salinity, measured pH, and TA using CO2SYS (Lewis et al., 1998) using CO_2 dissociation constants defined by Mehrbach et al. (1973) and refit by Dickson and Millero (1987).

Experimental uncertainty

The experimental error corresponding to the rate measurements was calculated according to the standard rules of error propagation. In all experiments, the overall error was found to be significantly smaller than the variation in the rates determined by each reactor. Although every precaution was taken to insure the subsamples in each reactor were as similar as possible, the considerable heterogeneity in the untreated bulk sediments is likely responsible for the relatively large variation between reactors.

Normalization of field and laboratory rates

Although both laboratory and field derived dissolution rates can be expressed as the rate of change of total alkalinity (ΔTA; $\mu mol\ kg^{-1}\ h^{-1}$) as a function of Ω_{Ar}, direct comparison of these rates is problematic. Dissolution rates from laboratory experiments are typically normalized to the weight or specific surface area of experimental substrate (e.g., Walter and Morse, 1984b, 1985) whereas rates from benthic field studies are normalized to planar surface area (Cyronak et al., 2013b). It is challenging to normalize laboratory rates to a surface area because it is unknown what portion of the total surface area is participating in the reaction. On the other hand, seawater Ω_{Ar} within and above the sediments in the in situ field incubation chambers may not be equal, and thus, it is unknown how much substrate was in contact with

$\Omega < 1$ seawater and potentially contributing to the flux of total alkalinity in terms of either weight or surface area.

To meaningfully compare the laboratory and field dissolution rates, we calculated what we refer to as the relative sensitivity of dissolution rates to changes in Ω_{Ar}, or simply, the relative slope for each experiment (Fig. 2.1D). To calculate this, the slope of the relationship from normalized laboratory dissolution rates (to weight, Supplemental Fig. 2.5) versus average Ω_{Ar} for each site was calculated and then divided by the greatest slope from the laboratory setting (i.e., $[\Delta\text{dissolution rate}/\Delta\Omega_{Ar}]_{site}/[\Delta\text{dissolution rate}/\Delta\Omega_{Ar}]_{greatest}$). The same was done for normalized field rates (to planar surface area, Fig. 2.1C – inset) for each site and then divided by the greatest slope from the field experiments. The rankings of the relative slopes from the laboratory and field were then compared (Fig. 2.1D).

Statistical analyses

All statistical analyses were carried out using R 3.5.2. We used a multiple linear regression model to examine the dependency of dissolution rates in the laboratory and the field on changes in average seawater saturation state Ω_{Ar} (continuous) and site (categorical) (Fig. 2.1C, Supplemental Fig. 2.5). The model results were generated using the lm function (Supplemental Table 2.2) (Lenth, 2016). Linear regression was used to examine the dependency of dissolution rates in the laboratory and the field on changes in the following physical properties: median grain size, the ratio of high-magnesian calcite to aragonite (wt%/wt%), and the amount of sediment with a grain size less than 63 μm (wt%). The linear regressions were also generated using the lm function. Estimated marginal means for trends, along with SE and 95% CI, were calculated (Supplemental Table 2.3) using the emmtrends

function (Lenth, 2019). To determine significant differences between trends, Tukey's multiple comparisons test on estimated marginal means for linear trends was conducted (Supplemental Table 2.3) using CLD function (Lenth, 2019). Alpha levels of 0.05 were considered significant for all statistical tests.

Model description

A simple box model was constructed to assess the effect of the initial seawater Ω_{Ar}, the solubility of the most soluble mineral phase, and also varying respiration rates on seawater carbonate chemistry in the incubation chambers. The objective of the model was not to create a full-fledged numerical replica of the reaction chambers, but simply to create a model that could be used to conceptually validate the experimental results and interpretations. The approach was similar to that employed by Morse et al. (2006). The model was comprised of a seawater and a pore water domain (Supplemental Fig. 2.6) parameterized based on the fixed physical properties of the chambers and approximate average values of other parameters such a porosity, carbonate chemistry, and advective flux rates (Supplemental Table 2.4). Each domain contained a DIC and TA reservoir. The model was run for nighttime conditions only (12 h). DIC flux owing to respiration was a prescribed forcing of the model in both the seawater and pore water reservoir. $CaCO_3$ dissolution fluxes only occurred if the seawater or pore water saturation state with respect to the most soluble mineral phase in the sediment was less than 1. At that stage, $CaCO_3$ dissolved in stoichiometric proportion to respiration in a ratio of 1:1 (i.e., metabolic dissolution). Numerical integration was conducted with Matlab R2018a (The MathWorks, Inc.) using an ordinary differential equation solver (ode45) based on an explicit Runge-Kutta (4, 5) formula. Multiple sensitivity analyses were conducted with

respect to the initial carbonate chemistry starting conditions by manipulating the initial DIC value, the solubility of the most soluble mineral phase in the sediments, and rates of respiration. Total fluxes of TA and DIC owing to $CaCO_3$ dissolution or respiration processes (F_{NCC} and F_{NCP}) were calculated based on start and end conditions in the chambers to replicate field methodology. Carbonate chemistry calculations in the model were conducted with CO2SYS v1.1 for Matlab.

ACKNOWLEDGEMENTS

We are grateful for the assistance of Ms. Morgan Goodrich and Mr. Samuel Kekuewa with monitoring laboratory experiments and preparation of materials. We are also grateful for the guidance of Ms. Beverly French and Dr. Lynn Waterhouse in statistical approaches to the data. We thank Dr. Peggy O'Day, Mr. Paul Aronstein and Mr. Alexander Leven for XRD analysis and Dr. Kenneth Veccio and Dr. Tyler Harrington for assistance with use of XRD phase identification software.

Chapter 2, in part, is in preparation for submission for publication. Griffin, A. J., Cyronak, T., Eyre, B., Stoltenberg, L., Andersson, A. J.. The dissertation author was the primary investigator and author of this material.

FIGURES

Figure 2.1: Laboratory and field apparatuses and dissolution rates. (A) In situ field incubation chambers and (B) laboratory free-drift reactor. (C) Raw laboratory and field dissolution rates (μmol kg^{-1} hr^{-1}) from each experiment or incubation, respectively. Legend Key: BB = Bailey's Bay, CM = CRIMP, CR = Crescent, H0,-5,-7= Heron 0, -5,-7, HR = Hog Reef, SB = Shark's Bay, T1,-2,-3= Tahiti 1, -2,-3. (C, inset) Field dissolution rates normalized to planar surface area of chambers (mmol m^{-2} d^{-1}). Dashed line indicates threshold between net calcification (>0) and net dissolution (<0). Hog Reef field incubations were only conducted under control conditions and therefore, no relation between ΔTA or rate and Ω_{Ar} was established. (D) Relative ranking of slope ($[\Delta$dissolution rate$/\Delta\Omega_{Ar}]_{site}/[\Delta$dissolution rate$/\Delta\Omega_{Ar}]_{greatest}$) from normalized laboratory (to weight) and field (to planar surface area) rates versus average Ω_{Ar} over the course of experiment or incubation.

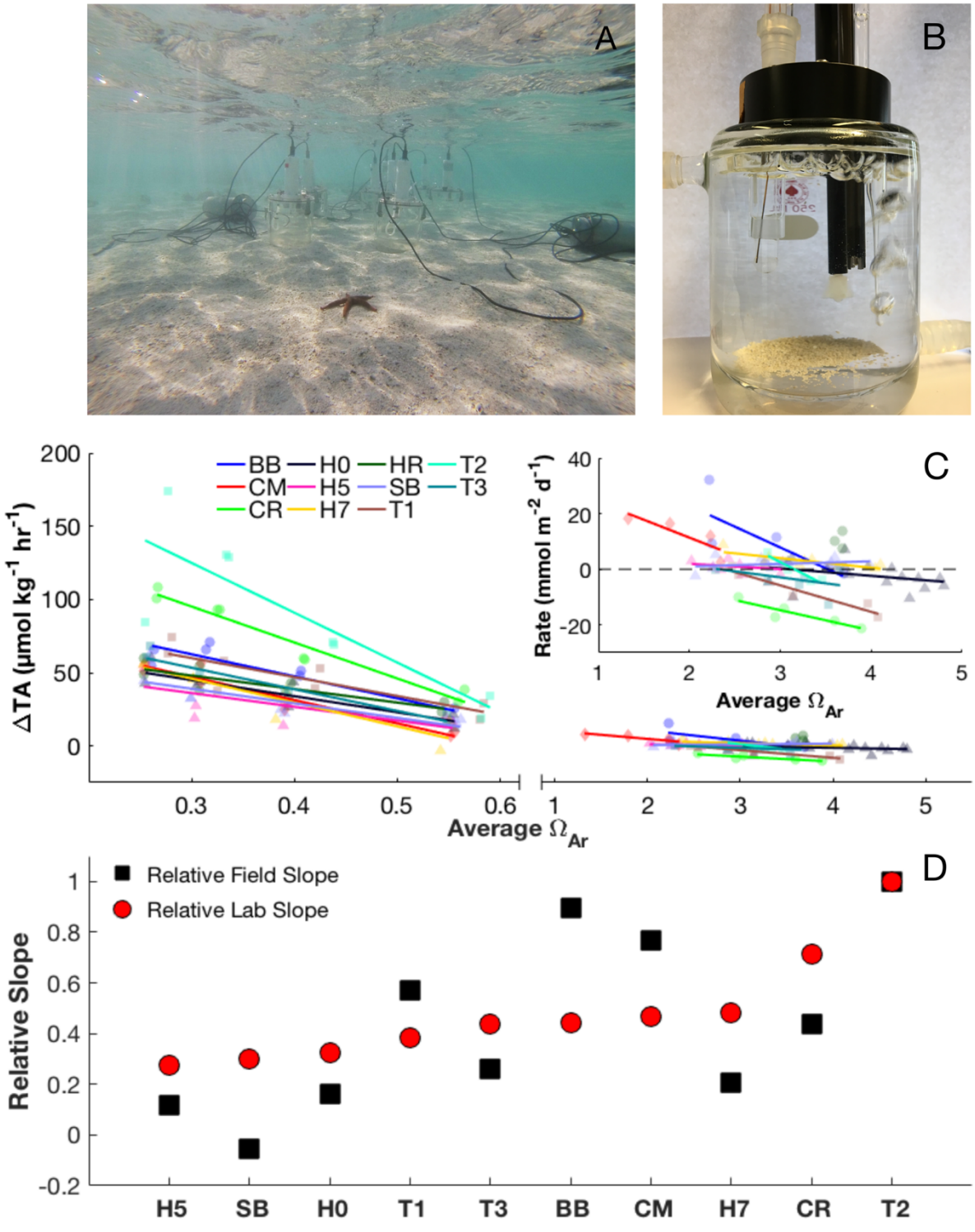
A
B
C
D
BB
H0
HR
T2
CM
H5
SB
T3
CR
H7
T1
ΔTA (μmol kg-1 hr-1)
Rate (mmol m-2 d-1)
Average ΩAr
Relative Field Slope
Relative Lab Slope
Relative Slope
H5
SB
H0
T1
T3
BB
CM
H7
CR
T2

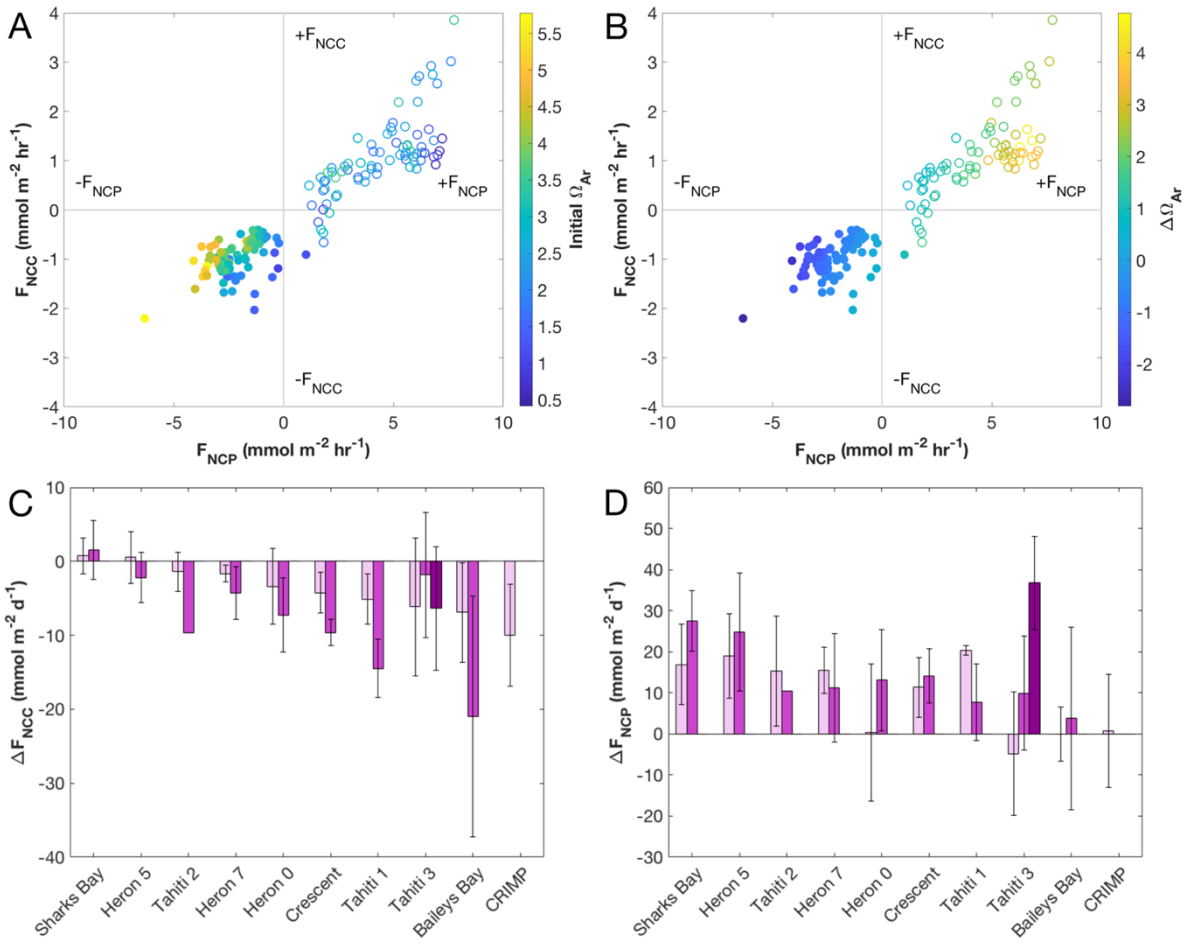

Figure 2.2: Metabolic activity and dissolution rates. (A and B) F_{NCC} versus F_{NCP} rates from all eleven field sites colored by (A) initial Ω_{Ar} at the beginning of nighttime (filled circles) and daytime (open circles) and (B) the change in Ω_{Ar} at over nighttime (filled circles) and daytime (open circles). (C and D) Difference between (C) average F_{NCC} and (D) average F_{NCP} rates for medium (light pink), high (pink) and ultra-high (dark pink) and controls for field incubations. Error bars shows one standard deviation. Rates in both (C) and (D) could not be compared statistically due to unbalanced design and the small number of replicates for many treatments ($n \leq 2$). Hog Reef not included in (C) and (D) because only control incubations were conducted at this site.

Figure 2.3: Average nighttime total alkalinity (TA) as a function of dissolved inorganic carbon (DIC). Vectors are superimposed on contours of Ω_{Ar} at average temperature and salinity from field incubations for each site. TA/DIC vectors are from average starting to final nighttime conditions for control (white triangles) and acidified (black circles) incubations. Asterisks (*) indicate nighttime data from incubations that began at dawn. In control incubations (see upper left hand corner for reference), respiration occurs along the horizontal dashed black line from the starting condition until equilibrium with respect to the most soluble bulk mineral phase is reached (white square). Once equilibrium with respect to the most soluble bulk mineral phase is reached (white square), additional DIC from continued respiration of organic matter drives dissolution (solid white lines) resulting in a 1:1 ratio of TA to DIC. This process is known as metabolic dissolution and drives changes along the dashed black line (labelled as such) until the final condition is reached. Starting conditions of acidified incubations have lower starting Ω_{Ar} and as a result, are already undersaturated with respect to the most soluble bulk mineral phase (Ω_{Ar} of white square). Therefore, DIC produced from respiration immediately drives metabolic dissolution which can result in greater dissolution, but smaller changes in Ω_{Ar} between starting and final conditions ($\Delta\Omega_{Ar}$).

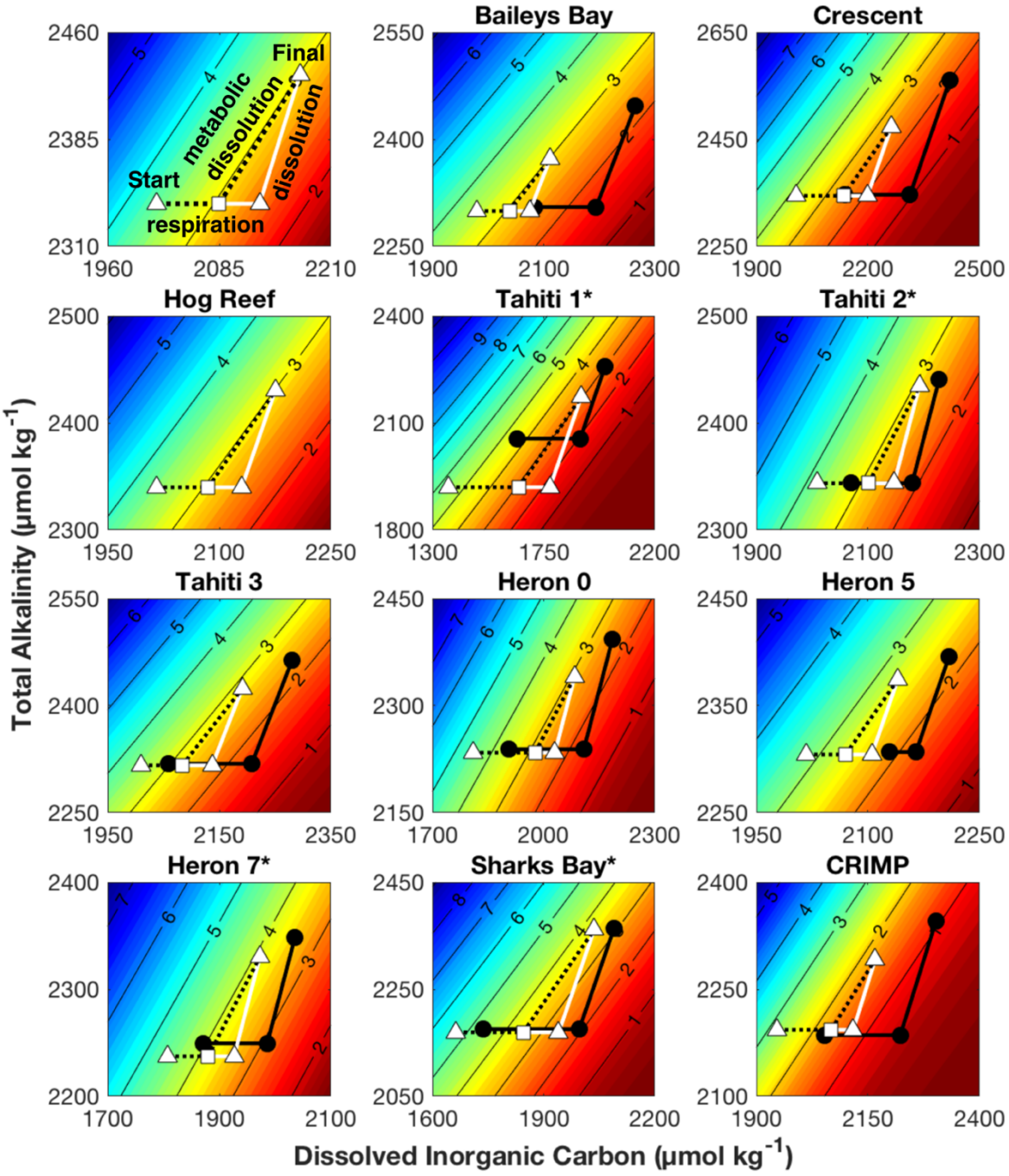
Baileys Bay
Crescent
Hog Reef
Tahiti 1*
Tahiti 2*
Tahiti 3
Heron 0
Heron 5
Heron 7*
Sharks Bay*
CRIMP
Final
metabolic dissolution
dissolution
Start
respiration
Total Alkalinity (µmol kg-1)
Dissolved Inorganic Carbon (µmol kg-1)

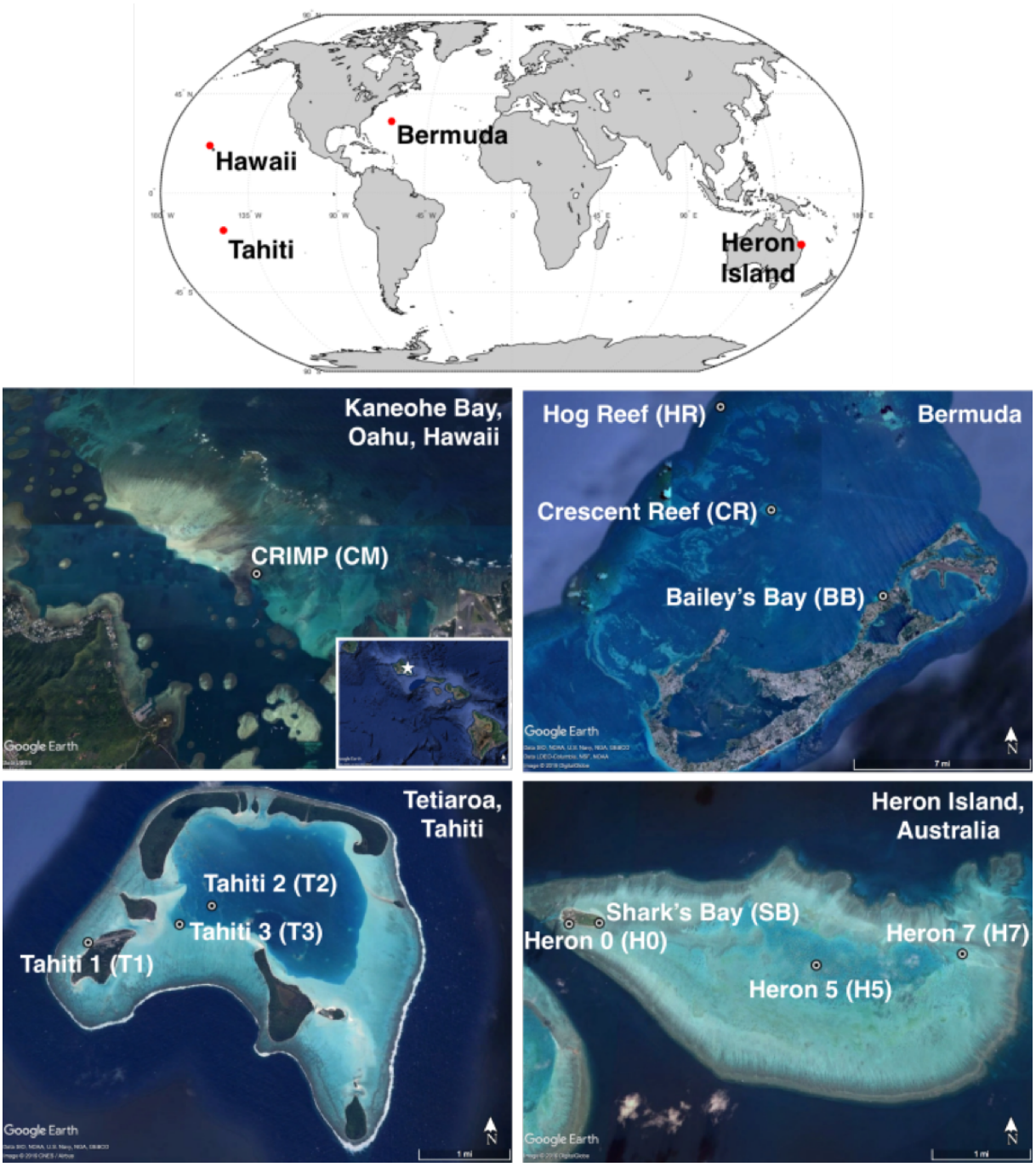

Supplemental Figure 2.1: Location maps of field incubation sites with site names and abbreviations.

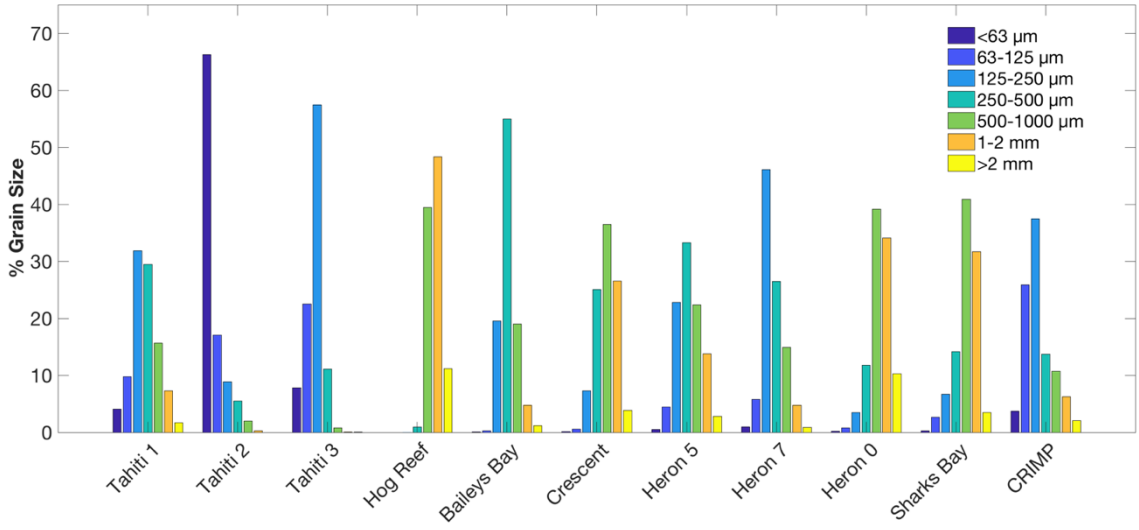

Supplemental Figure 2.2: **Grain size distribution.**

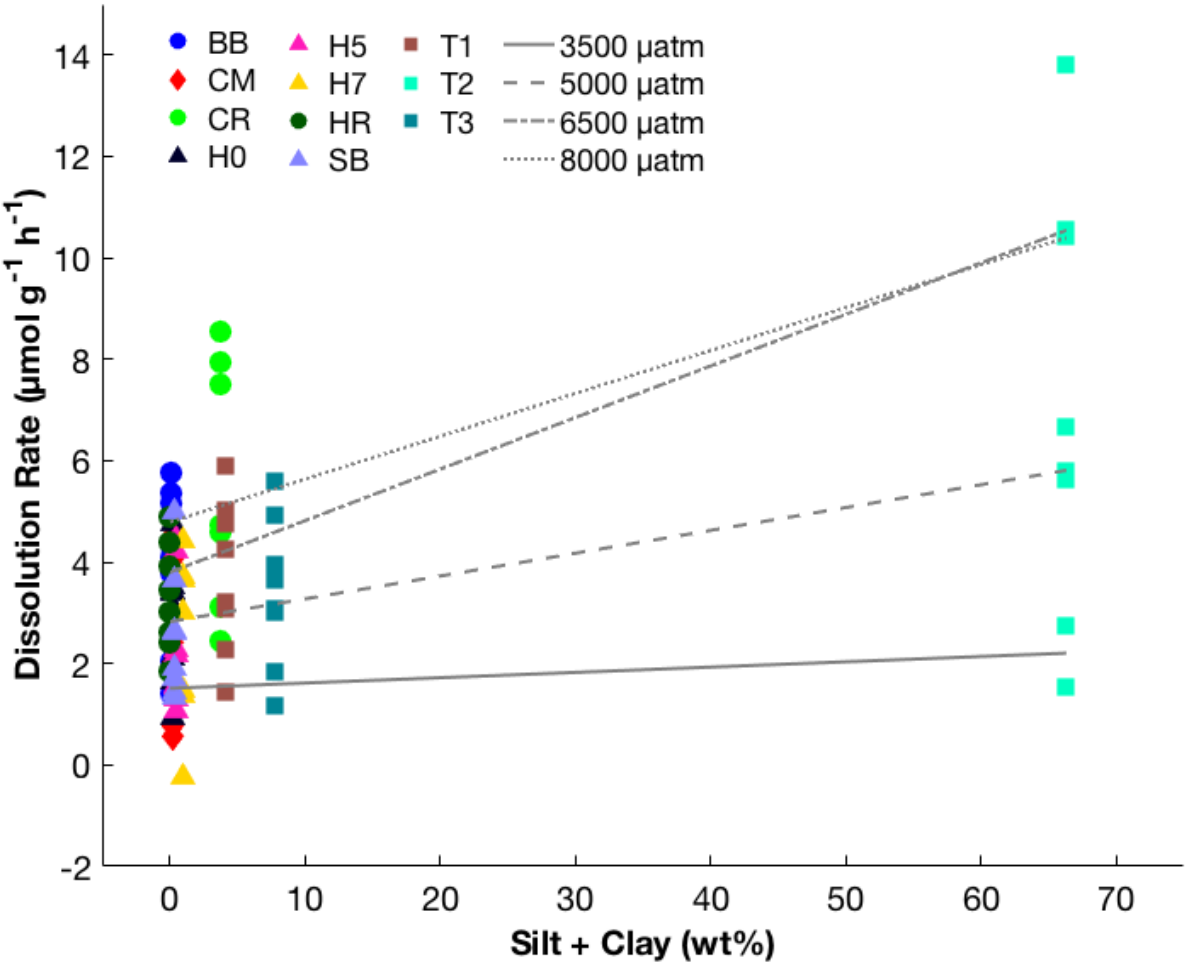

Supplemental Figure 2.3: Normalized laboratory dissolution rates versus weight percent (wt%) of silt and clay fraction (<63 µm). Trendlines represent relationship for rates measured at given experimental pCO_2 level.

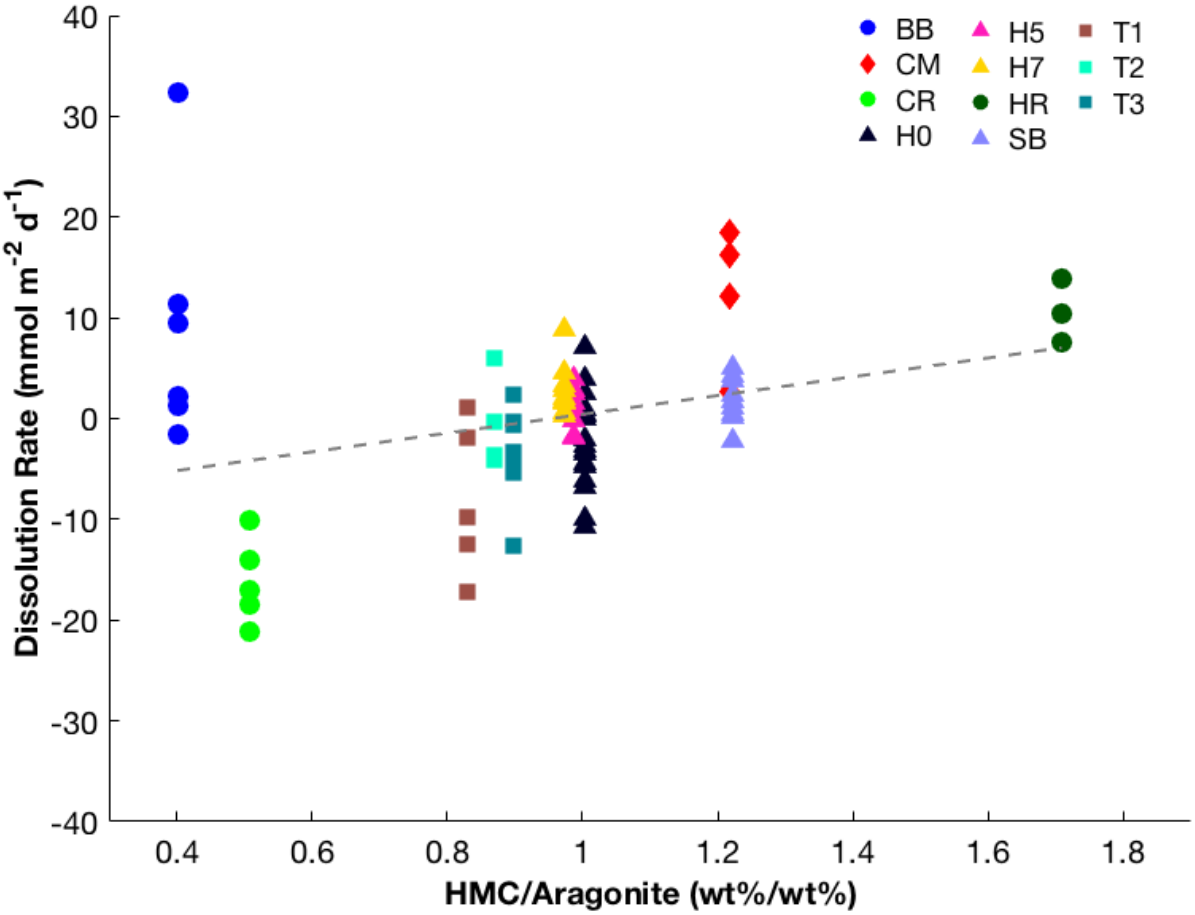

Supplemental Figure 2.4: Net daily field dissolution rates versus ratio of high-magnesian calcite (HMC; weight percent) to aragonite (weight percent).

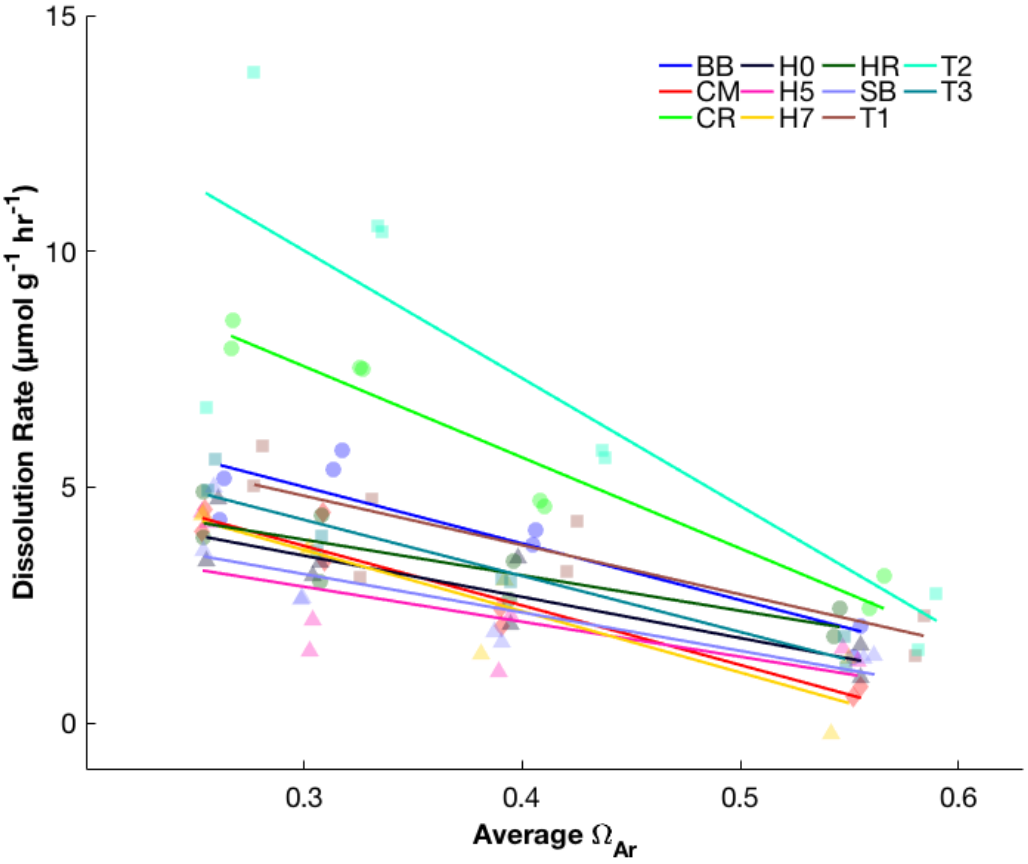

Supplemental Figure 2.5: Laboratory dissolution rates normalized to weight of substrate versus average Ω_{Ar} experienced during 2-hr experiment.

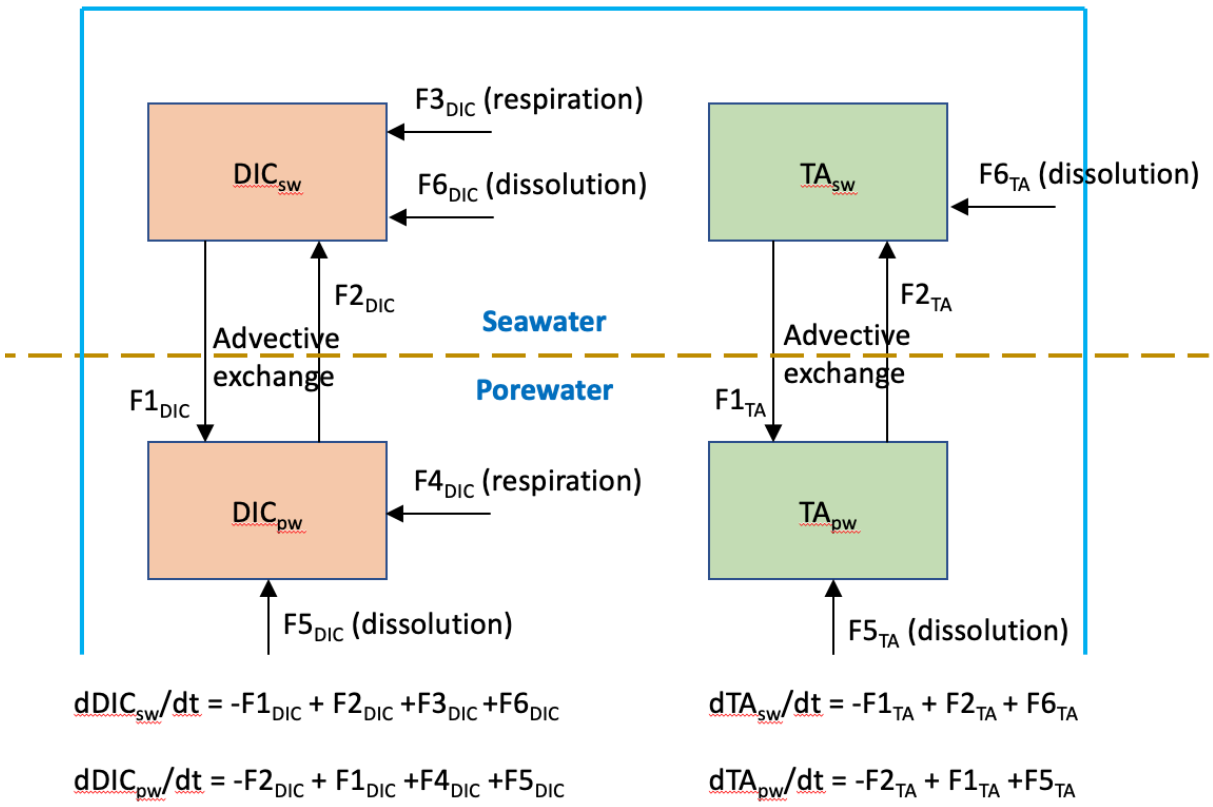

Supplemental Figure 2.6: Schematic of box model and mass balance equations used to assess the influence of varying respiration rates, initial seawater Ω_{Ar}, and sediment mineral solubility on changes in seawater chemistry within the incubation chambers. Model parameters are shown in Supplemental Table 1.4.

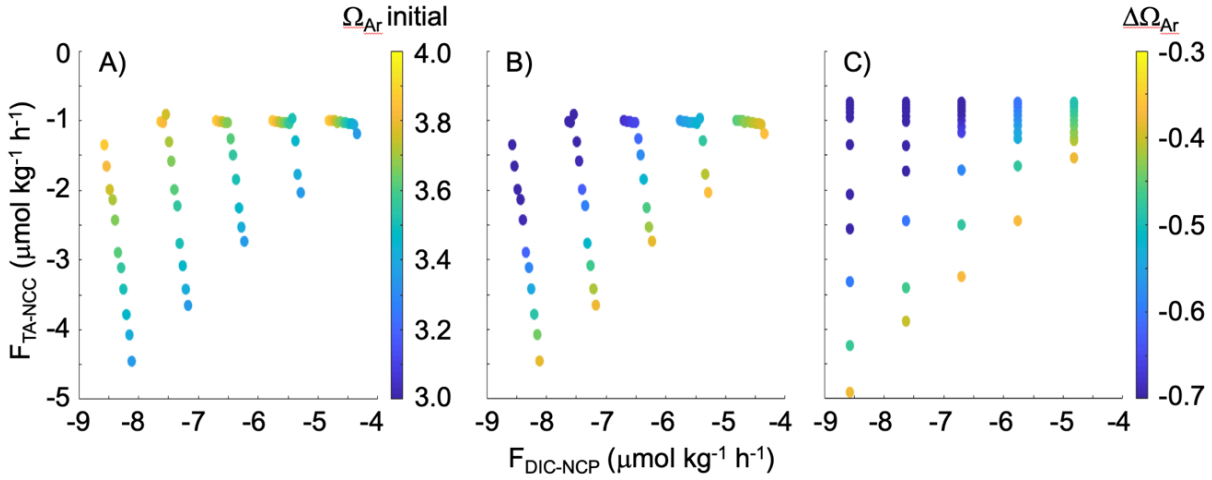

Supplemental Figure 2.7: Model output of sensitivity analyses investigating the effect of initial Ω_{Ar}, sediment mineral solubility, and varying respiration rates on the flux of DIC from respiration ($F_{DIC-NCP}$) and alkalinity from $CaCO_3$ dissolution (F_{TA-NCC}) in the incubation chambers and resulting changes in seawater Ω_{Ar}. (A) Effect of varying respiration rates and initial Ω_{Ar} (colorbar) and (B) the observed changes in seawater Ω_{Ar} (colorbar). (C) Effect of varying respiration rates and the solubility of the most soluble bulk mineral phase in the sediments corresponding to a range in Ω_{Ar} of 2.4-3.4 (i.e., in the most soluble scenario dissolution was initiated at Ω_{Ar}=3.4 and in the least soluble scenario at Ω_{Ar}=2.4).

TABLES

Table 2.1: Physical and chemical properties of sediment samples. N.D. = Not detectable. Asterisk (*) by location name indicates sites with data previously published in (Eyre et al., 2018). Weight percent (wt%).

Location	Median Grain Size (µm)	Mineralogy (wt%)			
		Aragonite	*Mg-Calcite*	*Calcite*	*Mg Content (mol%)*
Bailey's Bay*	365	67.7	27.2	5.1	13.3
Crescent*	182	66.4	33.6	N.D.	13.6
CRIMP*	689	43.1	52.5	4.4	14.3
Heron 0*	907	49.9	50.1	N.D.	14.1
Heron 5	397	49.3	48.6	2.0	13.3
Heron 7	239	50.7	49.3	N.D.	13.5
Hog Reef	1146	36.9	63.1	N.D.	12.6
Shark's Bay	778	45.0	55	N.D.	13.9
Tahiti 1*	276	54.6	45.4	N.D.	14.2
Tahiti 2*	32	53.5	46.5	N.D.	13.5
Tahiti 3*	158	52.7	47.3	N.D.	13.3

Supplemental Table 2.1: Average seawater conditions and NCP/NCC rates (± S.D.) for field incubations at each site. NCP/NCC rates in mmol m^{-2} h^{-1}. Depth values are approximate. Treatment types = Control (C), Medium (M), High (H), Ultra-high (UH). Asterisk (*) by location name indicates sites where 24-hr incubations began at dawn (as opposed to dusk for all other sites).

Location	Depth (m)	Salinity	Treat-ment	Temp. (°C)	NCP		NCC		Initial Ω_{Ar}		$\Delta\Omega_{Ar}$	
					Day	Night	Day	Night	Day	Night	Day	Night
Bailey's Bay	3	37.20 ± 0.00	C	25.93 ± 1.15	2.97 ± 0.77	-1.56 ± 0.22	0.63 ± 0.46	-0.62 ± 0.29	2.96 ± 0.08	3.53 ± 0.02	1.37 ± 0.18	-0.58 ± 0.05
			M	25.93 ± 1.15	3.05 ± 0.96	-1.65 ± 0.99	0.49 ± 0.31	-1.05 ± 0.85	2.23 ± 0.11	2.57 ± 0.05	1.64 ± 0.52	-0.34 ± 0.05
			H	25.93 ± 1.15	1.89 ± 0.1	-0.16 ± 1.66	-0.27 ± 0.55	-1.47 ± 0.80	2.02 ± 0.28	1.28 ± 0.08	1.38 ± 0.45	0.74 ± 0.3
Crescent	2.8	36.90 ± 0.00	C	29.09 ± 0.47	6.42 ± 0.53	-2.68 ± 0.04	2.69 ± 0.09	-0.91 ± 0.06	2.59 ± 0.19	3.81 ± 0.13	2.24 ± 0.12	-1.22 ± 0.06
			M	29.09 ± 0.47	7.17 ± 0.63	-2.47 ± 0.36	2.97 0.06	-1.51 ± 0.23	1.97 ± 0.08	2.52 ± 0.1	2.52 ± 0.37	-0.55 ± 0.07
			H	29.09 ± 0.53	6.17 ± 0.00	-1.32 ± 0.00	2.71 ± 0.00	-1.71 ± 0.00	1.95 ± 0.00	1.60 ± 0.00	2.11 ± 0.00	0.34 ± 0.00
CRIMP	3	35.00 ± 0.00	C	25.97 ± 0.54	1.54± 0.37	-2.47 ± 0.72	0.24 ± 0.21	-0.72 ± 0.33	1.70 ± 0.02	2.81 ± 0.01	0.66 ± 0.20	-1.11 ± 0.03
			M	25.98 ± 0.71	1.69 ± 0.17	-2.53 ± 0.06	-0.12 ± 0.18	-1.18 ± 0.25	1.08 ± 0.23	1.74 ± 0.43	0.76 ± 0.09	-0.65 ± 0.20

Supplemental Table 2.1, Continued

Heron 0	1	35.92 ± 0.05	C	22.63 ± 1.73	5.75 ± 0.66	-3.23 ± 0.32	1.19 ± 0.17	-0.78 ± 0.14	2.86 ± 0.44	4.54 ± 0.36	3.27 ± 0.68	-1.68 ± 0.17
			M	22.63 ± 1.73	5.43 ± 0.82	-2.87 ± 0.38	1.20 ± 0.34	-1.08 ± 0.13	2.43 ± 0.68	3.62 ± 0.66	3.15 ± 0.99	-1.19 ± 0.25
			H	22.63 ± 1.73	6.01 ± 0.41	-2.39 ± 0.32	1.12 ± 0.27	-1.34 ± 0.11	1.91 ± 0.52	2.54 ± 0.69	3.66 ± 0.69	-0.63 ± 0.19
Heron 5	4.7	35.91 ± 0.03	C	22.90 ± 1.36	1.42 ± 0.37	-1.22 ± 0.09	0.58 ± 0.12	-0.50 ± 0.13	2.67 ± 0.09	3.20 ± 0.03	0.50 ± 0.15	-0.53 ± 0.06
			M	22.90 ± 1.32	2.29 ± 0.44	-0.49 ± 0.38	0.78 ± 0.16	-0.61 ± 0.06	2.23 ± 0.04	2.14 ± 0.28	0.87 ± 0.19	0.08 ± 0.28
			H	22.90 ± 1.32	2.92 ± 1.08	-0.57 ± 0.18	0.91 ± 0.38	-0.92 ± 0.42	1.91 ± 0.24	1.63 ± 0.44	1.26 ± 0.46	0.28 ± 0.39
Heron 7*	3.4	35.82 ± 0.09	C	21.75 ± 0.95	2.34 ± 0.32	-1.59 ± 0.09	0.74 ± 0.07	-0.63 ± 0.01	3.66 ± 0.08	4.58 ± 0.09	0.91 ± 0.14	-0.69 ± 0.11
			M	21.75 ± 0.95	3.78 ± 0.42	-1.57 ± 0.09	0.64 ± 0.08	-0.68 ± 0.09	2.31 ± 0.21	4.07 ± 0.12	1.77 ± 0.30	-0.62 ± 0.04
			H	21.75 ± 0.95	3.19 ± 1.22	-1.42 ± 0.16	0.65 ± 0.21	-0.88 ± 0.26	1.92 ± 0.45	3.25 ± 0.31	1.33 ± 0.39	-0.36 ± 0.14
Hog Reef	11	36.90 ± 0.00	C	27.63 ± 0.10	1.86 ± 0.20	-1.36 ± 0.12	-0.31 ± 0.22	-0.54 ± 0.11	2.99 ± 0.06	3.64 ± 0.00	1.35 ± 0.06	-0.65 ± 0.06

Supplemental Table 2.1, Continued

Shark's Bay*	1	35.71 ± 0.00	C	23.24 ± 0.39	5.72 ± 0.52	-3.59 ± 0.10	1.15 ± 0.03	-1.24 ± 0.10	2.24 ± 0.01	5.30 ± 0.35	3.06 ± 0.34	-1.68 ± 0.08
			M	23.24 ± 0.39	6.75 ± 0.30	-3.18 ± 0.28	1.12 ± 0.04	-1.16 ± 0.16	0.94 ± 0.04	4.62 ± 0.06	3.68 ± 0.08	-1.52 ± 0.18
			H	23.24 ± 0.39	7.08 ± 0.15	-2.63 ± 0.06	1.19 ± 0.26	-1.16 ± 0.06	0.47 ± 0.05	3.58 ± 0.21	3.11 ± 0.25	-1.04 ± 0.07
Tahiti 1*	0.5	36.29 ± 0.00	C	29.33 ± 1.72	6.50 ± 1.79	-5.21 ± 1.57	3.02 ± 1.18	-1.62 ± 0.83	3.42 ± 0.09	5.61 ± 0.24	2.19 ± 0.15	-2.58 ± 0.32
			M	29.33 ± 1.92	6.99 ± 0.00	-4.04 ± 0.00	2.57 ± 0.00	-1.60 ± 0.00	1.98 ± 0.00	4.46 ± 0.00	2.48 ± 0.00	-1.49 ± 0.00
			H	29.33 ± 1.72	4.61 ± 0.74	-2.84 ± 0.05	1.28 ± 0.13	-1.16 ± 0.05	1.51 ± 0.16	3.58 ± 0.15	2.06 ± 0.31	-1.16 ± 0.01
Tahiti 2*	7.5	36.30 ± 0.00	C	28.77 ± 0.12	3.37 ± 0.00	-2.36 ± 0.00	1.46 ± 0.00	-0.78 ± 0.00	2.91 ± 0.00	3.80 ± 0.00	0.75 ± 0.00	-0.90 ± 0.00
			M	28.77 ± 0.10	3.87 ± 2.35	-1.62 ± 0.72	1.23 ± 0.65	-0.72 ± 0.28	2.62 ± 0.13	3.18 ± 0.11	1.21 ± 0.70	-0.56 ± 0.23
			H	28.77 ± 0.12	4.00 ± 0.00	-2.06 ± 0.00	0.84 ± 0.00	-1.03 ± 0.00	2.18 ± 0.00	2.78 ± 0.00	1.47 ± 0.00	-0.60 ± 0.00
Tahiti 3	3.5	36.00 ± 0.00	C	29.10 ± 0.69	4.52 ± 2.23	-1.75 ± 0.92	1.56 ± 0.89	-0.74 ± 0.08	2.81 ± 0.51	3.53 ± 0.09	1.64 ± 0.67	-0.71 ± 0.60

Supplemental Table 2.1, Continued

Tahiti 3			M	29.10 ± 0.69	4.56 ± 0.25	-2.14 ± 0.54	1.36 ± 0.26	-1.04 ± 0.09	2.34 ± 0.26	3.05 ± 0.03	1.72 ± 0.01	-0.72 ± 0.29
			H	29.10 ± 0.69	4.91 ± 0.03	-1.32 ± 0.58	1.64 ± 0.06	-0.94 ± 0.10	2.36 ± 0.33	2.59 ± 0.00	1.81 ± 0.10	-0.23 ± 0.32
			UH	29.10 ± 0.77	6.09 ± 0.00	-0.26 ± 0.00	1.53 ± 0.00	-1.19 ± 0.00	1.57 ± 0.00	0.97 ± 0.00	2.77 ± 0.00	0.60 ± 0.00

Supplemental Table 2.2: Results of linear regression model, rate = $ß_0 + ß_1(\Omega_{Ar}) + ß_2(site) + ß_3(\Omega_{Ar} \times site)$, of laboratory and field dissolution rates (rate) as a function of aragonite saturation state (Ω_{Ar}) and site. Bailey's Bay serves as the baseline and p-values for variables and interaction terms represent significant difference from reference group coefficients (Intercept and Ω_{Ar}). Significance values: *p ≤ 0.05, **p ≤ 0.01 , ***p ≤ 0.001.

	Laboratory		Field	
Model Terms	**F-statistics**	**p-value**	**F-statistics**	**p-value**
Ω_{Ar}	$F_{1,66}$=151.3809	< 2.2e-16	$F_{1,56}$=54.726	7.618e-10
site	$F_{10,66}$=20.5465	< 2.2e-16	$F_{10.56}$=17.001	1.303e-13
Ω_{Ar} × site	$F_{10,66}$= 3.7837	0.0004619	$F_{10,56}$= 2.853	0.006111
Variable	**Regression coefficient (ß)**	**Standard Error**	**Regression coefficient (ß)**	**Standard Error**
Intercept	8.6043***	1.2881	52.7686	8.8768
Ω_{Ar}	-12.0015***	3.2217	-14.9791	2.9939
Crescent	4.7448*	1.8312	-45.6274	15.3225
CRIMP	-1.0629	1.7855	-15.7818	13.4171
Heron 5	-3.4924	1.7858	-46.9361	14.4919
Heron 7	-1.0407	1.7889	-38.3985	12.0842
Heron 0	-2.4401	1.7881	-44.4321	11.0237
Hog Reef	-2.4578	1.8057	-49.1926	222.1795
Shark's Bay	-3.0096	1.7632	-53.6527	11.0233

Supplemental Table 2.2, Continued

Tahiti 1	-0.6565	1.8222	-29.9859	12.6256
Tahiti 2	9.5290***	1.7938	-0.1171	30.1608
Tahiti 3	-0.7315	1.8040	-42.7255	14.6466
Interaction Terms				
Ω_{Ar} × Crescent	-7.3005	4.5411	7.6944	4.8836
Ω_{Ar} × CRIMP	-0.6249	4.5011	2.1814	5.9311
Ω_{Ar} × Heron 5	4.5839	4.5114	13.0503	5.4025
Ω_{Ar} × Heron 7	-0.9890	4.5392	11.5231	3.8515
Ω_{Ar} × Heron 0	3.2713	4.4965	12.3045	3.4205
Ω_{Ar} × Hog Reef	4.4635	4.5658	16.8955	60.8334
Ω_{Ar} × Shark's Bay	3.8696	4.4439	15.9191	3.7014
Ω_{Ar} × Tahiti 1	1.5569	4.4530	5.4565	4.0402
Ω_{Ar} × Tahiti 2	-15.0649***	4.3667	-1.7145	9.5132
Ω_{Ar} × Tahiti 3	0.1106	4.5559	10.633	4.7582
Model Fit				
Adjusted R^2	0.8111		0.751	
F-statistic	$F_{21,66} = 18.79$		$F_{21,56} = 12.06$	
p-value	< 2.2e-16		6.559e-14	

Supplemental Table 2.3: Estimated marginal means of linear trends with 95% lower (L) and upper (U) confidence intervals: effect of saturation state on laboratory and field dissolution rates. Group information using Tukey method and 95% confidence. Trends that do not share the same number are significantly different from one another. SE = Standard Error

	Laboratory			Field		
Variable	**Trend (SE)**	**95% CI (L,U)**	**Group**	**Trend (SE)**	**95% CI (L, U)**	**Group**
Bailey's Bay	-12.00 (3.22)	-18.4, -5.57	2	-14.98 (2.99)	-20.98, -8.982	1
Crescent	-19.30 (3.20)	-25.7, -12.91	1,2	-7.28 (3.86)	-15.01, 0.444	1,2
CRIMP	-12.63 (3.14)	-18.9, -6.35	2	-12.80 (5.12)	-23.05, -2.541	1,2
Heron 5	-7.42 (3.16)	-13.7, -1.11	2	-1.93 (4.50)	-10.94, 7.080	1,2
Heron 7	-12.99 (3.20)	-19.4, -6.61	1,2	-3.46 (2.42)	-8.31, 1.398	1,2
Heron 0	-8.73 (3.14)	-15.0, -2.47	2	-2.67 (1.65)	-5.99, 0.639	2
Hog Reef	-7.54 (3.24)	-14.0, -1.08	2	1.92 (60.76)	-119.80, 123.633	1,2
Shark's Bay	-8.13 (3.06)	-14.2, -2.02	2	0.94 (2.18)	-3.42, 5.300	2
Tahiti 1	-10.44 (3.07)	-16.6, -4.31	2	-9.52 (2.71)	-14.96, -4.088	1,2
Tahiti 2	-27.07 (2.96)	-33.0, -21.18	1	-16.69 (9.03)	-34.78, 1.395	1,2
Tahiti 3	-11.89 (3.22)	-18.3, -5.46	2	-4.32 (3.70)	-11.72, 3.093	1,2

Supplemental Table 2.4: Parameters used in model.

Model Parameters for Chambers	
Inner diameter (m)	0.19
Height (m)	0.33
Area of sediments (m^2)	0.028
Average water height (m)	0.17
Average sediment height (m)	0.16
Water volume (L)	4.82
Sediment volume (L)	4.54
Sediment mass (g) @ 0% porosity	13291.83
x% porosity	0.50
Sediment mass (g) @ x% porosity	6645.9
Pore water volume (L)	2.268
Average salinity	36.1
Average temperature	25.0
Seawater average starting DIC @ night (μmol kg^{-1})	1946
Seawater average starting TA @ night (μmol kg^{-1})	2252
Pore water average starting DIC @ night (μmol kg^{-1})	2125
Pore water average starting TA @ night (μmol kg^{-1})	2400
Advective exchange (L m^{-2} d^{-1})	43.0
Advective exchange (L h^{-1})	0.05
Pore water residence time (h)	44.7

REFERENCES

Albright, R., Caldeira, L., Hosfelt, J., Kwiatkowski, L., Maclaren, J.K., Mason, B.B., Nebuchina, Y., Ninokawa, A., Pongratz, J., Ricke, K.L., Rivlin, T., Schneider, K., Sesboüé, M., Shamberger, K., Silverman, J., Wolfe, K., Zhu, K. and Caldeira, K. (2016) Reversal of ocean acidification enhances net coral reef calcification. Nature 531, 1-4.

Albright, R., Takeshita, Y., Koweek, D.A., Ninokawa, A., Wolfe, K., Rivlin, T., Nebuchina, Y., Young, J. and Caldeira, K. (2018) Carbon dioxide addition to coral reef waters suppresses net community calcification. Nature 555, 516-519.

Andersson, A.J. (2015) A fundamental paradigm for coral reef carbonate sediment dissolution. Frontiers in Marine Science 2.

Andersson, A.J. and Gledhill, D. (2013) Ocean acidification and coral reefs: effects on breakdown, dissolution, and net ecosystem calcification. Annual Review of Marine Science 5, 321-348.

Andersson, A.J., Kuffner, I.B., Mackenzie, F.T., Jokiel, P.L., Rodgers, K.S. and Tan, A. (2009) Net Loss of $CaCO_3$ from a subtropical calcifying community due to seawater acidification; mesocosm-scale experimental evidence. Biogeosciences 6, 1811-1823.

Bischoff, W.D., Bishop, F.C. and Mackenzie, F.T. (1983) Biogenically produced magnesian calcite: inhomogeneities in chemical and physical properties; comparison with synthetic phases. American Mineralogist 68, 1183-1188.

Bischoff, W.D., Mackenzie, F.T. and Bishop, F.C. (1987) Stabilities of synthetic magnesian calcites in aqueous solution: Comparison with biogenic materials. Geochimica et Cosmochimica Acta 51, 1413-1423.

Burdige, D.J. and Zimmerman, R.C. (2002) Impact of sea grass density on carbonate dissolution in Bahamian sediments. Limnology and Oceanography 47, 1751-1763.

Comeau, S., Carpenter, R.C., Lantz, C.A. and Edmunds, P.J. (2015) Ocean acidification accelerates dissolution of experimental coral reef communities. Biogeosciences 12, 365-372.

Cyronak, T., Santos, I.R. and Eyre, B.D. (2013a) Permeable coral reef sediment dissolution driven by elevated pCO_2 and pore water advection. Geophysical Research Letters 40, 4876-4881.

Cyronak, T., Santos, I.R., McMahon, A. and Eyre, B.D. (2013b) Carbon cycling hysteresis in permeable carbonate sands over a diel cycle: Implications for ocean acidification. Limnology and Oceanography 58, 131-143.

Deffeyes, K.S. (1965) Carbonate equilibria: A graphic and algebraic approach 1. Limnology and Oceanography 10, 412-426.

Dickson, A.G. (1993) pH buffers for sea water media based on the total hydrogen ion concentration scale. Deep Sea Research Part I: Oceanographic Research Papers 40, 107-118.

Dickson, A.G. and Millero, F.J. (1987) A comparison of the equilibrium constants for the dissociation of carbonic acid in seawater media. Deep Sea Research Part A. Oceanographic Research Papers 34, 1733-1743.

Eyre, B.D., Andersson, A.J. and Cyronak, T. (2014) Benthic coral reef calcium carbonate dissolution in an acidifying ocean. Nature Climate Change 4, 969-976.

Eyre, B.D., Cyronak, T., Drupp, P., De Carlo, E.H., Sachs, J.P. and Andersson, A.J. (2018) Coral reefs will transition to net dissolving before end of century. Science 359, 908-911.

Glud, R.N., Eyre, B.D. and Patten, N. (2008) Biogeochemical responses to mass coral spawning at the Great Barrier Reef: Effects on respiration and primary production. Limnol. Oceanogr. 53, 1014-1024.

Hoegh-Guldberg, O., Mumby, P.J., Hooten, A.J., Steneck, R.S., Greenfield, P., Gomez, E., Harvell, C.D., Sale, P.F., Edwards, A.J., Caldeira, K., Knowlton, N., Eakin, C.M., Iglesias-Prieto, R., Muthiga, N., Bradbury, R.H., Dubi, A. and Hatziolos, M.E. (2007) Coral Reefs Under Rapid Climate Change and Ocean Acidification. Science 318, 1737-1742.

Jeanson, M., Anthony, E.J., Etienne, S. and Dolique, F. (2014) Morphodynamic characterization of beaches on a Pacific atoll island: Tetiaroa, French Polynesia. Journal of Coastal Research 70, 176-182.

Jell, J.S. and Webb, G.E. (2012) Geology of Heron Island and Adjacent Reefs, Great Barrier Reef, Australia. Episodes 35, 110-119.

Kroeker, K.J., Kordas, R.L., Crim, R.N. and Singh, G.G. (2010) Meta-analysis reveals negative yet variable effects of ocean acidification on marine organisms. Ecology Letters 13, 1419-1434.

Lantz, C.A., Schulz, K.G. and Eyre, B.D. (2019) The effect of warming and benthic community acclimation on coral reef carbonate sediment metabolism and dissolution. Coral Reefs 38, 149-163.

Lenth, R.V. (2016) Least-Squares Means: The R Package lsmeans. Journal of Statistical Software 69, 1-33.

Lenth, R.V. (2019) emmeans: Estimated Marginal Means, aka Least-Squares Means. R package version 1.3.3.

Lewis, D.W. and McConchie, D. (2012) Analytical sedimentology. Springer Science & Business Media.

Lewis, E., Wallace, D. and Allison, L.J. (1998) Program developed for CO_2 system calculations. Carbon Dioxide Information Analysis Center, managed by Lockheed Martin Energy Research Corporation for the US Department of Energy Tennessee.

Mehrbach, C., Culberson, C.H., Hawley, J.E. and Pytkowicx, R.M. (1973) Measurement of the apparent dissociation constants of carbonic acid in seawater at atmospheric pressure. Limnology and Oceanography 18, 897-907.

Moberg, F. and Folke, C. (1999) Ecological goods and services of coral reef ecosystems. Ecological Economics 29, 215-233.

Morse, J.W., Andersson, A.J., Mackenzie, F.T., Canfield, D.E. and Lyons, T.W. (2006) Initial responses of carbonate-rich shelf sediments to rising atmospheric pCO_2 and "ocean acidification": Role of high Mg calcites. Geochimica et Cosmochimica Acta 70, 5814-5830.

Morse, J.W., Arvidson, R.S. and Lüttge, A. (2007) Calcium Carbonate Formation and Dissolution. Chemical Reviews 107, 342-381.

Morse, J.W., Zullig, J.J., Bernstein, L.D., Millero, F.J., Milne, P., Mucci, A. and Choppin, G.R. (1985a) Chemistry of calcium carbonate-rich shallow water sediments in the Bahamas. American Journal of Science 285, 147-185.

Morse, J.W., Zullig, J.J., Bernstein, L.D., Millero, F.J., Milne, P.J., Mucci, A. and Choppin, G.R. (1985b) Chemistry of calcium carbonate-rich shallow water sediments in the Bahamas. American Journal of Science 285, 147-185.

Muehllehner, N., Langdon, C., Venti, A. and Kadko, D. (2016) Dynamics of carbonate chemistry, production, and calcification of the Florida Reef Tract (2009-2010): Evidence for seasonal dissolution. Global Biogeochemical Cycles 30, 661-688.

Pandolfi, J.M., Connolly, S.R., Marshall, D.J. and Cohen, A.L. (2011) Projecting Coral Reef Futures Under Global Warming and Ocean Acidification. Science 333, 418-422.

Perry, C.T. and Alvarez-Filip, L. (2018) Changing geo-ecological functions of coral reefs in the Anthropocene. Functional Ecology, 976-988.

Pickett, M. and Andersson, A.J. (2015) Dissolution Rates of Biogenic Carbonates in Natural Seawater at Different pCO_2 Conditions: A Laboratory Study. Aquatic Geochemistry 21, 459-485.

Plummer, L.N. and Mackenzie, F.T. (1974) Predicting mineral solubility from rate data; application to the dissolution of magnesian calcites. American Journal of Science 274, 61-83.

Rao, A.M.F., Polerecky, L., Ionescu, D., Meysman, F.J.R. and de Beer, D. (2012) The influence of pore-water advection, benthic photosynthesis, and respiration on calcium carbonate dynamics in reef sands. Limnology and Oceanography 57, 809-825.

Reaka-Kudla, M.L. (1997) The global biodiversity of coral reefs: a comparison with rain forests. Biodiversity II: Understanding and protecting our biological resources 2, 551.

Ries, J.B., Ghazaleh, M.N., Connolly, B., Westfield, I. and Castillo, K.D. (2016) Impacts of seawater saturation state (Ω_A = 0.4–4.6) and temperature (10, 25 °C) on the dissolution kinetics of whole-shell biogenic carbonates. Geochimica et Cosmochimica Acta 192, 318-337.

Schmalz, R.F. and Chave, K.E. (1963) Calcium carbonate: Factors affecting saturation in ocean waters off Bermuda. Science 139, 1206-1207.

Schönberg, C.H., Fang, J.K., Carreiro-Silva, M., Tribollet, A. and Wisshak, M. (2017) Bioerosion: the other ocean acidification problem. ICES Journal of Marine Science 74, 895-925.

Silverman, J., Lazar, B., Cao, L., Caldeira, K. and Erez, J. (2009) Coral reefs may start dissolving when atmospheric CO_2 doubles. Geophysical Research Letters 36, L05606.

Subhas, A.V., Rollins, N.E., Berelson, W.M., Erez, J., Ziveri, P., Langer, G. and Adkins, J.F. (2018) The dissolution behavior of biogenic calcites in seawater and a possible role for magnesium and organic carbon. Marine Chemistry 205, 100-112.

Takeshita, Y.T., Cyronak, T., Martz, T.R., Kindeberg, T. and Andersson, A.J. (2018) Coral reef carbonate chemistry variability at different functional scales. Frontiers in Marine Science 5, 175.

Towle, E.K., Enochs, I.C. and Langdon, C. (2015) Threatened Caribbean coral is able to mitigate the adverse effects of ocean acidification on calcification by increasing feeding rate. PloS one 10, e0123394.

Tribble, G.W. (1993) Organic matter oxidation and aragonite diagenesis in a coral reef. Journal of Sedimentary Petrology 63, 523-527.

Walter, L.M. and Morse, J.W. (1984a) Magnesian calcite stabilities: A reevaluation. Geochimica et Cosmochimica Acta 48, 1059-1069.

Walter, L.M. and Morse, J.W. (1984b) Reactive surface area of skeletal carbonates during dissolution; effect of grain size. Journal of Sedimentary Petrology 54, 1081-1090.

Walter, L.M. and Morse, J.W. (1985) The dissolution kinetics of shallow marine carbonates in seawater: A laboratory study. Geochimica et Cosmochimica Acta 49, 1503-1513.

Yamamoto, S., Kayanne, H., Terai, M., Watanabe, A., Kato, K., Negishi, A. and Nozaki, K. (2012) Threshold of carbonate saturation state determined by CO_2 control experiment. Biogeosciences 9, 1441-1450.

Yates, K.K., Zawada, D.G., Smiley, N.A. and Tiling-Range, G. (2017) Divergence of seafloor elevation and sea level rise in coral reef ecosystems. Biogeosciences 14, 1739-1772.

Yeakel, K.L., Andersson, A.J., Bates, N.R., Noyes, T.J., Collins, A. and Garley, R. (2015) Shifts in coral reef biogeochemistry and resulting acidification linked to offshore productivity. Proceedings of the National Academy of Sciences 112, 14512-14517.

Chapter 3: Inhibition of shallow carbonate sediment dissolution by organic coatings

Alyssa J. Griffin, Tyler Cyronak, Bradley D. Eyre, Andreas J. Andersson

ABSTRACT

As a result of ocean acidification, calcium carbonate mineral dissolution will increase. This is of particular concern in carbonate dominated environments, such as coral reefs, where ecosystem function rely on net accumulation of carbonate sediments and substrates. Despite the importance of this process, dissolution rates of carbonate sediments and the influence of factors such as seawater carbonate chemistry grain size distribution, mineralogy, and surface characteristics are not well constrained.

In this study, free-drift dissolution experiments were conducted under different pCO_2 conditions using shallow biogenic carbonate sediments from Bermuda and Heron Island, Australia to explore the relative influence of physical and chemical properties on bulk sediment dissolution rates. Dissolution rates (R) for all bulk sediment samples increased with increasing seawater pCO_2, but the absolute rate and the sensitivity ($dR/dpCO_2$) were different between samples. No relationships were found between bulk dissolution rates and grain size distribution or mineralogy. Instead, targeted experiments revealed that organic matter associated with the mineral grains could influence dissolution rates. Sediment samples free from organic coatings resulted in significantly higher (~2-3 times) dissolution rates compared to untreated samples. Furthermore, bulk sediment dissolution rates at Heron Island were inversely correlated with the total organic matter content of the sediments. These results suggest that the presence of organic coatings on the surface of sediment grains may inhibit

dissolution by preventing direct interaction between the surrounding seawater and mineral surface. To better understand the effect of ocean acidification on carbonate sediment dissolution, the role of organic matter inhibition requires further attention.

INTRODUCTION

As a result of anthropogenic CO_2 emissions (Le Quéré et al., 2018), oceanic uptake of CO_2 has led to a global decrease in open ocean surface seawater pH and saturation state with respect to calcium carbonate ($CaCO_3$) minerals (Ω) (Bates et al., 2014; Doney et al., 2009). These changes in seawater carbonate chemistry are collectively referred to as ocean acidification (OA) and are expected to reduce biological calcification rates (Kroeker et al., 2010) while also increasing bioerosion (Schönberg et al., 2017) and carbonate mineral dissolution rates (Andersson et al., 2009; Morse et al., 2006; Tynan and Opdyke, 2011). Because of these anticipated changes, shallow water carbonate mineral dissolution has recently received increased attention (e.g., Andersson et al., 2003; 2007; 2009; Morse et al., 2006; Silverman et al., 2009; Andersson and Gledhill, 2013; Cyronak et al., 2013; Eyre et al., 2014).

Nearly half of global carbonate sediments accumulate in shallow marine environments such as coral reefs, banks, and tropical shelves (Milliman, 1993). In fact, the current function and persistence of coral reefs depend on net accumulation of $CaCO_3$ which occurs when constructive processes (i.e., calcification and import) exceed or are equal to destructive processes (i.e., $CaCO_3$ dissolution and export) (Andersson and Gledhill, 2013; Erez et al., 2011; Eyre et al., 2014; Hutchings, 1986; Kleypas et al., 1999; Kleypas and Langdon, 2006).

Although coral reefs are typically associated with complex $CaCO_3$ structures and framework, as much as 95% of the areal benthic coverage is made up of permeable carbonate sediments (Eyre et al., 2014; Gattuso et al., 1998), making sediments an important reservoir of $CaCO_3$ on coral reefs. Despite surface seawater that is supersaturated with respect to the most commonly occurring $CaCO_3$ mineral phases, carbonate mineral dissolution is an ubiquitous process in shallow carbonate sediments owing to microbial decomposition of organic matter generating acid and seawater undersaturation within interstitial pore waters (Aller, 1982; Andersson et al., 2007; Balzer and Wefer, 1981; Cyronak et al., 2013a; Walter et al., 1990; Walter et al., 1993). Furthermore, an increasing number of studies have shown strong evidence that $CaCO_3$ dissolution will increase in response to increasing surface seawater CO_2 and decreasing pH and Ω (Comeau et al., 2015; Cyronak and Eyre, 2016; Cyronak et al., 2013a; Eyre et al., 2018; Griffin et al., in prep.), with some studies even suggesting that carbonate dissolution is far more sensitive to these changes than biological calcification (Andersson et al., 2009; Eyre et al., 2018).

However, in spite of these projections, shallow water carbonate sediment dissolution has received relatively little attention in the context of OA (Eyre et al., 2014), and many questions remain in terms of the relative importance of different drivers and properties that influence $CaCO_3$ dissolution rates. This includes the influence of seawater and pore water carbonate chemistry (e.g., pCO_2, pH, Ω), sediment grain size distribution, mineralogy, and surface characteristics. As atmospheric CO_2 continues to increase, it is important to develop an understanding of 1) how fast will $CaCO_3$ sediments dissolve under different CO_2 scenarios, 2) where in the sediments will most of the dissolution occur, 3) what property and/or properties (e.g., mineralalogy, grain size, microarchitechture) will cause certain grains to

preferentially dissolve, and 4) are certain habitats and environments more or less sensitive to the projected changes in seawater CO_2 chemistry? Addressing these questions will be important to understand the full effect of OA on the accumulation and preservation of $CaCO_3$ in carbonate dominated ecosystems, such as coral reefs. Some insight to these questions can be found in the extensive body of work that has been dedicated to carbonate mineral dissolution in both the laboratory and the field (for comprehensive reviews, see Morse and Arvidson, 2002; Morse et al., 2007), but there is often a large disparity between field and laboratory observations making it challenging to develop robust quantitative predictions (Morse et al., 2007; Griffin et al., in prep., Griffin and Andersson, in prep.). Furthermore, the majority of laboratory studies have focused on relatively narrow ranges of grain sizes and specific mineral phases that may only represent a fraction of the bulk sediment, which is highly heterogeneous and made up of varying grain sizes and mineralogies. This heterogeneity of both physical and chemical properties between the individual grains that make up the bulk sediments could potentially influence dissolution rates in drastically different ways between contrasting carbonate depositional environments.

Based on the general dissolution literature and a small number of studies focused on bulk carbonate sediment dissolution (Pickett and Andersson, 2015; Walter and Morse, 1985; Yamamoto et al., 2012), existing paradigms suggest that shallow bulk carbonate sediment dissolution rates will increase with: 1) increasing seawater pCO_2 (decreasing pH and Ω) (Griffin et al., in prep.; Pickett and Andersson, 2015), 2) decreasing grain size owing to increasing reactive surface area to volume ratio (Walter and Morse, 1984b), and 3) with increasing proportion of Mg-calcite and/or their mol% $MgCO_3$ due to decreasing mineral stability (Busenberg and Plummer, 1986; Plummer and Mackenzie, 1974). Some studies have

already challenged these paradigms under certain conditions. For example, Walter and Morse (1985) demonstrated that differences in grain microstructural complexity can potentially override thermodynamic constraints and lead to selective dissolution of more stable mineral phases in shallow marine carbonate substrates. Furthermore, the presence of different inhibitors and/or adsorption of organic matter to mineral surfaces, may physically isolate or lower the free-energy of the carbonate mineral surface, affecting reactivity and reaction rates (Suess, 1970).

The overarching objective of this study was to evaluate the bulk carbonate sediment dissolution rates from different coral reef environments in response to increasing pCO_2 and decreasing pH and Ω in the laboratory. Carbonate sediments from Bermuda and Heron Island, Australia, characterized by different grain size distributions and mineral compositions, were exposed to a range of pCO_2/pH conditions using a free-drift reactor to test the following hypotheses:

H1: Bulk carbonate sediment dissolution rates from different coral reef depositional environments have different sensitivity to increasing pCO_2 ($dRate/dpCO_2$) and decreasing pH due to varying sediment properties.

H2: Bulk carbonate sediment dissolution rates and sensitivity increase with increasing proportion of grains classified as fine or smaller because of increasing reactive surface area to volume ratio.

H3: Bulk carbonate sediment dissolution rates and sensitivity increase with increasing proportion and mol% $MgCO_3$ of high Mg-calcite minerals, due to lower mineral stability.

In addition, a subset of experiments was conducted to evaluate the specific influence of grain size on carbonate dissolution rates as well as the influence of the presence of intracrystalline and non-intracrystalline organic matter (Ingalls et al., 2004).

METHODS

Sediment Collection and Analysis

Sample sediments were collected from two carbonate reef environments: Bermuda and Heron Island, Australia. Located in the Sargasso Sea, the Bermuda carbonate platform is a subtropical reef ecosystem comprised of patch reefs located across a central lagoon (i.e., North Lagoon), which is surrounded by outer rim and terrace reefs (Garrett et al., 1971; Scoffin and Garrett, 1974) (Fig. 3.1). Bulk sediment samples were collected from three sites across the Bermuda carbonate platform near Hog Reef (a rim reef), Crescent Reef (a patch reef), and within Bailey's Bay (a seagrass bed) (e.g., Takeshita et al., 2018; Yeakel et al., 2015). Sediment cores were also collected in September 2011 at two additional sites on the Bermuda platform (Fig. 3.1A) down to a sediment depth of 20 cm. The Heron Island lagoon is a platform reef located on the Great Barrier Reef off the eastern coast of Queensland, Australia (Jell and Flood, 1978). Seven surface sediment samples were collected from across the Heron Island lagoon in December 2013 (Fig. 3.1B).

Grain Size

Grain size analysis was performed using the Wet Sieving Analysis method (Lewis and McConchie, 2012) with deionized water and divided into the following grain size fractions: granule/gravel (>2mm), very coarse sand (1000-2000 μm), coarse sand (500-1000 μm), medium sand (250-500 μm), fine sand (125-250 μm), very fine sand (63-125 μm), and silt/clay (<63 μm). Each fraction was dried at 60°C and weighed following grain size separations.

Mineralogy

Mineral analysis was conducted using X-ray diffraction (XRD) to determine the relative composition of calcite, aragonite, and Mg-calcite, as well as the average mol% $MgCO_3$ content. Bermuda bulk and core samples were milled and spiked with 20 wt% fluorite and then mounted on zero diffraction silicon XRD plates. Core samples were analyzed using a Scintag PAD V powder X-Ray Diffractometer with a Cu X-ray tube whereas bulk samples were analyzed with a PANalytical X'Pert Pro XRD diffractometer equipped with a X'Celerator detector using Co K-α radiation. The X-ray data were analyzed and processed using JADE (Materials Data, Inc.). The offset of d-spacing of the calcite 104 peak was used to determine the mol% $MgCO_3$ using the calibration curve developed by Goldsmith et al. (1961) of the bulk samples and, for the core samples, Bischoff et al. (1983). The relative composition of calcite, aragonite, and Mg-calcite was determined based on calibration curves constructed using standards prepared from Iceland spar (calcite), *Diploria labyrinthiformis* (aragonite), and *Homotrema rubrum* (Mg-calcite) in variable composition containing 0, 25%, 50%, 75%,

and 100% of a given mineral phase. Relative mineral composition was calculated based on the mineral peak areas.

The mineralogy of the Heron Island bulk sediment samples was analyzed using a Siemens D501 Bragg–Brentano diffractometer equipped with a graphite monochromator and scintillation detector, using Cu K-α radiation, following the protocols of Nash et al. (2013).

Additional Heron Island Sediment Analyses

The Heron Island samples were also analyzed for permeability, total organic carbon content and $\delta^{13}C$ (organic and inorganic). In addition, six of the seven sediment samples were radiocarbon dated. Coefficients of permeability were measured using a constant head permeameter. Radiocarbon was measured on accelerator mass spectrometer (AMS) at the University of Tokyo on bulk powdered sediments.

For organic matter analyses, approximately one gram (1 g) of carbonate sediment was dissolved in trace-metal grade 6N HCl overnight in a combusted glass vial. Organic matter insoluble in 6 N HCl was removed from the dissolved sediment solution by filtration through a combusted Whatman GFF filter (0.7 m nominal pore size). The filter was rinsed with 1 mL of 1% HCl to remove any acid-soluble organic matter left on the filter, and filtrates were combined. HCl-soluble organic carbon in filtrates was analyzed using a dissolved inorganic carbon (DOC) analyzer. HCl-insoluble organic C on filters was analyzed by elemental analysis isotope ratio mass spectrometry (EA-IRMS). Standards (acetanilide) of known elemental and isotopic composition, and of measured weights, were run every 10-15 samples. The absolute calibration was made by referencing the acetanilide samples to primary working

standards of $CaCO_3$ and Ammonium Sulphate directly calibrated to NBS 19 and IAEA Ammonium Sulphate measured 3 times with every sample run. Soluble and insoluble fractions of samples were summed to obtain total organic carbon (TOC).

For two samples (L-17 and L-18) intracrystalline and non-intracrystalline OC were measured following the method of Ingalls et al. (2004). A fraction of each bulk sample was bleached in 5% NaOCl for eight days at room temperature and TOC was measured using the same protocol as above. Nonintracrystalline OC was calculated as the difference in TOC between the unbleached and bleached sample fractions.

Surface Area

The total surface areas of bleached and unbleached subsamples from L-17 and L-18 were analyzed using a Quantachrome Nova 4200e analyzer from 15-point BET (Brunauer–Emmett–Teller; Brunauer et al., 1938) N_2 adsorption isotherms. The total surface areas of the Bermuda core samples were also analyzed using a Quantachrome Monosorb surface area analyzer (Model MS-12) from the single-point BET method (Brunauer et al., 1938) with 75% N_2 - 25% He gas.

Free-drift Laboratory Experiments

A duplicate free-drift reactor previously described and validated by Pickett and Andersson (2015) was used for all laboratory experiments in this study, following the method of Griffin et al. (in prep.) (See Chapter 2). In brief, 2-hr dissolution experiments were

performed in temperature controlled jacketed beakers, with filtered, UV sterilized seawater. Experiments on each substrate were conducted at four pCO_2 conditions (~3500, 5000, 6500, 8000 μatm) using an N_2-CO_2 gas mixture. This range of pCO_2 values was chosen to represent pCO_2 conditions observed in sediments on representative carbonate platforms such as Bermuda (Pickett and Andersson, 2015) and the Bahamas (Morse et al., 1985b) as well as potentially higher conditions due to ocean acidification. Representative 1.5 gram subsamples of bulk sediments were dissolved in 245 grams of seawater. To assure that the sediment samples more closely represented conditions in the natural environment, the samples did not undergo any grinding, cleaning or sonicating prior to use in the dissolution experiments (Bischoff et al., 1987; Plummer and Mackenzie, 1974; Walter and Morse, 1984a), barring the coarse size fraction from the Bermdua core samples (see below).

The measured TA values between initial and final samples were used to calculate the average rate of dissolution during the 2 h incubation as follows:

$$R = 0.5 \times W_{SW}\left(\frac{\Delta TA - TA_E}{\Delta t \times W_C}\right) \quad (2)$$

where W_{SW} designates the weight of the seawater (kg), ΔTA represents the final minus initial TA (μmol kg^{-1}), TA_E represents the correction for the increase in TA due to evaporation (2.31 ± 1.44 μmol kg^{-1}), t is the length of the experiment (h), and W_C is the weight of the carbonate substrate (g). The total value is multiplied by 0.5 because the dissolution of one mole of $CaCO_3$ results in a two mole increase in TA.

The complete carbonic acid system was calculated based on reactor temperature, salinity, measured pH, and TA using CO2SYS (Lewis et al., 1998) using CO_2 dissociation constants defined by Mehrbach et al. (1973) and refit by Dickson and Millero (1987).

In addition to the bulk sediment dissolution experiments, dissolution rates were also measured for three different grain size fractions (500 – 1000 μm [coarse], 125 – 250 μm [fine]. and 63 – 125 μm [very fine]) from two contrasting locations on the Bermuda carbonate platform (Stations 3 and 6, see Fig. 3.1A). Samples were chosen to minimize mineralogical differences between the size fractions and across sites as much as possible. The coarse size fractions were sonicated in ethanol to remove adhered submicron particles, but the fine and very fine fractions were not prepared in any way.

Statistical analyses

All statistical analyses were carried out using R 3.5.2. A multiple linear regression model was used to examine the dependency of measured dissolution rates to changes in average pCO_2 levels (continuous) and sample (categorical) for all experiments. Model results were generated using the lm function (Lenth, 2016). Linear regression was also used to examine the dependency of measured dissolution rates on changes in physical or chemical properties of interest (i.e., median grain size, the ratio of high-magnesian calcite to aragonite (wt%/wt%), the mol% $MgCO_3$). Estimated marginal means for trends, along with SE and 95% CI, were calculated using the emmtrends function (Lenth, 2019). To determine significant differences between trends, Tukey's multiple comparisons test on estimated marginal means for linear trends was conducted using the cld function (Lenth, 2019). Alpha levels of 0.05 were considered significant for all statistical tests.

RESULTS AND DISCUSSION

Bulk sediment dissolution rates

Dissolution rates for the ten Bermuda and Heron Island bulk sediment samples exposed to pCO_2 levels from 3000 to 8000 µatm ranged from approximately 0.6 to 8.5 µmol kg^{-1} hr^{-1} with a few samples experiencing net precipitation at lower pCO_2 conditions (Fig. 3.2). The overall highest dissolution rates from individual experiments were observed from the Crescent Reef sample or from Heron Island sample L-27 and the lowest from Heron Island samples L-18, L-25, or L-22, depending on the pCO_2 condition. Overall, the dissolution rates of all bulk sediment samples increased with increasing pCO_2, with significant differences in slopes (i.e. the sensitivity of dissolution rate to changes in pCO_2) between sites (Supplemental Tables 3.1 and 3.2), with the highest and lowest sensitivities observed in L-18 and L-22, respectively.

In support of hypothesis 1, there were significant differences in the sensitivity ($dRate/dpCO_2$) to increasing pCO_2 between the different bulk sediment samples (Supplemental Tables 3.1 and 3.2). However, median grain size (hypothesis 2), the ratio of high-magnesian calcite to aragonite (wt%/wt%) and the mol% $MgCO_3$ (hypothesis 3) were not found to be significant predictors of the sediments' sensitivities.

Dissolution rates of specific grain size fractions

Although median grain size was not a significant predictor, different grain size fractions may play more or less important roles in overall dissolution rates. For example, smaller grains have higher surface area to volume ratio than larger grains and are more susceptible to dissolution (Chave and Schmalz, 1966; Pytkowicz, 1969). Median grain size may not fully capture these differences between size fractions, since it is only a metric of the

overall grain size distribution. For this reason, the dissolution rates of three different grain size fractions with near-identical mineralogy from two locations in Bermuda were measured (Supplemental Table 3.3). Counter to the existing paradigm, the results for these experiment showed that the largest (coarse) grain sizes dissolved significantly faster than the smaller (fine, very fine) grain sizes (Fig. 3.3A; Supplemental Tables 3.4 and 3.5) for both locations. No correlation was found between dissolution rates and mineralogy or BET surface area of the grains that could elucidate this unexpected pattern (Supplemental Table 3.3). Because of the counterintuitive nature of these results, identical experiments were conducted on sonicated, calcite (Icelandic spar) of the same grain size fractions to eliminate the possibility of any experimental design artifacts or issues with the reactor. Calcite grains dissolved in accordance with the established paradigm, with dissolution rates increasing with decreasing grain size, but this trend was not apparent until the highest pCO_2 treatment (Fig. 3.3B). Nonetheless, because of the clear separation in dissolution rates as a function of grain size (albeit inverse to expectations) for the Bermuda sediment samples, other properties must be responsible for the unexpected trends.

Substrate preparation

All samples were prepared identically to the maximum extent possible, but the coarse fractions were sonicated whereas sonication was not possible for the fine and very fine fractions. The purpose of sonication is to remove microscopic particles that adhere to the grains' surfaces and initially dissolve very quickly, therefore increasing integrated dissolution rates. Thus, sonication typically results in lower dissolution rates compared to non-sonicated

samples. However, when an identical fine sediment subsample was sonicated, it resulted in slightly higher dissolution rates than its unsonicated equivalent (Supplemental Fig. 3.1; Supplemental Table 3.6). Nonetheless, the observed change was small relative to the observed difference between the very fine, fine and coarse samples.

Inhibition via organic coatings

One hypothesis that may explain the counterintuitive grain size results could be inhibition by organic coatings that act as a protective barrier between the mineral surface and the surrounding seawater (Morse, 1983; Pytkowicz, 1969; Suess, 1968). Biogenic carbonates can contain organic matter (OM) that is both intracrystalline and nonintracrystalline in nature (Ingalls et al., 2004). Intracrystalline OM is incorporated into the carbonate mineral structure during biogenic precipitation, whereas nonintracrystalline OM may have a variety of mineral associations (e.g., intercrystalline, adsorbed or detrital) (Ingalls et al., 2004). When OM physically attaches to mineral surfaces, it may isolate the carbonate mineral surface and in turn, have a strong regulatory influence on the carbonate-seawater equilibration at the mineral-seawater interface. Several studies have shown that certain dissolved organic compounds can inhibit abiotic calcite dissolution (Barwise et al., 1990; Compton and Sanders, 1993; Morse, 1974; Suess, 1968, 1970, 1973) and that organic coatings may inhibit biogenic calcite dissolution (Honjo and Erez, 1978; Keir, 1980). However, few studies have investigated the role of OM as an inhibitor of dissolution in shallow-water biogenic carbonate sediments (Suess, 1968). Using sediment samples from Bermuda, Suess (1968) demonstrated the presence of extensive organic coatings on mineral grains via staining with methylene blue.

Coincidentally, these samples were collected nearby the Bermuda sampling locations of the present study. Furthermore, Suess (1968) showed that carbonate grains did not dissolve significantly when exposed to undersaturated solution, but dissolved rapidly after treatment with H_2O_2 that destroyed the organic coatings. Regrettably, we were unable to carry out similar experiments with our Bermuda sediment samples due to limited sample volume, but were instead able to assess OM properties of the samples from Heron Island.

Bulk sediment dissolution sensitivity vs organic matter content

In addition to grain size distribution (Supplemental Table 3.7) and mineralogy (Supplemental Table 3.8), the bulk sediment samples from Heron Island were also analyzed for TOC, $\delta^{13}C$ of TOC, $\Delta^{14}C$, and sediment permeability (Supplemental Table 3.9). Pairwise linear correlation analyses (Pearson r) between these properties and the dissolution rate sensitivity to pCO_2 ($dR/dpCO_2$) for the different stations were used to identify and explore any potential relationships. The only significant correlations from this analysis were negative correlations between the dissolution sensitivity and weight percent of organic carbon in the bulk samples ($r=-0.78$, $p<0.05$) as well as the $\delta^{13}C$ signatures of the associated organic carbon ($r=-0.93$, $p<0.01$; Fig. 3.4). These results suggested that $dR/dpCO_2$ increases with decreasing TOC and as the $\delta^{13}C$ of the OM becomes more depleted. No other sediment properties showed any significant correlations with $dR/dpCO_2$. Although these correlations support the hypothesis that organic coatings may inhibit dissolution rates of the sediment samples, they do not unequivocally prove it. Consequently, additional experiments were conducted to explicitly demonstrate the role of organic matter coatings and their impact on shallow biogenic carbonate dissolution rates.

Influence of intracrystalline vs nonintracrystalline organic matter

To explicitly evaluate the role of organic coatings on dissolution rates, OM was removed via surficial oxidation (bleaching) from the bulk samples with the highest and lowest TOC values (L-17 and L-18, respectively). This method is capable of distinguishing between intracrystalline OC (OC of bleached subsamples) and nonintracrystalline OC (the difference in OC between unbleached and bleached subsamples) because surficial oxidation during the bleaching process does not degrade or remove organic compounds incorporated in the mineral lattice (Gaffey and Bronnimann, 1993). The bleached L-17 and L-18 subsamples were then used in identical dissolution experiments to those run with their unbleached counterparts (Fig. 3.5). As with all other samples, the dissolution rates of the bleached samples increased with increasing pCO_2, but overall, the rates were significantly higher than those of the unbleached samples (Fig 3.5; Supplemental Table 3.10). In addition, the sensitivity of the bleached samples' dissolution rates to changes in pCO_2 were no longer significantly different, as they were in the unbleached samples, following the removal of the nonintracrystalline OM. These results confirm that OM coatings are indeed inhibiting carbonate dissolution in these carbonate sediments (Suess, 1968) and influencing their sensitivity to changes in pCO_2, although, the exact mechanism is unknown. Previous studies have suggested that if the particle is completely isolated from the surrounding seawater, the OM simply blocks chemical interactions between the mineral solid and surrounding solution (Suess, 1968, 1970). The presence of organic matter could also lower the free-energy of mineral surfaces (Suess, 1970). In the present study, the average total surface area increased approximately 1.4 and 2.2 times in the bleached subsamples of L-17 and L-18, respectively, relative to their unbleached subsamples (Fig. 3.5, inset), suggesting that the organic coatings reduced the reactive surface

area, and thus, the total free-energy of the mineral surface (Suess, 1970). However, it is unknown to what extent grain surfaces were isolated in the unbleached samples. Analyses of the ratio between nonintracrystalline and intracrysatalline OC were approximately 1.2 and 1.0 in L-17 and L-18, respectively (Fig. 3.6; Supplemental Table 3.11).

The observed correlation between the $\delta^{13}C$ and $dR/dpCO_2$ may further support the role of organic coating as inhibitors of dissolution. In this study, the $\delta^{13}C$ of the insoluble OC pool was isotopically heavier for nonintracrystalline OC relative to the intracrystalline OC for both samples (Fig. 3.6; Supplemental Table 3.11). If $\delta^{13}C$ of nonintracrystalline OC is consistently heavier than intracrystalline OC in these carbonate sediments, the overall $\delta^{13}C$ of the TOC (intracrystalline + nonintracrystalline) associated with a mineral grain would become heavier with greater ratios of nonintracrystalline:intracrystalline OC. This could explain the observed trend of decreasing $dR/dpCO_2$ in samples with both higher TOC and enriched $\delta^{13}C$, as indicated by the strong correlations between sensitivities and these variables (Fig. 3.4).

Organic matter coatings and sediment grain size

Although additional OM analysis was not performed on the Bermuda size fractions due to sample limitations, Carter and Mitterer (1978) determined that OM compounds tend to be preferentially associated with smaller grain sizes due to their larger surface area to volume ratio, whereas larger grain-sizes (>250 um) tend to have greater intracrystalline material. This suggests that coarse grains may have less nonintracrystalline OM to inhibit dissolution, leading to higher dissolution rates than smaller size fractions with greater nonintracrystalline organic matter associated with their surfaces. This could explain the higher dissolution rates

observed in the coarse fraction relative to the finer fractions, but further experimentation is needed to elucidate the relationship between grain size and organic matter coatings.

Comparison to previous studies

Several other studies have investigated the influence of numerous organic compounds on carbonate mineral dissolution when chemically adsorbed onto the mineral surface (Barwise et al., 1990; Chave, 1965; Compton et al., 1989; Compton and Sanders, 1993; Morse, 1974; Müller and Suess, 1977; Naviaux et al., 2019; Suess, 1970, 1973; Unwin and Compton, 1990), but the majority of experiments in these studies were conducted on abiotic substrates, in dilute solutions and through the addition of various known organic compounds to the experimental solution. Therefore, any extrapolations of their findings to shallow biogenic carbonates must be made with considerable caution, if at all. Also, the range of magnitude in the effects of organic matter on reaction rates observed across these studies is also quite variable and some studies even report little to no effect (Morse, 1974; Sjöberg, 1978).

The latter is also true for the few studies on deep-sea biogenic carbonates, where some suggest that coatings are responsible for the inhibition of dissolution (Honjo and Erez, 1978; Keir, 1980), but another study, using identical methods for organic matter removal through surficial oxidation, showed no change in dissolution rates between bleached and unbleached subsamples (Subhas et al., 2018).

Dissolution rates from our experiments in the bleached sediments were approximately 2-3 times greater than those in the unbleached samples, which is of similar magnitude in for coccoliths (Honjo and Erez, 1978; Keir, 1980) and foraminifera (Honjo and Erez, 1978) when

organic matter is removed via similar surface oxidation methods. Although, it is important to note that these studies were done on subsamples of deep-sea sediments (Honjo and Erez, 1978) or cultured coccoliths (Keir, 1980), which have very different physical and chemical properties from shallow carbonate sediments due to differences in source (i.e., original calcifying organism) as well as varying life and diagenetic histories (Morse et al., 2007).

The results of this study suggest that the presence of organic coatings may override the influence of grain size and mineralogy on dissolution rates in shallow bulk sediments. For this reason, conducting experiments with shallow, bulk carbonate sediments with little to no preparation may improve applicability of laboratory dissolution rates to natural shallow carbonate environments. However, the pervasiveness of inhibited dissolution via organic coatings is unknown. Certain results from this study and the work of Suess (1968) suggest that inhibition of dissolution via organic coatings in shallow carbonate sediments may be an important and widespread mechanism.

In this study, the relationship between TOC and $\delta^{13}C$ and the sensitivities of dissolution rates to changes in pCO_2 was significant across all seven Heron samples analyzed. These samples, although from one carbonate environment, represent a wide range in numerous physical and chemical properties and yet no other properties demonstrated any significant controls on dissolution rates. Inhibition via organic coatings also seems to be a plausible explanation for the surprising results in dissolution rates between grain size fractions from the Bermuda sediments. These results are in keeping with the work of Suess (1968) which reported that sediments from across the Bermuda platform were shown to dissolve as anticipated according to mineralogy and grain size (see hypotheses 2 and 3) only after organic

coatings were removed (Suess, 1968). Suess (1968) also reported that organic coatings were ubiquitous across grain size fractions and spatial and vertical distributions, as observed in recent Bermuda sediments with no significant variations between environments.

The relationship between organic matter and carbonate dissolution rates remains highly complex and multi-faceted. In stark contrast to organic coatings potentially inhibiting dissolution, the respiration of organic matter associated with sinking carbonate aggregates or in sediment pore waters can increase dissolution by creating undersaturated microenvironments that increase dissolution through the release of metabolic CO_2 (Aller, 1982; Burdige and Zimmerman, 2002; Cyronak et al., 2013b; Eyre et al., 2014; Milliman et al., 1999; Morse et al., 1985a; Schiebel et al., 2007; Troy et al., 1997). The interplay of these two contradictory roles of organic matter may be particularly complex in shallow carbonate sediments, which undergo diel cycles of photosynthesis and respiration (Cyronak et al., 2013b; Werner et al., 2008; Yates and Halley, 2006) and often times are subject to increased organic matter input from terrestrial sources (Fabricius, 2005; Hoegh-Guldberg et al., 2007).

Clearly, further experimentation is needed to determine the chemical nature of the organic material associated with shallow carbonate mineral surfaces and how these it may interact with both the mineral surface and changes in surrounding seawater chemistry (particularly those that are expected to enhance dissolution- e.g., ocean acidification).

CONCLUSIONS

The findings of this study support the hypothesis (H1), that bulk carbonate sediment dissolution rates from different coral reef depositional environments have different sensitivity

to increasing pCO_2 ($dRate/dpCO_2$) and decreasing pH due to varying sediment properties. However, these differences could not be attributed to increasing dissolution sensitivity with increasing proportion of grains classified as fine/smaller (H2) or with increasing proportion and mol% $MgCO_3$ of high Mg-calcite minerals (H3), Instead, evidence from this study suggests that $dR/dpCO_2$ in bulk shallow carbonate sediments may differ due to the presence of organic matter which acts as a protective coating on mineral surfaces. This trend appears to be applicable across a diverse sedimentary carbonate environment (Heron Island), but additional analyses on carbonate sediments from various carbonate environments will help elucidate the pervasiveness of this mechanism in shallow carbonate sediments. Previous work, however, suggests that this may be a widespread phenomenon in vastly different shallow carbonate environments (Suess, 1968). Inhibition via this mechanism may also be greater in smaller grain sizes which tend to adsorb higher amounts of organic matter, but further investigation is needed to confirm this trend. The use of molecular level analytical techniques with the ability to characterize the surfaces of the sediments in greater detail would be of particular use in determining the precise mechanism for dissolution inhibition via organic matter coatings at the surface-seawater interface.

In a time where shallow carbonate environments, such as coral reefs, are under threat from ocean acidification, increased terrestrial inputs of organic matter and a suite of other anthropogenically-driven changes, it is critical that we strengthen our understanding of what seems to be the very complex, but equally important roles of organic matter in shallow carbonate dissolution processes. This understanding will have important implications for early diagenesis in carbonate sediments, the accumulation and preservation of both organic matter

and carbonate minerals, and both the short- and long-term cycling of carbonates in marine environments.

ACKNOWLEDGEMENTS

This project was funded by the U.S. National Science Foundation (NSF) OCE 14-16518 (AJA, RJ) and OCE 12-55042 (AJA). We are grateful for the assistance of Ms. Margot White, Ms. Tran Nguyen, and Mr. Bruce Deck for their assistance with organic matter analyses.

Chapter 3, in part, is in preparation for submission for publication. Griffin, A. J., Cyronak, T., Eyre, B., Andersson, A. J.. The dissertation author was the primary investigator and author of this material.

FIGURES

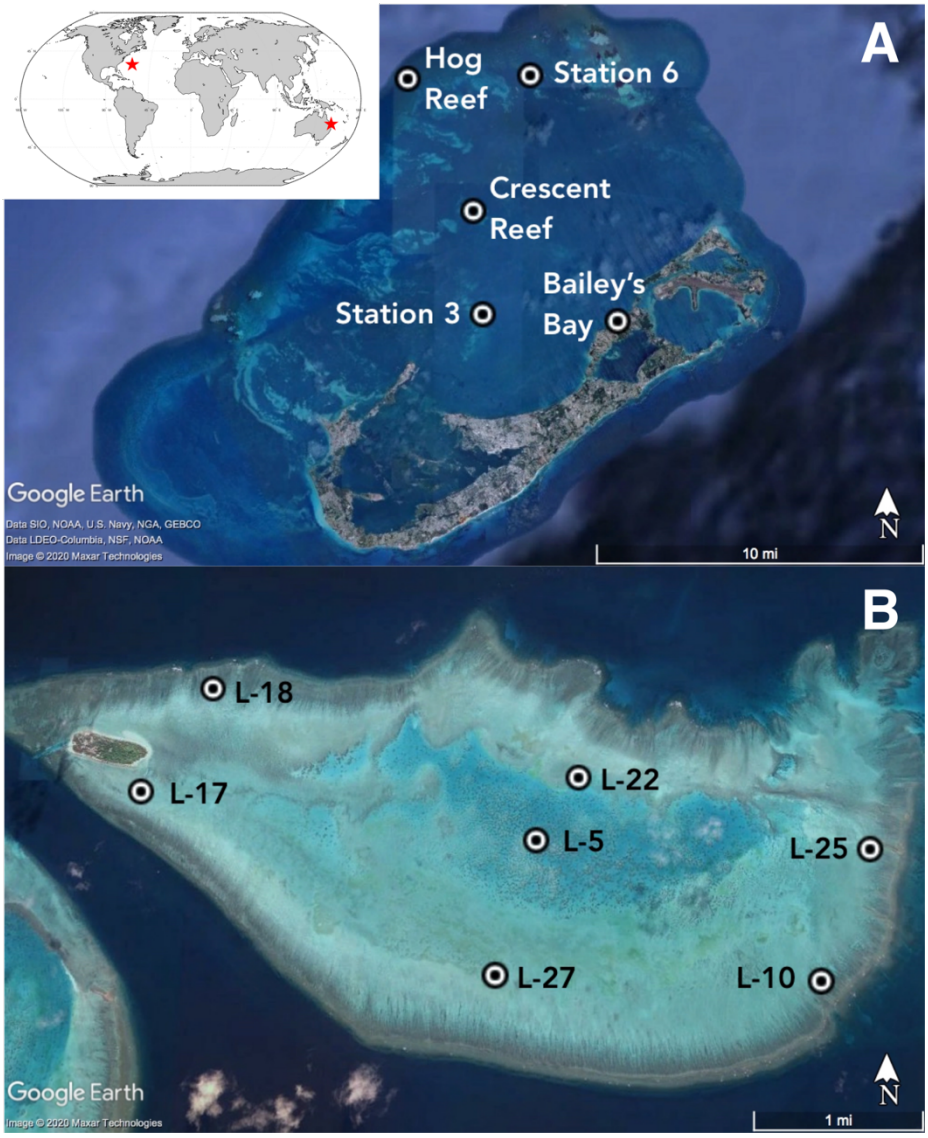

Figure 3.1: Location maps for A) Bermuda and B) Heron sample collection sites. Samples used in Heron Island experiments labelled in magenta.

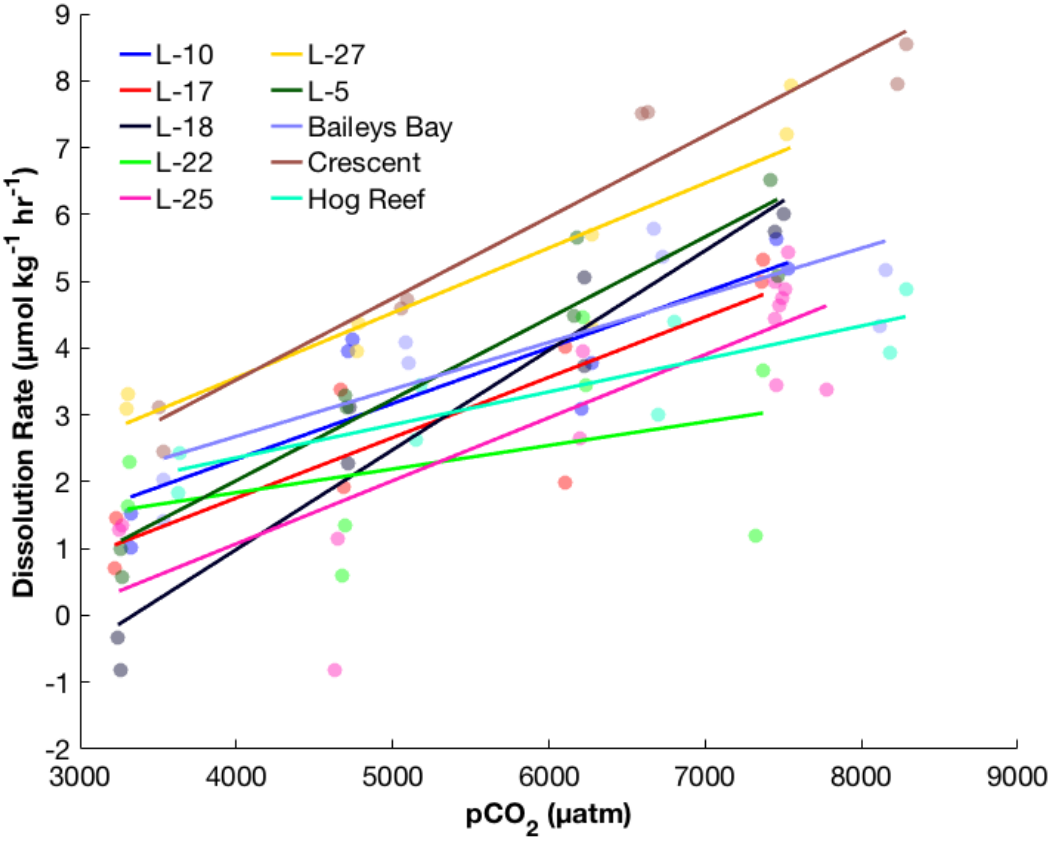

Figure 3.2: Heron Island bulk sediment dissolution rates (µmol g^{-1} hr^{-1}). Each point represents a measurement from one duplicate reactor.

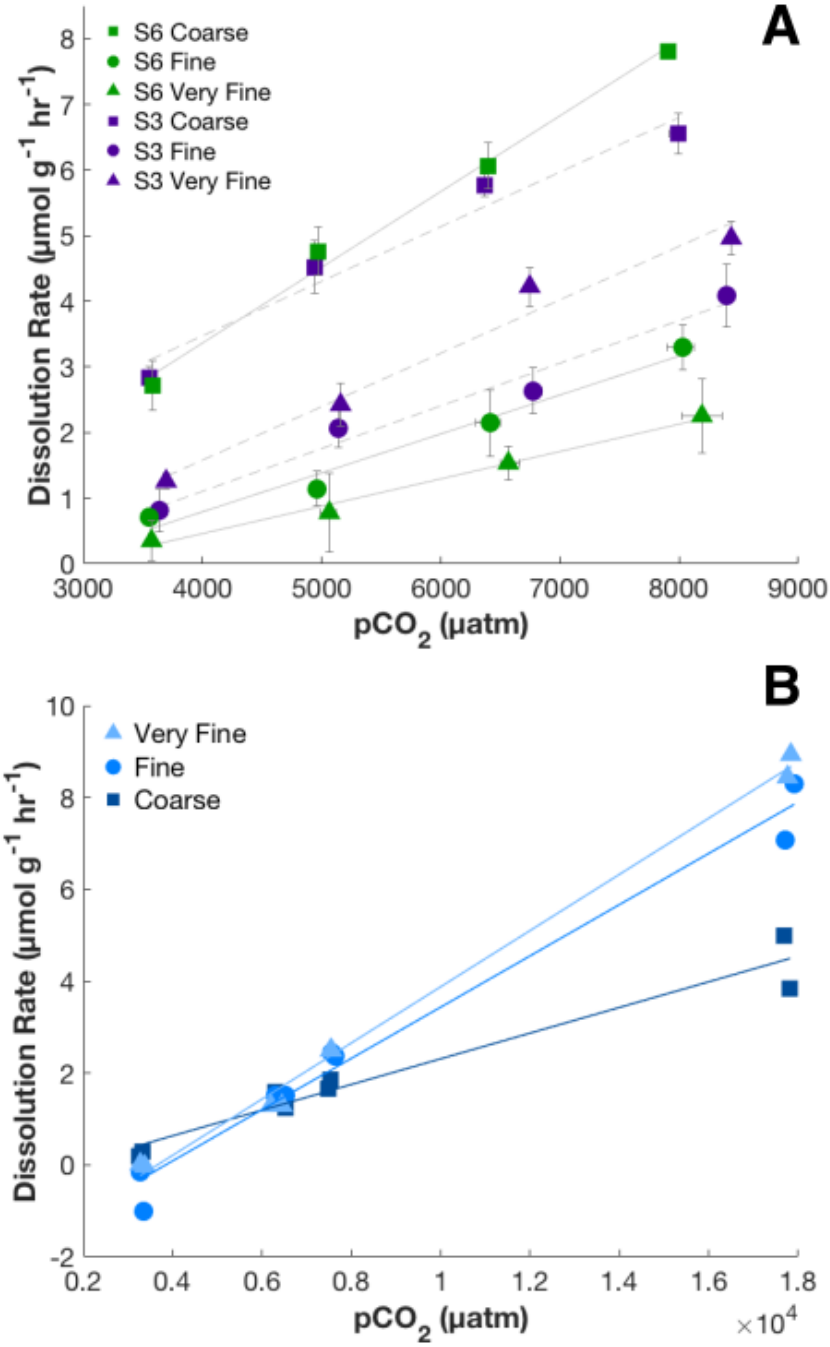

Figure 3.3: Dissolution rates (µmol g^{-1} hr^{-1}) of Bermuda grain size fractions. Coarse (squares), fine (circles) and very fine (triangles) size fractions from Station 6 (green) and Station 3 (purple) on the Bermuda platform. X-error represents range of pCO_2 experienced over the course of the 2-hr. experiment. Y-error represents one standard deviation of duplicate measurements (n=4).

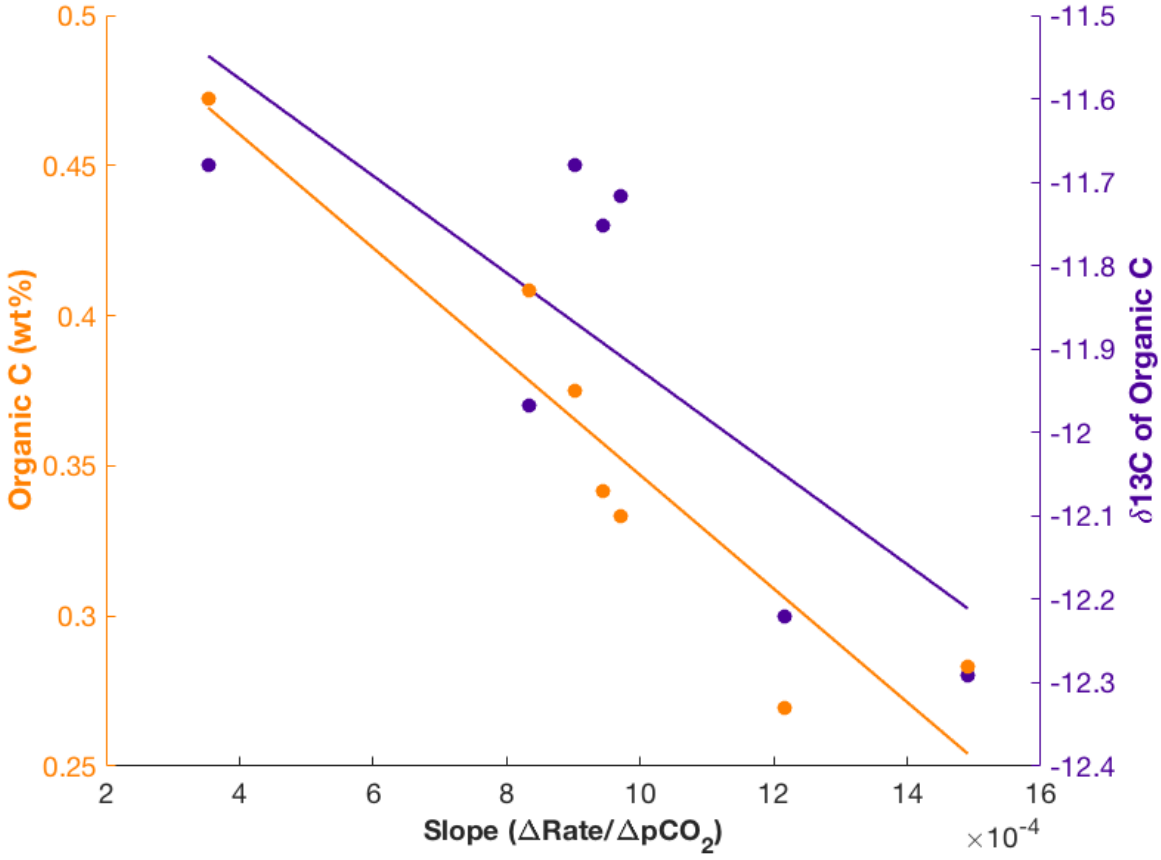

Figure 3.4: Correlations between the sensitivity of dissolution rates to changes in pCO_2 and total organic carbon (wt%; left axis) and $\delta^{13}C$ of the organic carbon (right axis). TOC values are in orange and $\delta^{13}C$ values are in purple.

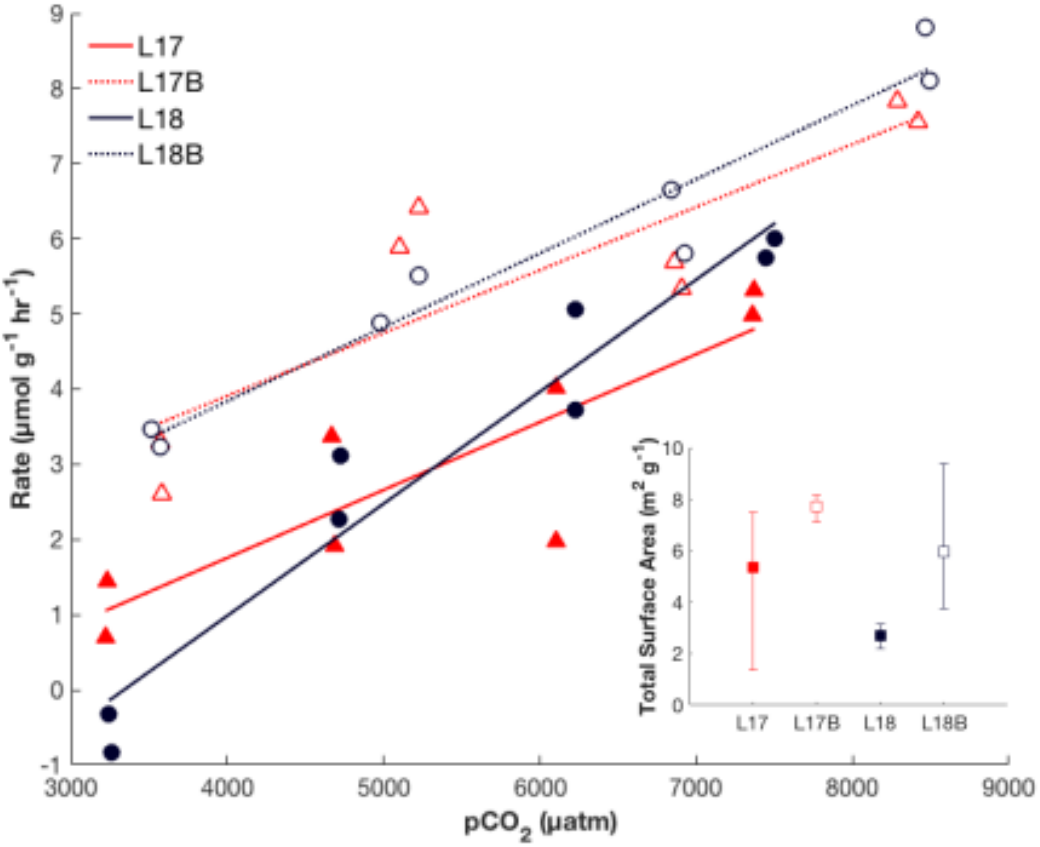

Figure 3.5: Dissolution rates (µmol g^{-1} hr^{-1}) and total specific surface areas (m^2 g^{-1}; inset) of bleached (L17B, L18B; open symbols) and unbleached (L17, L18; closed symbols) subsamples. L-17 samples are represented with red triangles and L-18 samples are represented with dark blue circles. Mean surface area represented with squares and range of triplicate measurements with error bars. Triplicate measurements were done on different splits of the subsamples.

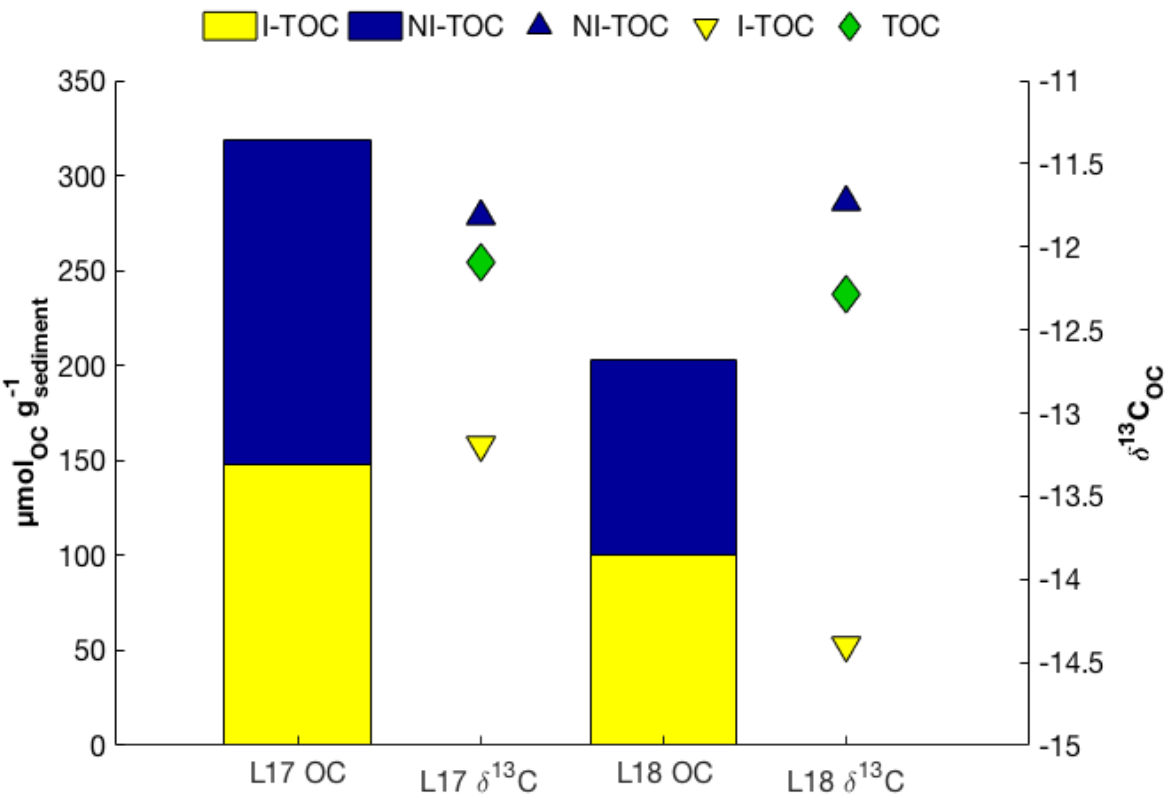

Figure 3.6: Characteristics of organic matter associated with sediment samples. Amount of intracrystalline (I-TOC; yellow bar) and non-intracrystalline (NI-TOC; blue bar) organic carbon in µmol of organic carbon per gram of sediment (left axis). $\delta^{13}C$ values in per mil (‰; right axis) for I-TOC (yellow up-side down triangle), NI-TOC (blue triangle) and TOC (green diamond). Isotopic values for TOC and I-TOC were measured and used to calculate NI-TOC values.

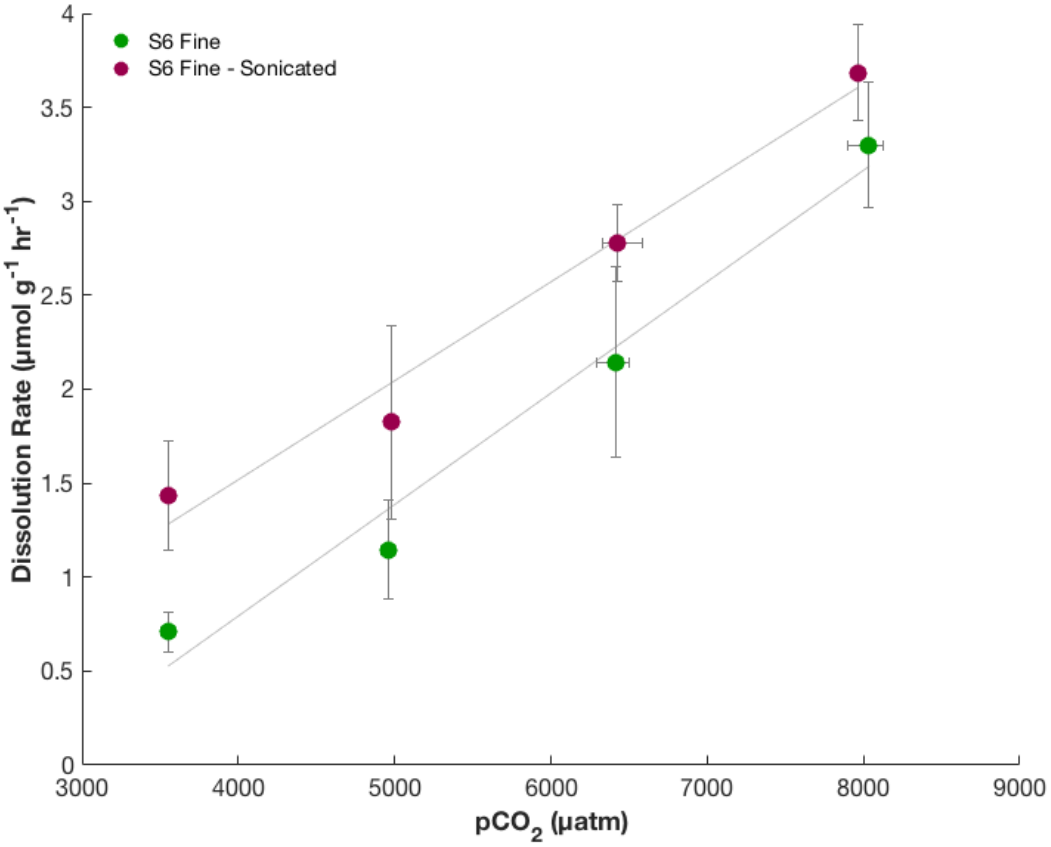

Supplemental Figure 3.1: Dissolution rates of sonicated (pink circles) and unsonicated subsamples (green circles).

TABLES

Supplemental Table 3.1: Results of linear regression model, rate = $ß_0$+ $ß_1(pCO_2)$ + $ß_2$(sample) + $ß_3(pCO_2 \times$ sample), for bulk sediment dissolution rates (rate) as a function of the partial pressure of carbon dioxide (pCO_2) and sample. Bailey's Bay serves as the baseline and p-values for variables and interaction terms represent significant difference from reference group coefficients (Intercept and pCO_2). Significance values: *p-val ≤ 0.05, **p-val ≤ 0.01 , ***p-val ≤ 0.001.

Model Terms	**F-statistics**	**p-value**
pCO_2	$F_{1,66}$=234.9480	< 2.2e-16***
sample	$F_{9,66}$=10.8805	3.613e-10***
$pCO_2 \times$ sample	$F_{9,66}$=3.0996	0.003645**
Variable	**Regression coefficient (ß)**	**Standard Error**
Intercept	-0.1373	1.1173
pCO_2	0.0007***	0.0002
L-5	-2.7071	1.5886
L-10	-0.8608	1.5947
L-17	-1.7171**	1.5896
L-18	-4.8385	1.5819
L-22	0.5619	1.6068
L-25	-2.5638	1.4780
L-27	-0.1879	1.5886
Crescent	-1.2086	1.5637
Hog Reef	0.5244	1.5904
Interaction Terms		
$pCO_2 \times$ L-5	0.0005	0.0003
$pCO_2 \times$ L-10	0.0001	0.0003
$pCO_2 \times$ L-17	0.0002	0.0003

pCO_2 × L-18	0.0008**	0.0003
pCO_2 × L-22	-0.0004	0.0003
pCO_2 × L-25	0.0002	0.0002
pCO_2 × L-27	0.0003	0.0003
pCO_2 × Crescent	0.0005*	0.0003
pCO_2 × Hog Reef	-0.0002	0.0003
Model Fit		
Adjusted R^2	0.8008	
F-statistic	$F_{19,66} = 18.99$	
p-value	< 2.2e-16	

Supplemental Table 3.2: Estimated marginal means of linear trends with 95% for bulk sediment dissolution rates. Group information using Tukey method and 95% confidence (L=Lower, U=Upper). Trends that do not share the same number are significantly different from one another. SE = Standard Error.

Variable	Trend (SE)	Standard Error	95% CI (L,U)	Group
L-22	3.53e-04	2.06e-04	-5.81e-05, 7.64E-04	1
L-25	9.43e-04	1.49e-04	6.47e-04, 1.24E-03	1
Hog Reef	4.93e-04	1.83e-04	1.28e-04, 8.58E-04	1,2
L-17	9.03e-04	2.03e-04	4.97e-04, 1.31E-03	1,2
L-18	1.49e-03	1.98e-04	1.09e-03, 1.89E-03	1,2
L-10	8.34e-04	2.01e-04	4.33e-04, 1.23E-03	1,2,3
Bailey's Bay	7.04e-04	1.83e-04	3.39e-04, 1.07E-03	1,2,3
L-5	1.22e-03	2.01e-04	8.14e-04, 1.62E-03	2,3
L-27	9.71e-04	1.98e-04	5.75e-04, 1.37E-03	3,4
Crescent	1.22e-03	1.79e-04	8.61e-04, 1.57E-03	4

Supplemental Table 3.3: Mineralogical and specific surface area data (m^2 g^{-1}) for Bermuda grain size fraction samples. HMC=High-magnesian calcite. mol% Mg=average molar % magnesium of HMCs. Mean surface area ± 1 S.D. of replicate measurements. N/A = insufficient sample volume for analysis.

Sample	Aragonite	Calcite	HMC	mol% Mg	Surface Area
Station 3					
Coarse	83	3	14	8.83	3.34 ± 0.04
Fine	84	2	14	14.26	4.43 ± 0.34
Very Fine	68	5	27	14.23	6.79 ± 0.12
Station 6					
Coarse	70	4	26	15.95	3.79 ± 0.37
Fine	53	7	40	16.11	N/A
Very Fine	61	5	34	16.42	3.87 ± 0.15

Supplemental Table 3.4: Results of linear regression model, rate = $ß_0$+ $ß_1(pCO_2)$ + $ß_2$(grain size) + $ß_3(pCO_2 \times$ grain size), for dissolution rates (rate) of Bermuda grain size fractions as a function of the partial pressure of carbon dioxide (pCO_2) and grain size. The coarse fraction serves as the baseline and p-values for variables and interaction terms represent significant difference from reference group coefficients (Intercept and pCO_2). Significance values: *p-val ≤ 0.05, **p-val ≤ 0.01 , ***p-val ≤ 0.001.

Model Terms	**F-statistics**	**p-value**
pCO_2	$F_{1,80}$= 231.0745	< 2.2e-16***
grain size	$F_{2,80}$= 211.0933	< 2.2e-16***
$pCO_2 \times$ grain size	$F_{2,80}$= 7.8637	7.624e-4***
Variable	**Regression coefficient (ß)**	**Standard Error**
Intercept	-4.60e-01	4.50e-01
pCO_2	9.75e-04***	7.69e-05
Fine	-1.14e+00	6.21e-01
Very Fine	-1.05e+00	6.69e-01
Interaction Terms		
$pCO_2 \times$ Fine	-3.426e-03**	1.040e-04
$pCO_2 \times$ Very Fine	-3.984e-04***	1.113e-04
Model Fit		
Adjusted R^2	0.8865	
F-statistic	$F_{5,80}$ = 133.8	
p-value	< 2.2e-16	

Supplemental Table 3.5: Estimated marginal means of linear trends with 95% for dissolution rates of Bermuda grain size fractions. Group information using Tukey method and 95% confidence (L=Lower, U=Upper). Trends that do not share the same number are significantly different from one another. SE = Standard Error.

Variable	Trend (SE)	Standard Error	95% CI (L,U)	Group
Very Fine	5.76e-04	7.69e-05	8.22e-04, 1.13E-03	1
Fine	6.32e-04	7.00e-05	4.93e-04, 7.72e-04	1
Coarse	9.75e-04	8.05e-05	4.16e-04, 7.37E-04	2

Supplemental Table 3.6: Results of linear regression model, rate = $ß_0$+ $ß_1(pCO_2)$ + $ß_2$(preparation) for dissolution rates (rate) of sonicated and unsonicated sediment as a function of the partial pressure of carbon dioxide (pCO_2) and preparation. The unsonicated sample serves as the baseline and p-values for variables represent significant difference from reference group coefficients (Intercept and pCO_2). Significance values: *p-val ≤ 0.05, **p-val ≤ 0.01 , ***p-val ≤ 0.001.

Model Terms	**F-statistics**	**p-value**
pCO_2	$F_{1,29}$= 237.233	1.694e-15***
Sonicated	$F_{1,29}$= 25.674	2.106e-5***
Variable	**Regression coefficient (ß)**	**Standard Error**
Intercept	-2.391***	2.253e-01
pCO_2	5.602e-04***	3.635e-05
Sonicated	6.098e-01***	1.204e-01
Model Fit		
Adjusted R^2	0.8938	
F-statistic	$F_{2,29}$ = 131.5	
p-value	2.876e-15	

Supplemental Table 3.7: Grain size distribution of Heron Island samples. G=Gravel, VC=Very coarse, C=Coarse, M=Medium, F=Fine, VF=Very fine. All grain size fractions in wt %. Median and mean values in mm.

Sample	G	VC	C	M	F	VF	Mud	Median	Mean
L-05	2%	3%	4%	11%	25%	41%	14%	0.16	0.21
L-10	43%	29%	20%	6%	2%	0%	0%	2.52	0.64
L-17	2%	22%	38%	29%	9%	0%	0%	1.12	0.88
L-18	7%	10%	15%	34%	31%	3%	0%	0.55	0.56
L-22	17%	19%	24%	20%	14%	5%	1%	1.06	0.89
L-25	42%	12%	23%	15%	8%	0%	0%	1.51	3.90
L-27	7%	15%	37%	29%	11%	1%	0%	0.98	0.84

Supplemental Table 3.8: Mineralogical data for Heron Island samples. HMC=High-magnesian calcite, LMC=Low=magnesian calcite, Arag=Aragonite.

Sample	%Ca	%Mg	%Sr	mol% Mg	Arag	HMC	LMC	HMC: Arag
L-05	40.8	1.5	0.63	14.57	60.80	38.90	0.30	0.64
L-10	38.7	2.0	0.50	14.78	46.78	52.54	0.68	1.12
L-17	40.7	1.2	0.72	14.96	69.74	29.91	0.35	0.43
L-18	39.9	1.2	0.71	14.97	74.81	24.42	0.77	0.33
L-22	41.7	1.6	0.67	15.22	66.92	32.71	0.38	0.49
L-25	37.5	1.9	0.51	14.76	37.76	62.24	0.00	1.65
L-27	39.1	1.2	0.69	14.88	59.85	40.15	0.00	0.67

Supplemental Table 3.9: Total organic carbon, carbon isotopes and physical parameters of Heron Island samples. TOC=Total Organic Carbon, OM=Organic Matter

Sample	Carbon Characteristics			Physical Parameters	
	TOC	$\delta^{13}C$ of OM	$\Delta^{14}C$ of sample	Depth (m)	Permeability (m^2)
L-05	0.30	-12.33	N/A	4.7	7.54E-12
L-10	0.37	-11.83	561	3	8.15E-11
L-17	0.45	-11.95	1193	2.2	6.04E-11
L-18	0.28	-12.28	875	2.3	5.00E-11
L-22	0.45	-11.60	1278	3.1	2.80E-11
L-25	0.43	-12.07	1078	2.3	6.30E-11
L-27	0.44	-12.10	1281	3.3	5.61E-11

Supplemental Table 3.10: Results of linear regression model, rate = $ß_0$+ $ß_1(pCO_2)$ + $ß_2$(preparation) for dissolution rates (rate) of bleached and unbleached sediments as a function of the partial pressure of carbon dioxide (pCO_2) and preparation. The bleached sample serves as the baseline and p-values for variables represent significant difference from reference group coefficients (Intercept and pCO_2). Significance values: *p-val ≤ 0.05, **p-val ≤ 0.01 , ***p-val ≤ 0.001.

Model Terms	**F-statistics**	**p-value**
pCO_2	$F_{1,29}$= 175.747	7.762e-14***
Unbleached	$F_{1,29}$= 44.598	2.525e-07***
Variable	**Regression coefficient (ß)**	**Standard Error**
Intercept	-5.222e-01	5.651e-01
pCO_2	1.037e-03***	8.745e-05
Unbleached	-2.021***	3.026e-01
Model Fit		
Adjusted R^2	0.8757	
F-statistic	$F_{2,29}$ = 110.2	
p-value	2.826e-14	

Supplemental Table 3.11: Characteristics of intracrystalline and non-intracrystalline organic matter.
OC=Organic carbon, TOC=Total organic carbon, (µmol C/g dry sediment).

		Insoluble OC (µmol/g)	**Soluble OC** (µmol/g)	**OC** (µmol/g)	**Pool % TOC**	**% Pool soluble**	**% Pool Insoluble**	**$\delta^{13}C$**
L-17	Total	159	160	320	100	50	50	-12.09
	Intracrystalline	31	117	148	46	79	21	-13.19
	Non intracrystalline	128	43	171	54	25	75	-11.82
L-18	Total	98	105	204	100	52	48	-12.29
	Intracrystalline	21	79	100	49	79	21	-14.40
	Non intracrystalline	78	26	103	51	25	75	-11.73

REFERENCES

Aller, R.C. (1982) Carbonate dissolution nearshore terrigenous muds; the role of physical and biological reworking. Journal of Geology 90, 79-95.

Andersson, A.J., Bates, N.R. and Mackenzie, F.T. (2007) Dissolution of Carbonate Sediments Under Rising pCO_2 and Ocean Acidification: Observations from Devil's Hole, Bermuda. Aquatic Geochemistry 13, 237-264.

Andersson, A.J. and Gledhill, D. (2013) Ocean acidification and coral reefs: effects on breakdown, dissolution, and net ecosystem calcification. Annual Review of Marine Science 5, 321-348.

Andersson, A.J., Kuffner, I.B., Mackenzie, F.T., Jokiel, P.L., Rodgers, K.S. and Tan, A. (2009) Net Loss of $CaCO_3$ from a subtropical calcifying community due to seawater acidification; mesocosm-scale experimental evidence. Biogeosciences 6, 1811-1823.

Balzer, W. and Wefer, G. (1981) Dissolution of carbonate minerals in a subtropical shallow marine environment. Marine Chemistry 10, 545-558.

Barwise, A.J., Compton, R.G. and Unwin, P.R. (1990) The Effect of Carboxylic Acids on the Dissolution of Calcite in Aqueous Solution. Part 2.-d-, l- and *meso*-Tartaric Acids. Journal of the Chemical Society, Faraday Transactions 86, 137-144.

Bates, N.R., Astor, Y.M., Church, M.J., Currie, K., Dore, J.E., Gonzalez-Davila, M., Lorenzoni, L., Muller-Karger, F., Olafsson, J. and Santana-Casiano, J.M. (2014) A Time-Series View of Changing Surface Ocean Chemistry Due to Ocean Uptake of Anthropogenic CO_2 and Ocean Acidification. Oceanography 27, 126-141.

Bischoff, W.D., Bishop, F.C. and Mackenzie, F.T. (1983) Biogenically produced magnesian calcite: inhomogeneities in chemical and physical properties; comparison with synthetic phases. American Mineralogist 68, 1183-1188.

Bischoff, W.D., Mackenzie, F.T. and Bishop, F.C. (1987) Stabilities of synthetic magnesian calcites in aqueous solution: Comparison with biogenic materials. Geochimica et Cosmochimica Acta 51, 1413-1423.

Brunauer, S., Emmett, P.H. and Teller, E. (1938) Adsorption of gases in multimolecular layers. Journal of the American chemical society 60, 309-319.

Burdige, D.J. and Zimmerman, R.C. (2002) Impact of sea grass density on carbonate dissolution in Bahamian sediments. Limnology and Oceanography 47, 1751-1763.

Busenberg, E. and Plummer, L.N. (1986) A Comparative Study of the Dissolution and Crystal Growth Kinetics of Calcite and Aragonite. U. S. Geological Survey Bulletin, 139-168.

Carter, P.W. and Mitterer, R.M. (1978) Amino acid composition of organic matter associated with carbonate and non-carbonate sediments. Geochimica et Cosmochimica Acta 42, 1231-1238.

Chave, K.E. (1965) Carbonates: Association with Organic Matter in Surface Seawater. Science 148, 1723-1724.

Chave, K.E. and Schmalz, R.F. (1966) Carbonate-seawater interactions. Geochimica et Cosmochimica Acta 30, 1037-1048.

Comeau, S., Carpenter, R.C., Lantz, C.A. and Edmunds, P.J. (2015) Ocean acidification accelerates dissolution of experimental coral reef communities. Biogeosciences 12, 365-372.

Compton, R.G., Pritchard, K.L., Unwin, P.R., Grigg, G., Silvester, P., Lees, M. and House, W.A. (1989) The effect of carboxylic acids on the dissolution of calcite in aqueous solution. Part 1.—Maleic and fumaric acids. Journal of the Chemical Society, Faraday Transactions 1: Physical Chemistry in Condensed Phases 85, 4335-4366.

Compton, R.G. and Sanders, G.H.W. (1993) The Dissolution of Calcite in Aqueous Acid: The Influence of Humic Species. Journal of Colloid and Interface Science 158, 439-445.

Cyronak, T. and Eyre, B.D. (2016) The synergistic effects of ocean acidification and organic metabolism on calcium carbonate (CaCO3) dissolution in coral reef sediments. Marine Chemistry 183, 1-12.

Cyronak, T., Santos, I.R. and Eyre, B.D. (2013a) Permeable coral reef sediment dissolution driven by elevated pCO_2 and pore water advection. Geophysical Research Letters 40, 4876-4881.

Cyronak, T., Santos, I.R., McMahon, A. and Eyre, B.D. (2013b) Carbon cycling hysteresis in permeable carbonate sands over a diel cycle: Implications for ocean acidification. Limnology and Oceanography 58, 131-143.

Dickson, A.G. and Millero, F.J. (1987) A comparison of the equilibrium constants for the dissociation of carbonic acid in seawater media. Deep Sea Research Part A. Oceanographic Research Papers 34, 1733-1743.

Doney, S.C., Fabry, V.J., Feely, R.A. and Kleypas, J.A. (2009) Ocean Acidification: The Other CO_2 Problem. Annual Review of Marine Science 1, 169-192.

Erez, J., Reynaud, S., Silverman, J., Schneider, K. and Allemand, D. (2011) Coral calcification under ocean acidification and global change, Coral reefs: an ecosystem in transition. Springer, pp. 151-176.

Eyre, B.D., Andersson, A.J. and Cyronak, T. (2014) Benthic coral reef calcium carbonate dissolution in an acidifying ocean. Nature Climate Change 4, 969-976.

Eyre, B.D., Cyronak, T., Drupp, P., De Carlo, E.H., Sachs, J.P. and Andersson, A.J. (2018) Coral reefs will transition to net dissolving before end of century. Science 359, 908-911.

Fabricius, K.E. (2005) Effects of terrestrial runoff on the ecology of corals and coral reefs: review and synthesis. Marine pollution bulletin 50, 125-146.

Gaffey, S.J. and Bronnimann, C.E. (1993) Effects of bleaching on organic and mineral phases in biogenic carbonates. Journal of Sedimentary Research 63.

Garrett, P., Smith, D.L., Wilson, A.O. and Patriquin, D. (1971) Physiography, ecology, and sediments of two Bermuda patch reefs. The Journal of Geology 79, 647-668.

Gattuso, J.-P., Frankignoulle, M. and Wollast, R. (1998) Carbon and carbonate metabolism in coastal aquatic ecosystems. Annual Review of Ecology and Systematics 29, 405-434.

Goldsmith, J.R., Graf, D.L. and Heard, H.C. (1961) Lattice constants of the calcium magnesium carbonates. Mineralogical Society of America.

Griffin, A.J., Andersson, A., Cyronak, T., Eyre, B.D. and Stoltenberg, L. (in prep.) Seawater carbonate chemistry and organic matter decomposition control calcium carbonate dissolution in coral reefs sediments.

Hoegh-Guldberg, O., Mumby, P.J., Hooten, A.J., Steneck, R.S., Greenfield, P., Gomez, E., Harvell, C.D., Sale, P.F., Edwards, A.J., Caldeira, K., Knowlton, N., Eakin, C.M., Iglesias-Prieto, R., Muthiga, N., Bradbury, R.H., Dubi, A. and Hatziolos, M.E. (2007) Coral Reefs Under Rapid Climate Change and Ocean Acidification. Science 318, 1737-1742.

Honjo, S. and Erez, J. (1978) Dissolution rates of calcium carbonate in the deep ocean; an in-situ experiment in the North Atlantic Ocean. Earth and Planetary Science Letters 40, 287-300.

Hutchings, P. (1986) Biological destruction of coral reefs. Coral reefs 4, 239-252.

Ingalls, A.E., Aller, R.C., Lee, C. and Wakeham, S.G. (2004) Organic matter diagenesis in shallow water carbonate sediments. Geochimica et Cosmochimica Acta 68, 4363-4379.

Jell, J.S. and Flood, P.G. (1978) Guide to the geology of reefs of the Capricorn and Bunker Groups, Great Barrier Reef Province, with special reference to Heron Reef. The University of Queensland Papers Department of Geology 8, 1-85.

Keir, R.S. (1980) The dissolution kinetics of biogenic calcium carbonates in seawater. Geochimica et Cosmochimica Acta 44, 241-252.

Kleypas, J.A., Buddemeier, R.W., Archer, D., Gattuso, J.-P., Langdon, C. and Opdyke, B.N. (1999) Geochemical Consequences of Increased Atmospheric Carbon Dioxide on Coral Reefs. Science 284, 118-120.

Kleypas, J.A. and Langdon, C. (2006) Coral reefs and changing seawater carbonate chemistry. Coastal and Estuarine Studies: Coral Reefs and Climate Change Science and Management 61, 73-110.

Kroeker, K.J., Kordas, R.L., Crim, R.N. and Singh, G.G. (2010) Meta-analysis reveals negative yet variable effects of ocean acidification on marine organisms. Ecology Letters 13, 1419-1434.

Le Quéré, C., Andrew, R.M., Friedlingstein, P., Sitch, S., Hauck, J., Pongratz, J., Pickers, P.A., Korsbakken, J.I., Peters, G.P. and Canadell, J.G. (2018) Global carbon budget 2018. Earth System Science Data 10, 2141-2194.

Lenth, R.V. (2016) Least-Squares Means: The R Package lsmeans. Journal of Statistical Software 69, 1-33.

Lenth, R.V. (2019) emmeans: Estimated Marginal Means, aka Least-Squares Means. R package version 1.3.3.

Lewis, D.W. and McConchie, D. (2012) Analytical sedimentology. Springer Science & Business Media.

Lewis, E., Wallace, D. and Allison, L.J. (1998) Program developed for CO_2 system calculations. Carbon Dioxide Information Analysis Center, managed by Lockheed Martin Energy Research Corporation for the US Department of Energy Tennessee.

Mehrbach, C., Culberson, C.H., Hawley, J.E. and Pytkowicx, R.M. (1973) Measurement of the apparent dissociation constants of carbonic acid in seawater at atmospheric pressure. Limnology and Oceanography 18, 897-907.

Milliman, J.D. (1993) Production and accumulation of calcium carbonate in the ocean: Budget of a nonsteady state. Global Biogeochemical Cycles 7, 927-957.

Milliman, J.D., Troy, P.J., Balch, W.M., Adams, A.K., Li, Y.-H. and Mackenzie, F.T. (1999) Biologically mediated dissolution of calcium carbonate above the chemical lysocline? Deep-Sea Research. Part I: Oceanographic Research Papers 46, 1653-1669.

Morse, J.W. (1974) Dissolution kinetics of calcium carbonate in sea water. V. Effects of natural inhibitors and the position of the chemical lysocline. American Journal of Science 274, 638-647.

Morse, J.W. (1983) The kinetics of calcium carbonate dissolution and precipitation, Reviews in Mineralogy: Carbonates - mineralogy and chemistry. Mineralogical Society of America, pp. 227-264.

Morse, J.W., Andersson, A.J., Mackenzie, F.T., Canfield, D.E. and Lyons, T.W. (2006) Initial responses of carbonate-rich shelf sediments to rising atmospheric pCO_2 and "ocean acidification": Role of high Mg calcites. Geochimica et Cosmochimica Acta 70, 5814-5830.

Morse, J.W. and Arvidson, R.S. (2002) The dissolution kinetics of major sedimentary carbonate minerals. Earth-Science Reviews 58, 51-84.

Morse, J.W., Arvidson, R.S. and Lüttge, A. (2007) Calcium Carbonate Formation and Dissolution. Chemical Reviews 107, 342-381.

Morse, J.W., Zullig, J.J., Bernstein, L.D., Millero, F.J., Milne, P., Mucci, A. and Choppin, G.R. (1985a) Chemistry of calcium carbonate-rich shallow water sediments in the Bahamas. American Journal of Science 285, 147-185.

Morse, J.W., Zullig, J.J., Bernstein, L.D., Millero, F.J., Milne, P.J., Mucci, A. and Choppin, G.R. (1985b) Chemistry of calcium carbonate-rich shallow water sediments in the Bahamas. American Journal of Science 285, 147-185.

Müller, P.J. and Suess, E. (1977) Interaction of organic compounds with calcium carbonate—III. Amino acid composition of sorbed layers. Geochimica et Cosmochimica Acta 41, 941-949.

Nash, M.C., Opdyke, B.N., Wu, Z., Xu, H. and Trafford, J.M. (2013) Simple X-ray diffraction techniques to identify Mg calcite, dolomite, and magnesite in tropical coralline algae and assess peak asymmetry. Journal of Sedimentary Research 83, 1085-1099.

Naviaux, J.D., Subhas, A.V., Rollins, N.E., Dong, S., Berelson, W.M. and Adkins, J.F. (2019) Temperature Dependence of Calcite Dissolution Kinetics in Seawater. Geochimica et Cosmochimica Acta 246, 363-384.

Pickett, M. and Andersson, A.J. (2015) Dissolution Rates of Biogenic Carbonates in Natural Seawater at Different pCO_2 Conditions: A Laboratory Study. Aquatic Geochemistry 21, 459-485.

Plummer, L.N. and Mackenzie, F.T. (1974) Predicting mineral solubility from rate data; application to the dissolution of magnesian calcites. American Journal of Science 274, 61-83.

Pytkowicz, R.M. (1969) Chemical solution of calcium carbonate in sea water. American Zoologist 9, 673-679.

Schiebel, R., Barker, S., Lendt, R., Thomas, H. and Bollmann, J. (2007) Planktic foraminiferal dissolution in the twilight zone. Deep Sea Research Part II: Topical Studies in Oceanography 54, 676-686.

Schönberg, C.H., Fang, J.K., Carreiro-Silva, M., Tribollet, A. and Wisshak, M. (2017) Bioerosion: the other ocean acidification problem. ICES Journal of Marine Science 74, 895-925.

Scoffin, T. and Garrett, P. (1974) Processes in the formation and preservation of internal structure in Bermuda patch reefs, Proceedings of the 2nd international coral reef symposium, pp. 429-448.

Sjöberg, E.L. (1978) Kinetics and mechanism of calcite dissolution in aqueous solutions at low temperatures. Almqvist & Wiksell.

Subhas, A.V., Rollins, N.E., Berelson, W.M., Erez, J., Ziveri, P., Langer, G. and Adkins, J.F. (2018) The dissolution behavior of biogenic calcites in seawater and a possible role for magnesium and organic carbon. Marine Chemistry 205, 100-112.

Suess, E. (1968) Calcium carbonate interaction with organic compounds. Lehigh University.

Suess, E. (1970) Interaction of organic compounds with calcium carbonate—I. Association phenomena and geochemical implications. Geochimica et Cosmochimica Acta 34, 157-168.

Suess, E. (1973) Interaction of organic compounds with calcium carbonate-II. Organo-carbonate association in Recent sediments. Geochimica et Cosmochimica Acta 37, 2435-2447.

Troy, P.J., Li, Y.-H. and Mackenzie, F.T. (1997) Changes in surface morphology of calcite exposed to the oceanic water column. Aquatic Geochemistry 3, 1-20.

Tynan, S. and Opdyke, B.N. (2011) Effects of lower surface ocean pH upon the stability of shallow water carbonate sediments. Science of the Total Environment 409, 1082-1086.

Unwin, P.R. and Compton, R.G. (1990) Effect of carboxylic acids on the dissolution of calcite in aqueous solution. Part 3.—Polymaleic acid. Journal of the Chemical Society, Faraday Transactions 86, 1517-1525.

Walter, L., Bonnell, L. and Patterson, W. (1990) Syndepositional dissolution of shallow marine carbonates: American Association of Petroleum Geologists. Bulletin 74, 787.

Walter, L.M., Bischof, S.A., Patterson, W.P. and Lyons, T.W. (1993) Dissolution and recrystallization in modern shelf carbonates; evidence from pore water and solid phase chemistry. Philosophical Transactions - Royal Society of London, Physical Sciences and Engineering 344, 27-36.

Walter, L.M. and Morse, J.W. (1984a) Magnesian calcite stabilities: A reevaluation. Geochimica et Cosmochimica Acta 48, 1059-1069.

Walter, L.M. and Morse, J.W. (1984b) Reactive surface area of skeletal carbonates during dissolution; effect of grain size. Journal of Sedimentary Petrology 54, 1081-1090.

Walter, L.M. and Morse, J.W. (1985) The dissolution kinetics of shallow marine carbonates in seawater: A laboratory study. Geochimica et Cosmochimica Acta 49, 1503-1513.

Werner, U., Blazejak, A., Bird, P., Eickert, G., Schoon, R., Abed, R.M., Bissett, A. and de Beer, D. (2008) Microbial photosynthesis in coral reef sediments (Heron Reef, Australia). Estuarine, Coastal and Shelf Science 76, 876-888.

Yamamoto, S., Kayanne, H., Terai, M., Watanabe, A., Kato, K., Negishi, A. and Nozaki, K. (2012) Threshold of carbonate saturation state determined by CO_2 control experiment. Biogeosciences 9, 1441-1450.

Yates, K.K. and Halley, R.B. (2006) Diurnal variation in rates of calcification and carbonate sediment dissolution in Florida Bay. Estuaries and Coasts 29, 24-39.

Chapter 4: Seasonal changes in seawater calcium and alkalinity in the Sargasso Sea and across the Bermuda carbonate platform

Alyssa J. Griffin, John Ballard, Nicholas Bates, Rod Johnson, Todd Martz, Yuichiro Takeshita and Andreas J. Andersson

ABSTRACT

Ocean acidification may shift reefs from a state of net ecosystem calcification (+NEC) to net ecosystem dissolution (–NEC). Evidence of –NEC is typically inferred from either an increase in measured or calculated total alkalinity (TA) or the dissolved calcium (Ca) to salinity ratio relative to a reference value. The alkalinity anomaly technique has historically been the dominant method to estimate NEC due to the greater analytical challenges and uncertainty associated with Ca measurements. However, this method assumes that changes in salinity-normalized TA are exclusively the result of calcification and dissolution processes. In most cases, this assumption is valid, but in some environments additional processes may significantly influence seawater TA via nutrient fluxes or redox processes. Because seawater Ca is unaffected by these processes, Ca and TA anomalies can be used in conjunction to estimate absolute or relative changes in NEC with greater confidence. Here, we present a two-year time series of monthly seawater Ca and TA measurements across the Bermuda carbonate platform and the nearby Bermuda Atlantic Time-series Study (BATS) location offshore. High precision Ca measurements (±6.01 μmol kg^{-1}) were conducted using a novel spectrophotometric titration system and showed mostly good agreement with changes in TA

over the same spatial and temporal scales. Ca and TA measurements across the Bermuda platform showed seasonal fluctuations relative to offshore waters, with +NEC during summer months and near zero or even –NEC (dissolution) during winter months. These seasonal patterns were most pronounced at the inshore locations with the longest residence times (10+ days), which allow stronger biogeochemical signals to develop relative to the offshore source water. Parallel measurements of Ca and TA from both inshore and offshore over a multi-annual timescale could improve our predictions for why, when and where a reef system, such as the Bermuda platform, may shift from +NEC to –NEC, but obtaining high accuracy and precision Ca measurements is not trivial.

INTRODUCTION

Coral reefs are among the most biologically diverse and economically valuable ecosystems, but their future is threatened by a multitude of local and global anthropogenic perturbations (Hughes and Connell, 1999). One of these perturbations is ocean acidification, the lowering of ocean surface water pH and saturation state with respect to $CaCO_3$ minerals (Ω_{Ar}), resulting from oceanic uptake of anthropogenic carbon dioxide (Bates et al., 2014; Doney et al., 2009). Ocean acidification is expected to negatively impact organismal $CaCO_3$ production (Chan and Connolly, 2013; Kroeker et al., 2013; Kroeker et al., 2010) while increasing $CaCO_3$ destruction through enhanced bioerosion (Schönberg et al., 2017; Wisshak et al., 2012) and dissolution (Eyre et al., 2014). It has been suggested that these changes could shift coral reefs from a state of net calcification to net dissolution (Andersson et al., 2009; Dove et al., 2013; Eyre et al., 2018; Hoegh-Guldberg et al., 2007a; Kleypas et al., 1999;

Silverman et al., 2009). Positive net ecosystem calcification (+NEC) occurs when the production of $CaCO_3$ outpaces biologically and geochemically driven $CaCO_3$ dissolution (Eyre et al., 2014; Kleypas et al., 2001).

Several studies have predicted that the transition from net calcification to net dissolution will not be reached until atmospheric pCO_2 levels equal or exceed 500 μatm (Andersson et al., 2009; Hoegh-Guldberg et al., 2007b; Silverman et al., 2009; Yates and Halley, 2006). However, negative net ecosystem calcification (–NEC; net dissolution) has already been documented at night and during periods of decreased calcification in some reef systems. Because of low surface seawater [CO_3^{2-}] and Ω_{Ar} during wintertime in Bermuda, it has been suggested that this reef system may already experience periods of near zero NEC (Bates et al., 2010) and platform-wide negative NEC was indeed observed in Bermuda during the winter of 2010 (Yeakel et al., 2015). Other reef systems, such as the Florida Reef Tract, have also shown seasonal net dissolution or even annual net erosion (Muehllehner et al., 2016). The fact that certain reefs already undergo periods of net dissolution on seasonal or annual timescales is concerning for the future function and persistence of these ecosystems. It also highlights the urgency to improve predictions for when and where a reef may shift from net calcification to net dissolution, and what this would mean for the ecosystem as a whole.

Estimates of NEC can be calculated from the difference in measured or calculated total alkalinity (TA) (i.e., the alkalinity anomaly technique; Smith and Key, 1975), or the dissolved calcium (Ca) to salinity (S) ratio (Chisholm and Gattuso, 1991) relative to a reference value based on the following equation:

$$CaCO_3 + H_2O + CO_2 \rightleftharpoons Ca^{2+} + 2HCO_3^- \qquad \text{Eq. (1)}$$

where dissolution of one mole of $CaCO_3$ produces one mole of Ca and two moles of TA. The reverse reaction represents $CaCO_3$ formation, which removes one mole of Ca and two moles of TA. To calculate absolute rates of NEC, in addition to TA or Ca data, knowledge of seawater density, water column depth, and residence time are also required (Langdon et al., 2010; Smith and Key, 1975). Nonetheless, comparisons of salinity-normalized TA or Ca values between inshore and offshore locations can be used to infer relative changes in NEC on different temporal and spatial scales assuming constant residence time and depth conditions (Yeakel et al., 2015).

The alkalinity anomaly technique has by far been the dominant method to measure $CaCO_3$ dissolution and precipitation (Gattuso et al., 1999; Kinsey, 1978; Smith and Key, 1975; Smith and Kinsey, 1978), mostly due to the analytical challenges and uncertainty associated with Ca measurements. However, in order to use TA as a proxy for carbonate dissolution and precipitation, it is assumed that these processes are primarily responsible for modifying seawater TA and that other processes are negligible (Chisholm and Gattuso, 1991; Smith and Key, 1975). This assumption may not be valid in certain environments where other processes can significantly affect TA. For example, TA is unaffected by the exchange of CO_2 during photosynthesis and respiration, but the release and uptake of inorganic nutrients during these processes can significantly influence TA in certain environments (Brewer and Goldman, 1976; Goldman and Brewer, 1980). Similarly, processes within sediments, groundwater and other anoxic systems can also modify alkalinity, such as anaerobic remineralization of organic matter (Emerson and Hedges, 2003; Hu and Cai, 2011; Mackenzie et al., 2011; Thomas et al., 2009) and reduction of various elements, such as iron, manganese or sulfur (Burdige, 1993). Numerous studies have shown that TA contributions from dissolved organic matter (DOM)

can also be significant in organic-rich environments such as coastal waters, algal blooms, estuaries, rivers and mangroves (Cai et al., 1998; Hernández-Ayon et al., 2007; Hunt et al., 2011; Kim and Lee, 2009; Muller and Bleie, 2008; Yang et al., 2015).

In contrast to TA, alteration to the conservative behavior of Ca in seawater is almost exclusively dominated by $CaCO_3$ precipitation and dissolution. Therefore, Ca measurements could add rigor to studies in environments with multiple processes influencing TA. Furthermore, in coral reef environments, it could potentially be used to evaluate the relative importance of the formation/dissolution of Mg-calcite minerals ($Mg_xCa_{1-x}CO_3$) relative to the formation/dissolution of calcite and aragonite minerals (Andersson et al., 2007). Established methods for measuring Ca, however, are often limited in application due to lower absolute analytical precision relative to TA (~0.1% or ~10 μmol kg^{-1} for most methods; e.g. Jagner, 1974; Kanamori and Ikegami, 1980; Steiner et al., 2014) versus ~0.1% or typically 2-2.5 μmol kg^{-1} for TA (Dickson and Goyet, 1994) as well as considerable labor and time requirements. Nonetheless, a number of studies have employed joint Ca and TA measurements to validate the alkalinity anomaly technique (Chisholm and Gattuso, 1991), investigate the influence of different reef communities on TA:Ca ratios in mesocosm flumes (Gazeau et al., 2015; Murillo et al., 2014), and assess $CaCO_3$ sediment dissolution in a natural environment exposed to seasonally elevated pCO_2 conditions (Andersson et al., 2007). However, to our knowledge, Ca measurements have yet to be used on larger spatial and longer temporal scales in coral reef systems.

Regardless of the challenges and assumptions associated with Ca measurements, joint Ca and TA anomalies have the potential to provide more rigorous estimates of NEC, parse apart the contribution from different processes to changes in TA, and identify the relative

contribution of different mineral phases (i.e., $CaCO_3$ or $Mg_xCa_{1-x}CO_3$) on both small and large spatial and temporal scales. Here, we evaluate a novel spectrophotometric titration system for seawater Ca measurements, which addresses some of the analytical challenges faced by other methods. We assess the potential of Ca measurements from this system to infer in situ changes in reef-scale relative NEC using a multi-annual time-series of Ca and TA measurements across the Bermuda carbonate platform and offshore at the Bermuda Atlantic Time-series Station (BATS).

METHODS

Study Site

The Bermuda carbonate platform is located in the subtropical gyre of the North Atlantic and covers an area of approximately 665 km^2 (Bates et al., 2010) (Fig. 4.1). The platform is comprised of a range of habitats including a well-developed rim reef and large, exposed fore-reef zones, a central lagoon (<18 m) with numerous patch reefs and extensive carbonate sand areas, and also small enclosed bays and sounds (Bates, 2001). These environments are dominated by various benthic calcifiers, including hard corals, calcareous green, red and brown algae, foraminifera, bryozoans, echinoderms and bivalves. Dominant non-calcifying benthic organisms include seagrasses, macroalgae, and sponges (Bates et al., 2010; Goodbody-Gringley et al., 2019; Logan and Murdoch, 2011; Manuel et al., 2013). The Bermuda carbonate platform is surrounded by deep oceanic waters and is continuously exchanging surface waters with the surrounding Sargasso Sea (Bates, 2001). Residence times range from approximately 1-3 days on the outer rim reef to 10+ days nearshore (Venti et al.,

2012). There is no significant discharge of surface freshwater or runoff from the island of Bermuda into the reef, lagoonal, or inshore seawater basins, but groundwater may impact enclosed lagoons and bays (Smith and Warren, 2019).

Due to its high latitudinal location, it has been proposed that the Bermuda coral reef system will act as a "first responder" to the negative impacts of ocean acidification and climate change among tropical and subtropical reefs (Bates et al., 2010; Kleypas et al., 1999). Its location and importance as a first responder to anthropogenic stressors has led to an extensive historical record of carbonate chemistry measurements both inshore (e.g. (Andersson et al., 2014; Bates, 2001; Bates, 2002, 2017; Yeakel et al., 2015) and offshore at the ongoing BATS program (Bates, 2007; Bates et al., 2014). Carbonate chemistry measurements in this study are a subset of this ongoing record.

Sample Collection

Seawater samples have been collected monthly at various inshore locations across the platform since 2007 and at the nearby BATS station, located offshore, approximately 80 km southeast of the platform since 1988 (Fig. 4.1). Offshore samples were collected according to established BATS program protocols (Bates et al., 2012). Inshore samples were collected using a 5-liter Niskin bottle at a depth of 0.5 to 1.0 m in accordance with best practices (Dickson et al., 2007). TA samples were collected in 200-ml Kimax glass sample bottles and sterilized using 100 ml of saturated solution of $HgCl_2$. A YSI 556 Handheld Multiparameter Instrument was used to measure in situ temperature (accuracy, ±0.15°C) and salinity (accuracy, ±1%). In addition to the long-term sampling programs, Ca samples were collected monthly beginning in August of 2014 at the same inshore locations across the platform and at

BATS. Samples were collected for Ca analysis within the mixed layer using low density polyethylene bottles with phenolic polyseal lined caps and secondarily sealed to prevent evaporation prior to analysis. The time-series presented here spans from August 2014 to August 2016.

Total Alkalinity and Salinity Analyses

All samples were analyzed for total alkalinity (TA) and salinity (S) at the Bermuda Institute of Ocean Sciences. TA samples were analyzed via closed-cell potentiometric titrations using a Versatile Instrument for the Determination of Titration Alkalinity 3S (VINDTA 3S, Marianda) system, whereas BATS samples were analyzed on a VINDTA 2S (Marianda). The accuracy and precision of TA analyses were verified against certified reference material (CRM) prepared by the laboratory of Dr. Andrew Dickson of the Scripps Institution of Oceanography. Analysis of replicate CRMs yielded a typical accuracy and precision of ±1 to 2 μmol/kg for TA. Salinity was analyzed on an Autosal salinometer with accuracy <0.002, which was repeatedly checked against IAPSO seawater standards.

Calcium Titration System and Analysis

Ca samples were analyzed using a titration system developed by the Martz lab at Scripps Institution of Oceanography. The titration system determines Ca via an established photometric titration method with EGTA as the titrant (Anfält and Granéli, 1976). An indirect

indicator system consisting of zinc-zincon and Zn-EGTA, as first proposed by (Ringbom et al., 1958), was used to determine Ca concentrations, per the following equation:

Reaction: $Ca^{2+} + HIN^{3-} + Zn\text{-}EGTA^{2-} \rightleftharpoons Ca\text{-}EGTA^{2-} + ZnIn^{2-} + H^{+}$ Eq. (2)

Solution Appearance: Orange Blue

where HIN represents the acid-indicator complex and ZnIn represents the Zincon indicator. The system described here employs a spectrophotometric approach to perform the titration and detect the endpoint (Culkin and Cox, 1966; Jagner, 1974) using a custom spectrophotometer cell.

The cell is comprised of a white LED, 620 nm filter, and photodiode. The voltage of the cell is monitored with LabVIEW software (National Instruments, UK) and a 24-bit analog to digital converter (National Instruments, NI-9219). To analyze each sample, 1M borate buffer (10 mL) was added to 25 g of seawater sample and diluted 10-fold with MilliQ water. Zincon indicator (0.1 wt% zincon monosodium salt in ethanol; 0.9mL) was manually pipetted into this solution and an initial absorbance was measured (left side of Eq. 2). Following this, 0.01M equimolar Zn-EGTA (2.5mL) was then added via a Kloehn^{TM} V6 syringe pump (Norgen Inc., Littleton, CO USA), shifting Eq. 2 to the right. A gravimetric addition of EGTA (0.02 M; ~11 g) was introduced, followed by highly precise software controlled volumetric additions (~0.1 ml) of EGTA via a milliGAT Model M6 pump (GlobalFIA, Fox Island, WA, USA) until the endpoint was reached.

The precision of the Ca measurements was established using secondary standards of filtered, UV-sterilized, seawater collected from Scripps Pier. In the absence of an established

standard for Ca in seawater, accuracy was determined using IAPSO standards of known salinity and a calculated Ca concentration based on Marcet's principle (Marcet, 1819) and a Ca:S ratio of 10.28 mmol kg^{-1}:35 (Dickson and Goyet, 1994). For samples analyzed between 2016-2017, the titrant concentration was calibrated relative to the IAPSO standard before samples were measured. Due to a limited availability of IAPSO following this period, titrant concentrations were retroactively calibrated to IAPSO standards run immediately following all analyses and raw concentrations were adjusted accordingly. Following these protocols, precision and accuracy of the Ca measurements were ± 6 and ± 5 μmol kg^{-1}, respectively (Fig. 4.2). Measured Ca and TA values were salinity normalized (nCa, nTA) to the average salinity of all inshore and offshore measurements (S = 36.48).

RESULTS

Offshore variability

Monthly observations from BATS showed seasonal sea surface temperature (SST) variations ranging from 20.0ºC to 28.8 ºC with lowest temperatures observed in March or April and seasonal highs in September of each year. Salinity at BATS ranged from 36.29 to 36.70 (Fig. 4.3). Excluding statistical outliers, the salinity normalized Ca (nCa) averaged 10739 ± 11 μmol kg^{-1} (± 1σ) and ranged from 10714 to 10760 μmol kg^{-1} (Fig. 4.4). The salinity normalized alkalinity (nTA) averaged 2391 ± 4 μmol kg^{-1} (± 1σ) and ranged from 2381 to 2399 μmol kg^{-1}. Although the absolute variability in nCa is greater than for nTA, relative to the average concentrations of nCa and nTA, the variability is quite similar (0.13% and 0.16%, respectively). A theoretical Ca value (10723 μmol kg^{-1}; Fig. 4.3) was calculated

from the average salinity at BATS (S=36.51) using an established Ca:S ratio (Dickson and Goyet, 1994).

Inshore seasonal and spatial variability

Surface seawater temperature across the six inshore stations also varied seasonally, but to a greater extent than offshore (Fig. 4.3A). Maximum and minimum temperatures ranged from 17.8 to 29.7 ºC, respectively, with seasonal lows occurring between January and March and seasonal highs observed in July. Maximum and minimum salinities ranged from 35.73 to 36.95, respectively, with no apparent seasonal trends (Fig. 4.3B).

The inshore monthly average nCa and nTA showed distinct seasonal variability with the greatest depletion relative to offshore waters observed in late summer months (July through September) (Fig. 4.5). The monthly average nCa (± 1σ) across the inshore stations ranged from 10710 ± 13 to 10752 ± 11 μmol kg^{-1}(Fig. 4.5A) and the monthly average nTA (± 1σ) from 2322 ± 23 to 2390 ± 8 μmol kg^{-1}(Fig. 4.5B). The average inshore nCa exceeded the offshore average nCa (10741 μmol kg^{-1}) in winter months (January through March) during 2015 and 2016 by up to 11 μmol kg^{-1}. Individual stations also exceeded the offshore average nCa, primarily during winter months, by up to 34 μmol kg^{-1}. The average inshore nTA never exceeded the offshore average nTA (2391 μmol kg^{-1}), but most closely approached this value in winter months. However, a few individual stations exceeded the offshore average nTA during December 2015 and February 2016 by up to 11 μmol kg^{-1}.

The inshore nCa and nTA values across stations ranged from approximately 10685 to 10775 μmol kg^{-1} and 2282 to 2402 μmol kg^{-1}, respectively (Fig. 4.6). Tynes Bay demonstrated the strongest seasonal variability in both variables, which ranged from 10685 to

10756 μmol kg^{-1} in nCa and 2282 to 2392 μmol kg^{-1} in nTA. Dockyard and Mid-Platform also demonstrated strong seasonal variability, but of lesser magnitude compared to Tynes Bay. No clear seasonal trends were observed at Crescent Reef, North Channel or Hog Reef. The two variables became increasingly decoupled and their ranges of variability decreased with increasing distance from shore.

Assessment of the correlation between nTA and nCA for all inshore samples across the two-year time period revealed a slope of the linear regression of 1.70 ± 0.13 (r=0.75), with the majority of samples showing depletion in nCa and nTA relative to the average offshore nTA:nCa (Fig 4.7A). Data grouped by season to evaluate the nTA:nCa relationship during times of anticipated maximum (Summer/July – September) and minimum (Winter/January – March) calcification rates (Bates, 2001; Venti et al., 2014; Yeakel et al., 2015), revealed a nTA-nCa slope of 2.00 ± 0.26 (r=0.77), while no relationship was evident between the variables during winter (slope= 0.10 ± 0.15, r=0.12; Fig. 4.7C).

Further evidence of the seasonal variability was observed in the median nCa and nTA at each station during both winter and summer (Fig. 4.8). During winter months (January to March), nCa and nTA across the inshore stations approached or exceeded the offshore average and there was little variability across sites (Fig. 4.8B). To the contrary, nCa and nTA across stations were depleted relative to the offshore average during summer months (July to September), with greater depletion occurring at stations farther inshore (Fig.4.8A).

DISCUSSION

Evaluation of Calcium Titration System and Protocols

There are many advantages to using the automated photometric calcium titrator (APCT) system described in this study. The most novel aspect of the system described here is the automation of several components, which decreases titration time and minimizes human error. Human error is further reduced through the use of a spectrophotometer to precisely analyze the absorbance throughout the titration and to detect the endpoint. The system, however, is not fully automated and certain steps could also be automated to further improve titration time and, potentially, analytical precision.

There are also improvements that can be made to the standardization protocols for the system. The use of calculated Ca concentrations from IAPSO standards assumes 1) IAPSO water behaves according to the theoretical Ca:S (10.28 mmol kg^{-1}:35 mixing line, and 2) the variance around the theoretical relationship is less than the precision of the measurements (<6 μmol kg^{-1}). Using alternative methods to confirm the Ca concentration of IAPSO standards (e.g. – ICP-OES; Besson et al., 2014; Steiner et al., 2014) or creating standard solutions that closely mimic seawater ion composition could provide greater certainty in the absolute values of Ca concentration measured by the system. In addition, the system is currently calibrated using a single-point method. A multi-point calibration using standard dilutions or Ca spikes would improve the accuracy and precision of the system, particularly over salinity ranges farther from typical IAPSO salinities (~35). Until these improvements in standardization protocols are made, absolute Ca concentration measurements from this system and therefore, this study, must be interpreted with caution. However, since the interpretations in this study are drawn from changes in Ca relative to offshore waters, uncertainties in the absolute Ca values do not undermine its main conclusions.

Trends in Calcium and Alkalinity

Assuming conservative behavior of Ca and TA in the offshore environment, nCa and nTA were expected to demonstrate small variability at BATS. Excluding statistical outliers, the standard deviation (± 1σ) of nCa offshore was ±11 μmol kg^{-1} for the time-series. This variability was considerably higher relative to offshore nTA, which had a standard deviation of ±4 μmol kg^{-1} over the same time period. However, the offshore Ca:S ratio (311 ± 46 μmol kg^{-1}, p-val<0.01) was approximately four times higher than the TA:S ratio (75.50 ± 8.82 μmol kg^{-1}, p-val<0.01). Thus, variations in salinity, whether from uncertainty in the measurements or from normalization calculations, had approximately 4 times greater impact on nCa compared to nTA values, consequently, exacerbating uncertainties in the former by the same magnitude. The uncertainty associated with the nCa values (±6 μmol kg^{-1}) was approximately three times greater than nTA (±2 μmol kg^{-1}). Therefore, the greater variability in nCa values was due to a combination of the analytical uncertainty and the effect of salinity variations. The impact of these factors was more pronounced for comparisons of absolute nCa and nTA values offshore, where changes in Ca and TA were due primarily to changes in salinity and not strongly influenced by $CaCO_3$ precipitation and dissolution.

Relative to offshore averages, inshore nCa and nTA demonstrated seasonal cycles indicative of increased NEC across the platform during summer and depressed NEC during winter. These seasonal patterns have been established previously based on TA anomalies relative to BATS (Bates et al., 2010; Venti et al., 2014; Yeakel et al., 2015), but the same patterns in the Ca data provide confidence in these measurements and the potential for using Ca data in conjunction with other NEC proxies. Although previous studies observed periods of platform-wide near zero NEC or even –NEC (net dissolution) during winter months (Bates

et al., 2010; Yeakel et al., 2015), no periods of net dissolution were unequivocally identified in this time period. Only the average inshore nCa exceeded the offshore average over the duration of this study and although individual stations exceeded the offshore average in the winter of 2016, no corresponding offshore samples were taken at this time (January and February 2016), making it impossible to ascertain whether net dissolution occurred.

Residence times of water across the platform vary greatly (Venti et al., 2012). Stations located near the rim reef (Hog Reef, North Lagoon), mid-platform (Mid-Platform, Crescent Reef) and nearshore (Dockyard, Tynes Bay) have estimated average residence times of 2.6 ± 1.3 days, 4.4 ± 1.4 and 9.3 ± 2.1, respectively (Venti et al., 2012). If net calcification and/or dissolution continually modifies seawater as it remains on the platform, the most pronounced seasonal fluctuations in nCa and nTA would be expected at Tynes Bay, where residence times are longest (Andersson et al., 2014; Takeshita et al., 2018). Longer residence time of water allows for greater modification and a greater cumulative chemical signature relative to offshore source water (Falter et al., 2013; Page et al., 2018). Tynes Bay indeed demonstrated both the largest seasonal fluctuations in nCa and nTA, as well as the strongest coupling between the two variables. Slightly weaker seasonal fluctuations were observed at Dockyard and Mid-Platform, but seasonal trends quickly degraded with stations' increasing distance from shore and decreasing residence times. The coupling between nCa and nTA followed a similar pattern. At stations farthest offshore (North Channel and Hog Reef), the strong seasonal trend observed at other locations was largely absent. Instead, large inter-monthly variability and decoupling between nCa and nTA were observed. We speculate that the former could be related to tidal flow and differential influence of water masses of different ages (i.e., inshore vs. offshore waters), and thus, different chemical signatures. This also may

partly explain the increasing decoupling in nCa and nTA as seen for offshore samples at BATS. The contrast between stations is most clearly seen during summer (Fig. 4.8), where depletions in nCa and nTA relative to offshore averages become more pronounced farther inshore. This pattern is not observed during winter where all stations more closely resembled offshore waters, displayed less variability in nCa and nTA, and some stations even exceeded offshore nCa and nTA averages during this period.

Further evidence that calcification and dissolution were the dominant biogeochemical processes modifying seawater chemistry across the reef was found in nTA-nCa relationships across the platform (Fig. 4.7). According to Eq. 1, seawater modification via calcification and dissolution results in an nTA:nCa ratio of 2:1. During winter, no significant relationship existed between the two variables and little modification occurred relative to offshore waters, suggesting that NEC across the platform was near zero (Fig. 4.7B). In stark contrast, the nTA-nCa relationship during summer months was 2.00 ± 0.26 across stations with strong depletions in both nTA and nCa relative to the offshore summer average (Fig 4.7C), indicating that elevated rates of +NEC occurred as water moved around the platform. Consequently, the slope of the nTA-nCA relationship for all the inshore data from the two-year study (1.70 ± 0.13), represented a combination of the influence from the winter and summer observations.

Previous studies have demonstrated that calcification rates of corals determined by the TA and calcium anomaly techniques were in good agreement, and thus, conforming to Eq. 1 (Chisholm and Gattuso, 1991; Gazeau et al., 2015; Murillo et al., 2014). Murillo et al. (2014) showed that the TA flux to Ca^{2+} flux ratio ($\Delta TA:\Delta Ca^{2+}$) for a coral community incubated in an experimental flume was 2.06 ± 0.19, which is similar to the nTA-nCa relationship

observed during summer in this study (Fig. 4.7C). Although corals are typically the dominant calcifiers on coral reefs, Murillo et al. (2014) advised caution in extrapolating these results to the ecosystem-scale. This was, in part, due to the finding that the flux ratio was significantly different (1.60 ± 0.14) for a mixed-community (coral, algae and sediment) incubation. Additional incubations with only sediments revealed that the sediments were a source of TA not associated with carbonate dissolution that could account for the lower the $\Delta TA:\Delta Ca^{2+}$ ratio in the mixed-community incubations (Murillo et al., 2014). These results highlight that other processes not associated with $CaCO_3$ calcification or dissolution can skew calcification estimates based on TA data alone. However, it is important to recognize that this influence will be different depending on the scale of the system being considered (e.g. flume vs natural reef). There is currently no evidence suggesting that the overall nTA-nCa relationship throughout the year for this study (1.70 ± 0.13) was due to an additional TA source, but simply just reflects the differences between summer and winter data.

Application of system and measurements

Overall, Ca and TA measurements demonstrated similar trends that lead to consistent inferences regarding dominant processes on the reef. Because TA measurements had lower absolute uncertainty (± 2 μmol kg^{-1}) than Ca measurements (± 6 μmol kg^{-1}) and that changes associated with calcification and dissolution were twice as large for TA than Ca (see Eq. 1), the alkalinity anomaly technique is more appropriate to use in environments where TA is not expected to be significantly influenced by other processes. However, Ca measurements could add substantial value in environments where TA is influenced by other processes, particularly in certain experimental settings and coastal systems where significant sedimentary fluxes,

high concentrations of DOM, and strong diel cycles of photosynthesis and respiration occur. These processes could obscure the contribution from calcification and dissolution to TA variability and Ca measurements could offer additional insights (Burdige and Zimmerman, 2002). Ca and TA profiles could also be used in the open ocean to better constrain alkalinity budgets and inorganic carbonate particle flux dynamics (Horibe et al., 1974; Shiller and Gieskes, 1980). In addition, if the method could be modified to use smaller seawater sample volumes, Ca measurements could be made in anoxic sediment pore waters where various redox reactions are known to contribute to changes in TA (Burdige, 1993).

Ca measurements could also be used in environments where high Mg-calcites or other carbonate minerals are known to contribute to carbonate precipitation/dissolution dynamics. Two moles of TA are removed or added to the system regardless of the type of carbonate mineral participating in Eq. (1), therefore, measuring TA alone cannot differentiate the precipitation/dissolution dynamics of various carbonate mineral phases. Coral reefs are known to have several calcifiers that incorporate Mg^{2+} into their biogenic hard parts and in turn, significant volumes of Mg-calcites are found in reef sediments. Using Ca and TA measurements in reef environments could potentially help parse apart alkalinity contributions from different calcifiers and mineral phases (i.e., calcite, aragonite, Mg-calcites). However, these proposed uses for joint Ca and TA measurements would need to be explored and validated in other systems, and may in some cases require higher accuracy and precision than demonstrated here.

CONCLUSION

To our knowledge, this study represents the first multi-annual time-series of Ca measurements across a coral reef platform. The findings suggest that the use of long-term calcium measurements in conjunction with alkalinity measurements may provide useful insight into seasonal and inter-annual trends in biogeochemical processes occurring on coral reefs. Overall, the trends in Ca data mostly followed those in TA. However, the absence of appropriate standards and standardization protocols as well as additional automation made achieving highly accurate and precise Ca measurements challenging relative to the use of well-established alkalinity measurements, standards and protocols. Therefore, in certain reef environments where other processes are not anticipated to significantly influence alkalinity, the alkalinity anomaly technique is still more suitable.

Even so, there are several benefits to the Ca system relative to other Ca measurement methods including higher precision, reduced labor, and quicker titration times. However, improvements to the system and in particular, standardization protocols will need to be made to reduce uncertainty in the measurements. These improvements are quite feasible and could certainly be accomplished with dedicated efforts and funding. If higher precision Ca measurements (<6 $\mu mol\ kg^{-1}$) were achieved, these measurements could be used in conjunction with TA and other carbonate chemistry parameters, or independently, to characterize NEC and interpret the underlying processes with greater confidence. This could be particularly valuable in environments where calcification and dissolution are not the only processes significantly influencing TA. Time-series measurements of Ca and TA across coral reefs and open ocean could improve predictions of future reef conditions as well as why,

when and where a reef system may transition to net erosion on seasonal, annual, and/or different spatial scales.

ACKNOWLEDGEMENTS

This project was funded by the U.S. National Science Foundation (NSF) OCE 14-16518 (AJA, RJ) and OCE 12-55042 (AJA). We are grateful for the assistance of Mr. Taylor Wirth and Ms. Stephanie Smith for their assistance with maintaining and troubleshooting the calcium titration system.

Chapter 4, in part, is in preparation for submission for publication. Griffin, A. J., Ballard, J., Bates, N., Johnson, R., Martz, T., Takeshita, Y. and Andersson, A. J.. The dissertation author was the primary investigator and author of this material.

FIGURES

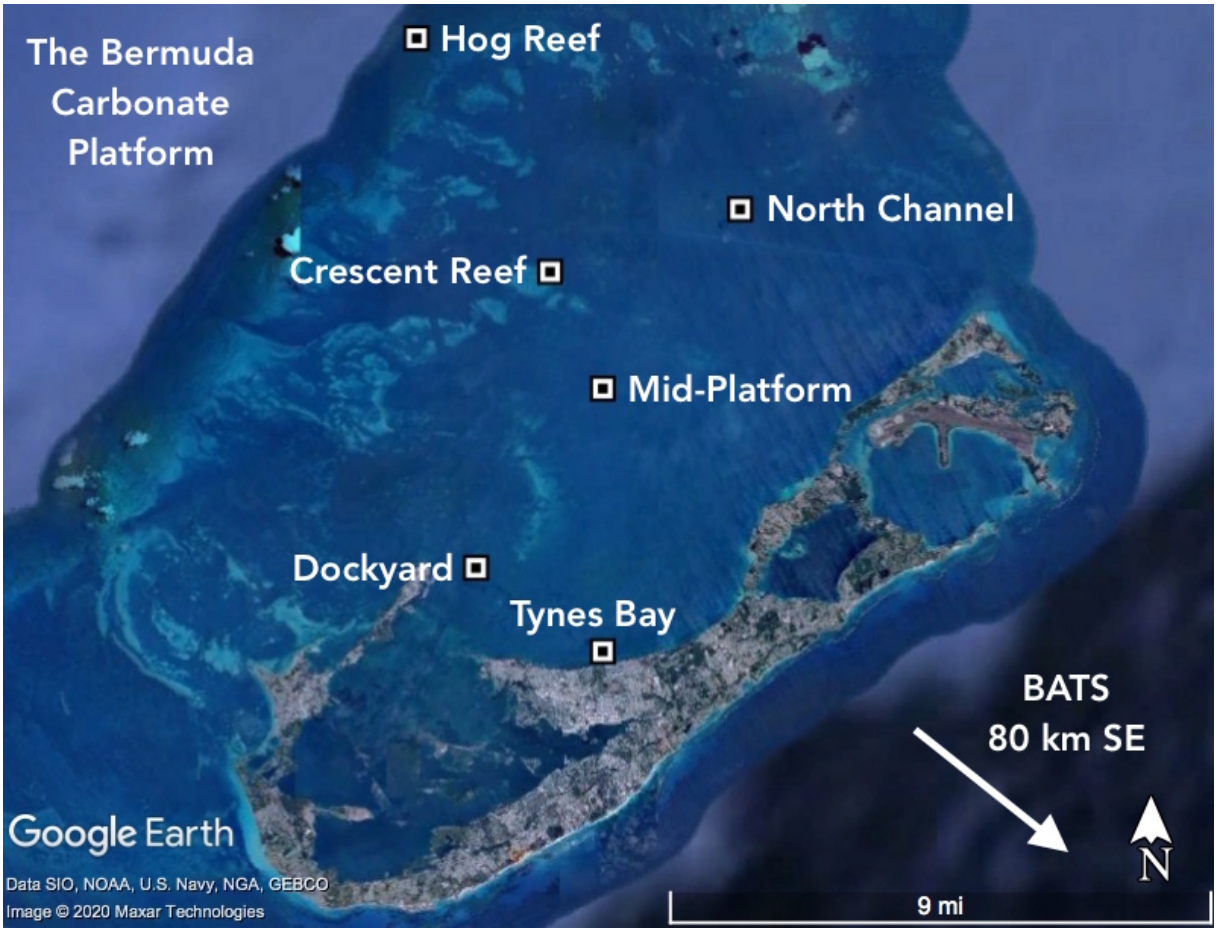

Figure 4.1: Spatial map of time-series inshore sample locations across the Bermuda carbonate platform. Sample locations are denoted by white and black squares.

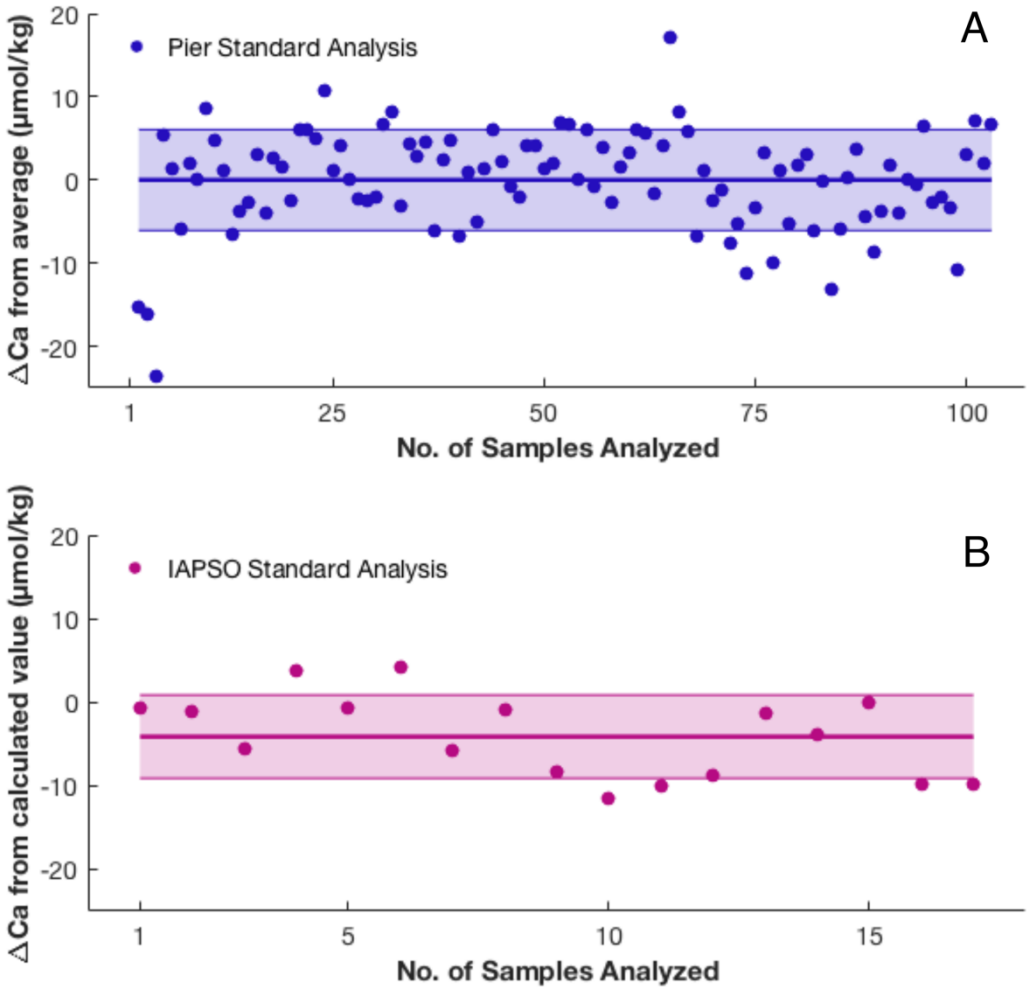

Figure 4.2: Repeated Ca measurements of (A) secondary pier standards and (B) IAPSO standards. Solid line represents average measurement value relative to standard value, ±1σ (shaded area).

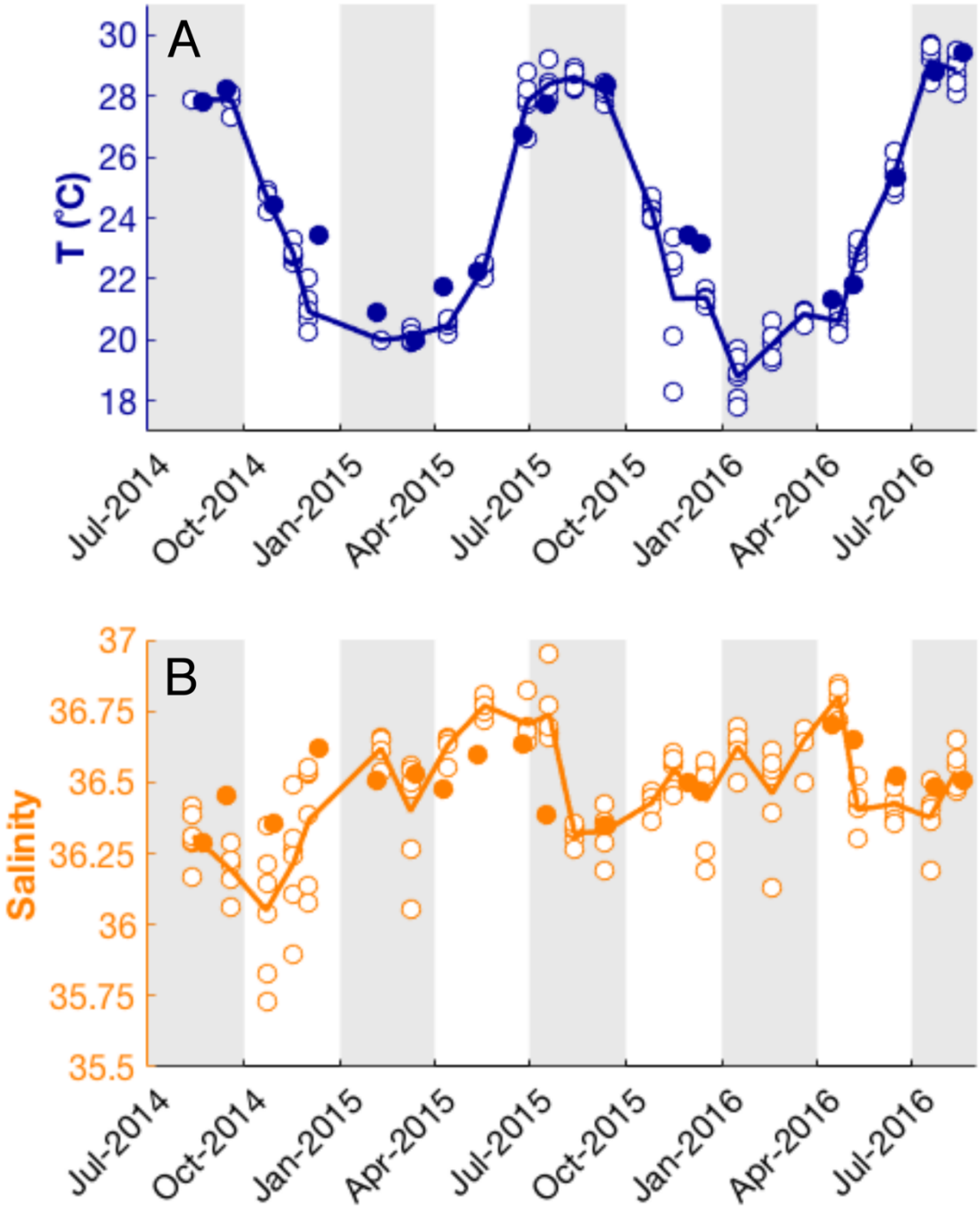

Figure 4.3: Offshore and inshore variability in (A) temperature and (B) salinity. Offshore and inshore data represented with filled and open symbols, respectively. Solid line is the monthly average of all inshore samples collected.

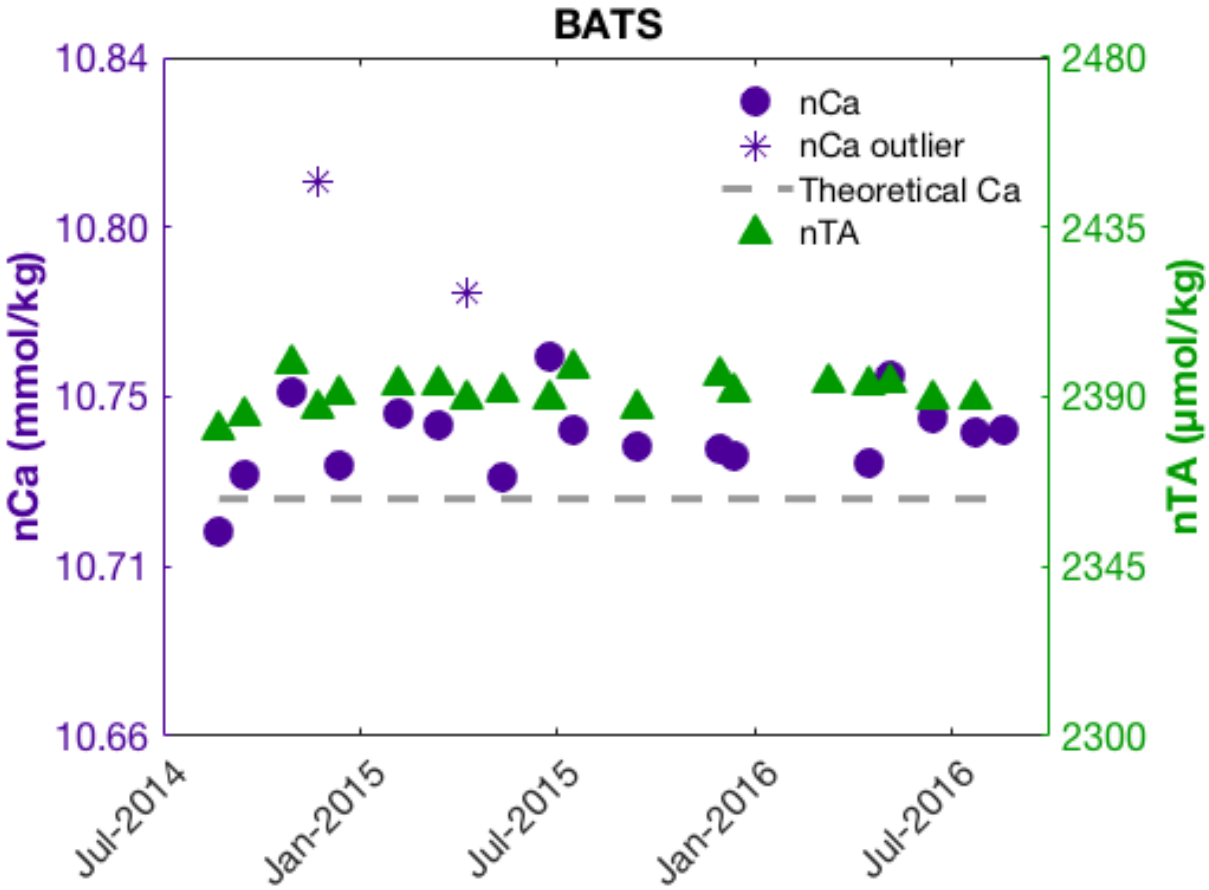

Figure 4.4: Offshore nCa and nTA at BATS. nCa (purple circles) and nTA (green triangles) values for samples collected at offshore BATS station between August 2014 and August 2016. Statistical nCa outliers denoted with purple asterisks. Theoretical nCa value (dashed line) was calculated from average offshore salinity and a Ca:S ratio of 10.28 mmol kg^{-1}:35.

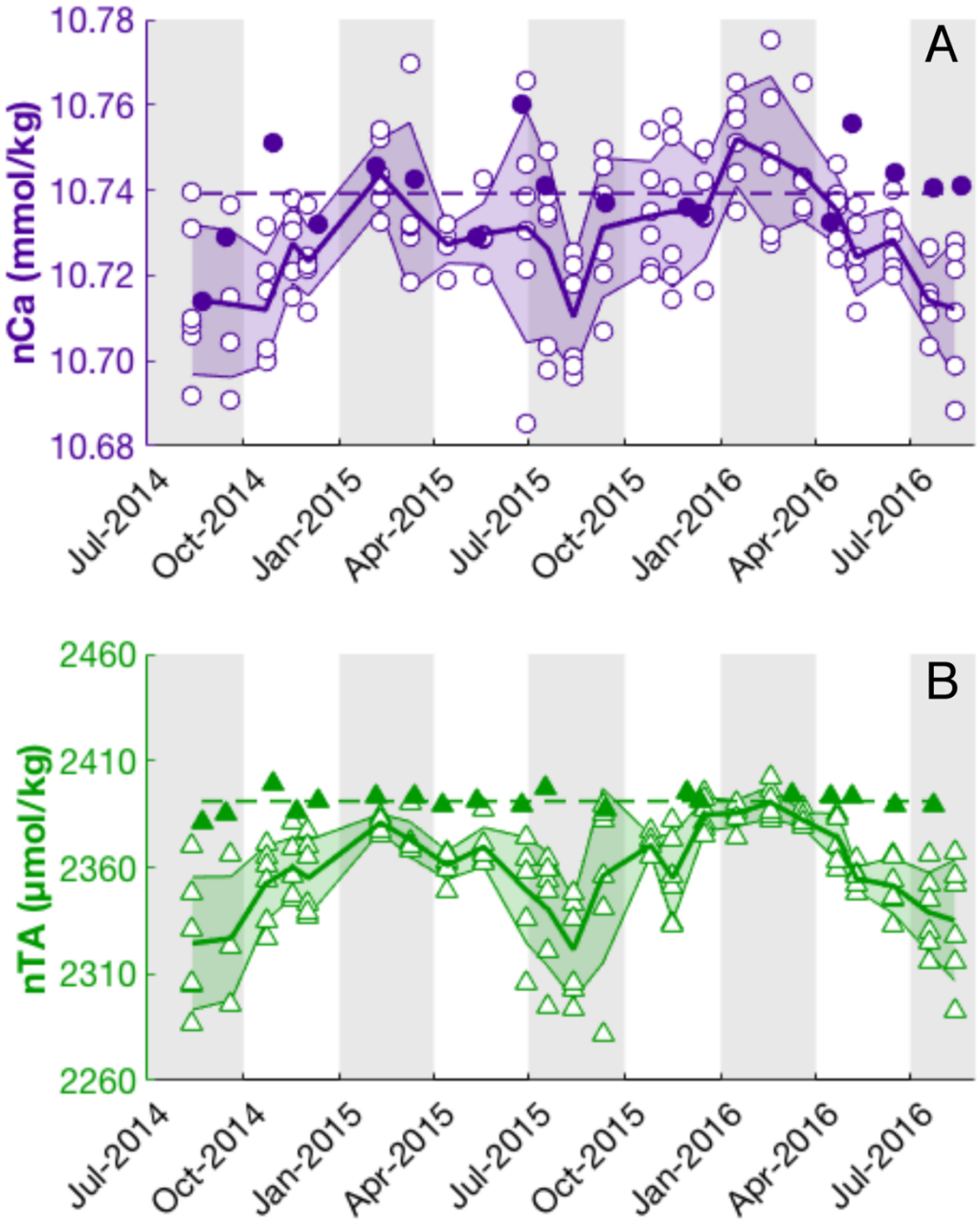

Figure 4.5: Offshore and inshore variability in (A) nCa and (B) nTA. Offshore and inshore data represented with filled and open symbols, respectively. Dashed line is the average of all offshore samples analyzed over the time-series (August 2014 to August 2016). Solid line is the monthly average of all inshore samples collected, ±1σ (shaded area).

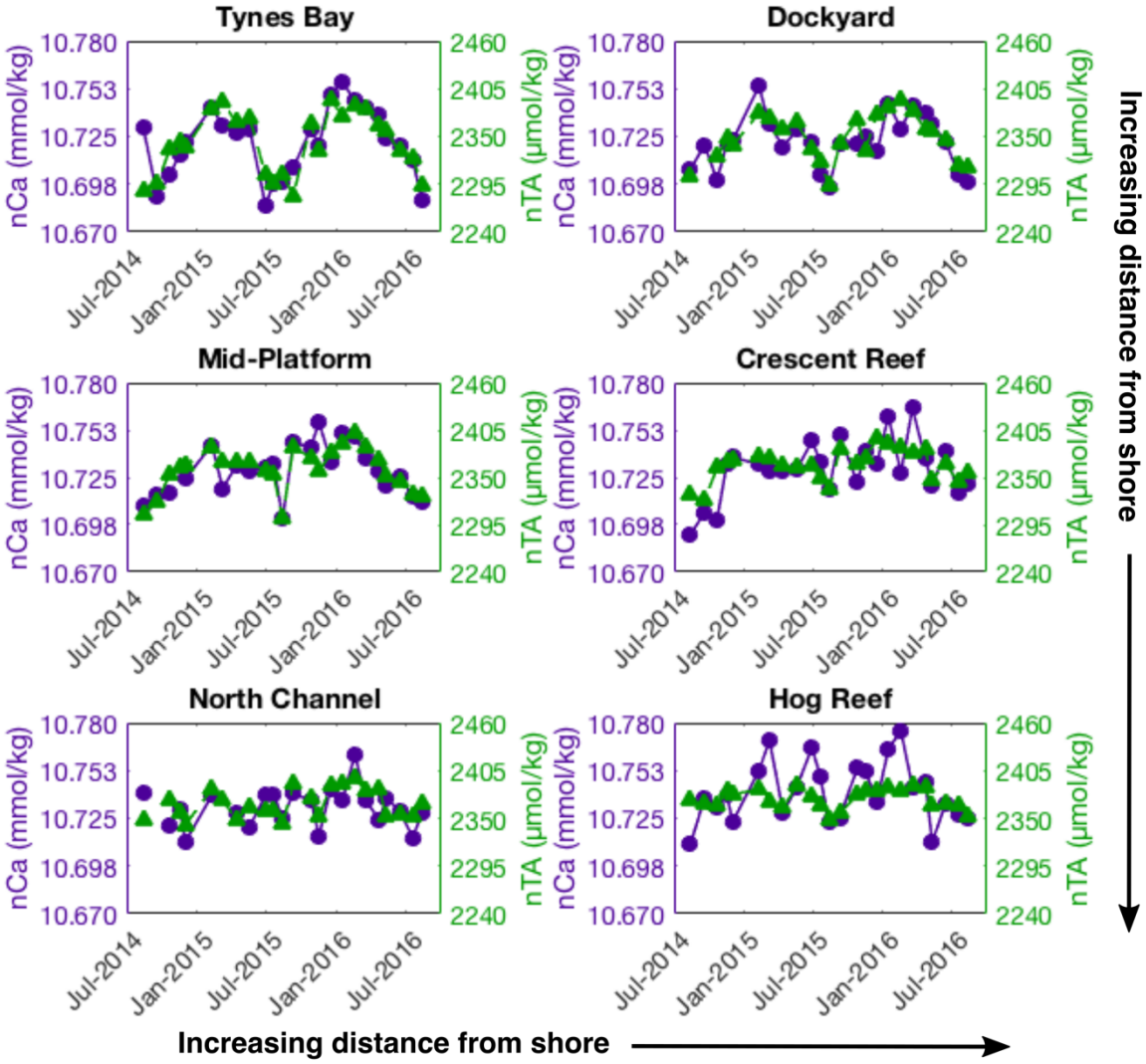

Figure 4.6: Time-series of nCa and nTA across inshore stations. nCa (purple circles) and nTA (green triangles) values for samples collected at each inshore location station between August 2014 and August 2016. Distance from shore increases from top-left to bottom-right.

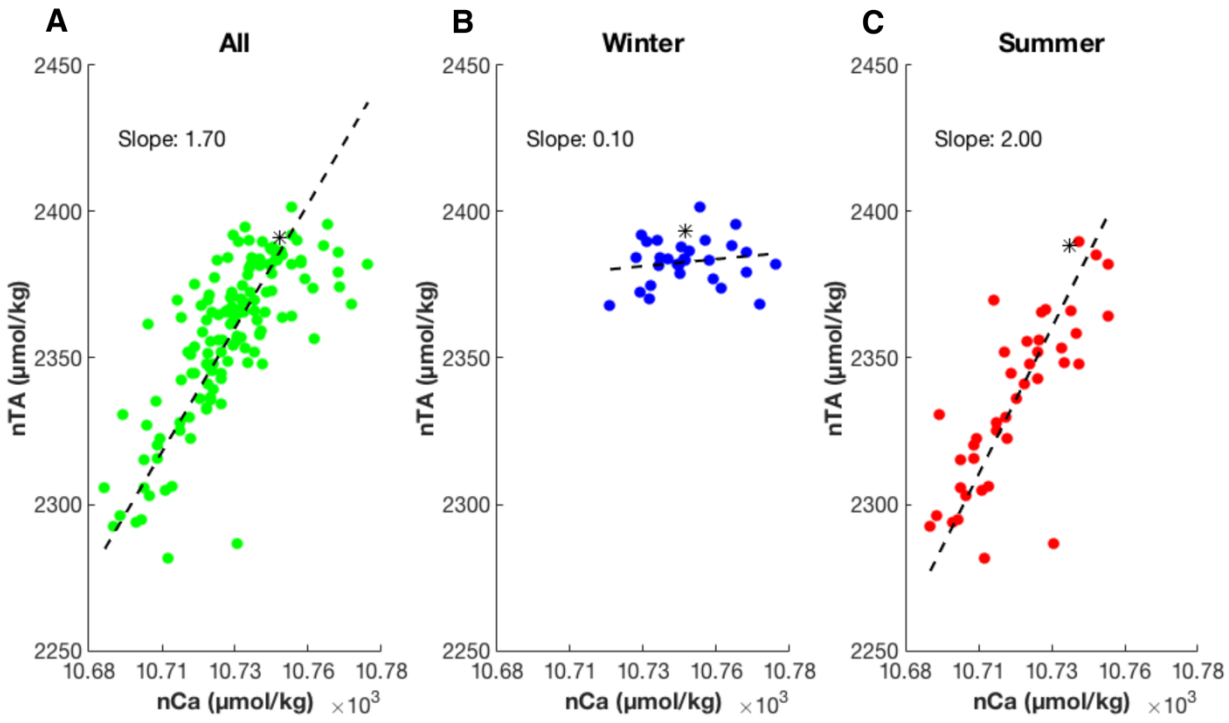

Figure 4.7: Seasonal variation in inshore nTA-nCa relationships. nTA-nCa values (filled symbols) for all inshore stations during A) full two-year time series from August 2014 to August 2016, B) winter months (January to March) and C) summer months (July to September). Offshore average nTA-nCa value for corresponding time periods denoted by asterisk.

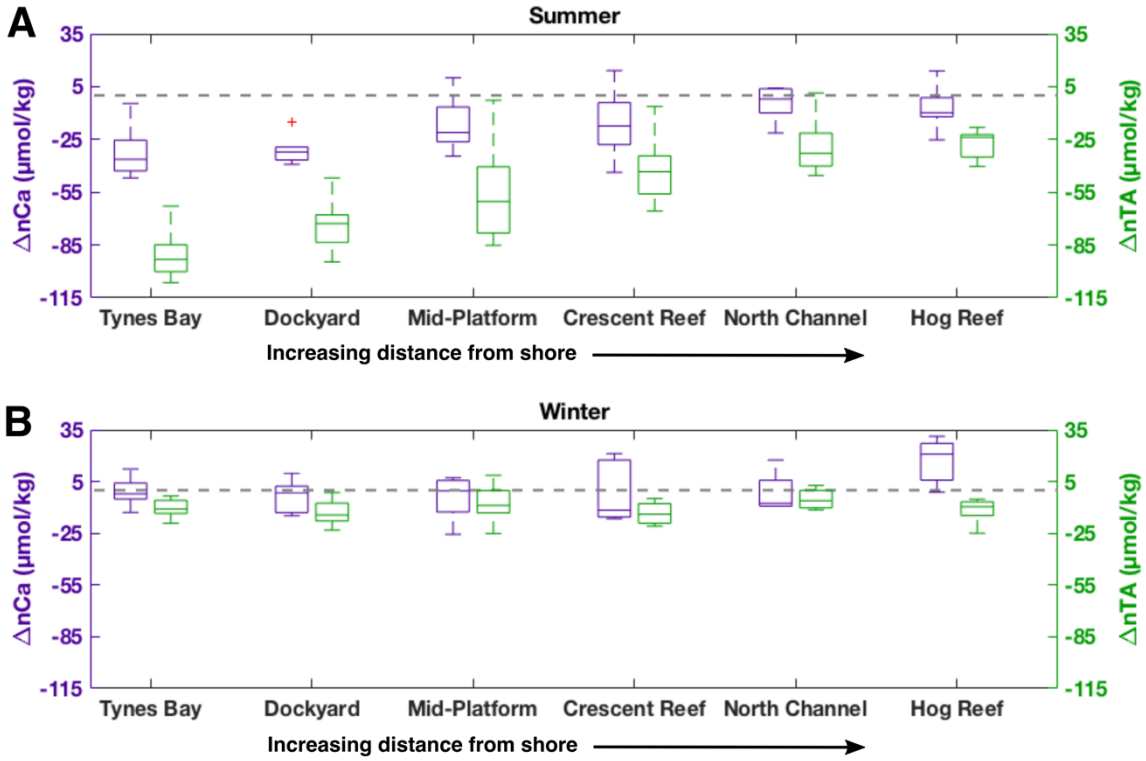

Figure 4.8: Inshore nCa and nTA across stations relative to offshore time-series average. A) Summer (July to September) and B) winter (January to March) distributions (central mark indicates the median, bottom and top edges of the box indicate the 25th and 75th percentiles, respectively, whiskers extend to the most extreme data points not considered outliers, and outliers are denoted with '+' symbol) of ΔnCa (purple) and ΔnTA (green) relative to offshore average nCa and nTA (dashed line = 0). Distance from shore increases from left to right.

REFERENCES

Andersson, A.J., Bates, N.R. and Mackenzie, F.T. (2007) Dissolution of Carbonate Sediments Under Rising pCO_2 and Ocean Acidification: Observations from Devil's Hole, Bermuda. Aquatic Geochemistry 13, 237-264.

Andersson, A.J., Kuffner, I.B., Mackenzie, F.T., Jokiel, P.L., Rodgers, K.S. and Tan, A. (2009) Net Loss of $CaCO_3$ from a subtropical calcifying community due to seawater acidification; mesocosm-scale experimental evidence. Biogeosciences 6, 1811-1823.

Andersson, A.J., Yeakel, K.L., Bates, N.R. and De Putron, S.J. (2014) Partial offsets in ocean acidification from changing coral reef biogeochemistry. Nature Climate Change 4, 56-61.

Anfält, T. and Granéli, A. (1976) Successive high-precision determination of calcium and magnesium in sea water with a new probe photometer. Analytica Chimica Acta 86, 13-19.

Bates, N., Best, M., Neely, K., Garley, R., Dickson, A. and Johnson, R. (2012) Detecting anthropogenic carbon dioxide uptake and ocean acidification in the North Atlantic Ocean. Biogeosciences 9, 2509-2522.

Bates, N.R. (2001) Interannual variability of oceanic CO_2 and biogeochemical properties in the Western North Atlantic subtropical gyre. Deep Sea Research Part II: Topical Studies in Oceanography 48, 1507-1528.

Bates, N.R. (2002) Seasonal variability of the effect of coral reefs on seawater CO2 and air—sea CO2 exchange. Limnology and Oceanography 47, 43-52.

Bates, N.R. (2007) Interannual variability of the oceanic CO2 sink in the subtropical gyre of the North Atlantic Ocean over the last 2 decades. Journal of Geophysical Research: Oceans 112.

Bates, N.R. (2017) Twenty years of marine carbon cycle observations at Devils Hole Bermuda provide insights into seasonal hypoxia, coral reef calcification, and ocean acidification. Frontiers in Marine Science 4, 36.

Bates, N.R., Amat, A. and Andersson, A.J. (2010) Feedbacks and responses of coral calcification on the Bermuda reef system to seasonal changes in biological processes and ocean acidification. Biogeosciences 7, 2509-2530.

Bates, N.R., Astor, Y.M., Church, M.J., Currie, K., Dore, J.E., Gonzalez-Davila, M., Lorenzoni, L., Muller-Karger, F., Olafsson, J. and Santana-Casiano, J.M. (2014) A Time-Series View of Changing Surface Ocean Chemistry Due to Ocean Uptake of Anthropogenic CO_2 and Ocean Acidification. Oceanography 27, 126-141.

Besson, P., Degboe, J., Berge, B., Chavagnac, V., Fabre, S. and Berger, G. (2014) Calcium, Na, K and Mg concentrations in seawater by inductively coupled plasma-atomic emission spectrometry: Applications to IAPSO seawater reference material, hydrothermal fluids and synthetic seawater solutions. Geostandards and Geoanalytical Research 38, 355-362.

Brewer, P.G. and Goldman, J.C. (1976) Alkalinity changes generated by phytoplankton growth. Limnology and Oceanography 21, 108-117.

Burdige, D.J. (1993) The biogeochemistry of manganese and iron reduction in marine sediments. Earth-Science Reviews 35, 249-284.

Burdige, D.J. and Zimmerman, R.C. (2002) Impact of sea grass density on carbonate dissolution in Bahamian sediments. Limnology and Oceanography 47, 1751-1763.

Cai, W.-J., Wang, Y. and Hodson, R.E. (1998) Acid-Base properties of dissolved organic matter in the estuarine waters of Georgia, USA. Geochimica et Cosmochimica Acta 62, 473-483.

Chan, N.C.S. and Connolly, S.R. (2013) Sensitivity of coral calcification to ocean acidification: a meta-analysis. Global Change Biology 19, 282-290.

Chisholm, J.R.M. and Gattuso, J.-P. (1991) Validation of the alkalinity anomaly technique for investigating calcification of photosynthesis in coral reef communities. Limnology and Oceanography 36, 1232-1239.

Culkin, F. and Cox, R. (1966) Sodium, potassium, magnesium, calcium and strontium in sea water, Deep Sea Research and Oceanographic Abstracts. Elsevier, pp. 789-804.

Dickson, A.G. and Goyet, C. (1994) Handbook of Methods for the Analysis of the Various Parameters of the Carbon Dioxide System in Sea Water. publisher not identified.

Dickson, A.G., Sabine, C.L. and Christian, J.R. (2007) Guide to best practices for ocean CO2 measurements. North Pacific Marine Science Organization.

Doney, S.C., Fabry, V.J., Feely, R.A. and Kleypas, J.A. (2009) Ocean Acidification: The Other CO_2 Problem. Annual Review of Marine Science 1, 169-192.

Dove, S.G., Kline, D.I., Pantos, O., Angly, F.E., Tyson, G.W. and Hoegh-Guldberg, O. (2013) Future reef decalcification under a business-as-usual CO_2 emission scenario. Proceedings of the National Academy of Sciences 110, 15342-15347.

Emerson, S. and Hedges, J. (2003) Sediment Diagenesis and Benthic Flux. Treatise on Geochemistry 6, 625.

Eyre, B.D., Andersson, A.J. and Cyronak, T. (2014) Benthic coral reef calcium carbonate dissolution in an acidifying ocean. Nature Climate Change 4, 969-976.

Eyre, B.D., Cyronak, T., Drupp, P., De Carlo, E.H., Sachs, J.P. and Andersson, A.J. (2018) Coral reefs will transition to net dissolving before end of century. Science 359, 908-911.

Falter, J.L., Lowe, R.J., Zhang, Z. and McCulloch, M. (2013) Physical and biological controls on the carbonate chemistry of coral reef waters: effects of metabolism, wave forcing, sea level, and geomorphology. PloS one 8.

Gattuso, J.-P., Frankignoulle, M. and Smith, S.V. (1999) Measurement of community metabolism and significance in the coral reef CO2 source-sink debate. Proceedings of the National Academy of Sciences 96, 13017-13022.

Gazeau, F., Urbini, L., Cox, T., Alliouane, S. and Gattuso, J.-P. (2015) Comparison of the alkalinity and calcium anomaly techniques to estimate rates of net calcification. Marine Ecology Progress Series 527, 1-12.

Goldman, J.C. and Brewer, P.G. (1980) Effect of nitrogen source and growth rate on phytoplankton-mediated changes in alkalinity 1. Limnology and Oceanography 25, 352-357.

Goodbody-Gringley, G., Noyes, T. and Smith, S.R. (2019) Bermuda, Mesophotic coral ecosystems. Springer, pp. 31-45.

Hernández-Ayon, J.M., Zirino, A., Dickson, A.G., Camiro-Vargas, T. and Valenzuela-Espinoza, E. (2007) Estimating the contribution of organic bases from microalgae to the titration alkalinity in coastal seawaters. Limnology and Oceanography: Methods 5, 225-232.

Hoegh-Guldberg, O., Mumby, P.J., Hooten, A.J., Steneck, R.S., Greenfield, P., Gomez, E., Harvell, C.D., Sale, P.F., Edwards, A.J. and Caldeira, K. (2007a) Coral reefs under rapid climate change and ocean acidification. science 318, 1737-1742.

Hoegh-Guldberg, O., Mumby, P.J., Hooten, A.J., Steneck, R.S., Greenfield, P., Gomez, E., Harvell, C.D., Sale, P.F., Edwards, A.J., Caldeira, K., Knowlton, N., Eakin, C.M., Iglesias-Prieto, R., Muthiga, N., Bradbury, R.H., Dubi, A. and Hatziolos, M.E. (2007b) Coral Reefs Under Rapid Climate Change and Ocean Acidification. Science 318, 1737-1742.

Horibe, Y., Endo, K. and Tsubota, H. (1974) Calcium in the South Pacific, and its correlation with carbonate alkalinity. Earth and Planetary Science Letters 23, 136-140.

Hu, X. and Cai, W.-J. (2011) An assessment of ocean margin anaerobic processes on oceanic alkalinity budget. Global Biogeochemical Cycles 25, n/a-n/a.

Hughes, T. and Connell, J. (1999) Multiple stressors on coral reefs: A long-term perspective. Limnology and oceanography 44, 932-940.

Hunt, C., Salisbury, J. and Vandemark, D. (2011) Contribution of non-carbonate anions to total alkalinity and overestimation of pCO 2 in New England and New Brunswick rivers. Biogeosciences 8, 3069-3076.

Jagner, D. (1974) High-precision determination of calcium in the presence of higher concentrations of magnesium by means of a computerized photometric titration: Application to sea water. Analytica chimica acta 68, 83-92.

Kanamori, S. and Ikegami, H. (1980) Computer-processed potentiometric titration for the determination of calcium and magnesium in sea water. Journal of the Oceanographical Society of Japan 36, 177-184.

Kim, H.-C. and Lee, K. (2009) Significant contribution of dissolved organic matter to seawater alkalinity. Geophysical Research Letters 36, n/a-n/a.

Kinsey, D.W. (1978) Alkalinity changes and coral reef calcification. Limnology and Oceanography 23, 989-991.

Kleypas, J.A., Buddemeier, R.W., Archer, D., Gattuso, J.-P., Langdon, C. and Opdyke, B.N. (1999) Geochemical Consequences of Increased Atmospheric Carbon Dioxide on Coral Reefs. Science 284, 118-120.

Kleypas, J.A., Buddemeier, R.W. and Gattuso, J.-P. (2001) The future of coral reefs in an age of global change. International Journal of Earth Sciences 90, 426-437.

Kroeker, K.J., Kordas, R.L., Crim, R., Hendriks, I.E., Ramajo, L., Singh, G.S., Duarte, C.M. and Gattuso, J.P. (2013) Impacts of ocean acidification on marine organisms: quantifying sensitivities and interaction with warming. Global Change Biology 19, 1884-1896.

Kroeker, K.J., Kordas, R.L., Crim, R.N. and Singh, G.G. (2010) Meta-analysis reveals negative yet variable effects of ocean acidification on marine organisms. Ecology Letters 13, 1419-1434.

Langdon, C., Gattuso, J.-P. and Andersson, A. (2010) Measurements of calcification and dissolution of benthic organisms and 13 communities. Guide to best practices for ocean acidification research and data reporting, eds U. Riebesell, VJ Fabry, L. Hansson and J.-P. Gattuso (Luxembourg: Publications Office of the European Union).

Logan, A. and Murdoch, T. (2011) Bermuda, in: Hopley, D. (Ed.), Encyclopedia of Modern Coral Reefs: Structure, Form and Process. Springer Netherlands, Dordrecht, pp. 118-123.

Mackenzie, F.T., Andersson, A.J., Arvidson, R.S., Guidry, M.W. and Lerman, A. (2011) Land–sea carbon and nutrient fluxes and coastal ocean CO_2 exchange and acidification: Past, present, and future. Applied Geochemistry 26, Supplement, S298-S302.

Manuel, S.A., Coates, K.A., Kenworthy, W.J. and Fourqurean, J.W. (2013) Tropical species at the northern limit of their range: composition and distribution in Bermuda's benthic habitats in relation to depth and light availability. Marine environmental research 89, 63-75.

Marcet, A.J.G. (1819) XII. On the specific gravity, and temperature of sea waters, in different parts of the ocean, and in particular seas; with some account of their saline contents. Philosophical Transactions of the Royal Society of London, 161-208.

Muehllehner, N., Langdon, C., Venti, A. and Kadko, D. (2016) Dynamics of carbonate chemistry, production, and calcification of the Florida Reef Tract (2009-2010): Evidence for seasonal dissolution. Global Biogeochemical Cycles 30, 661-688.

Muller, F.L.L. and Bleie, B. (2008) Estimating the organic acid contribution to coastal seawater alkalinity by potentiometric titrations in a closed cell. Analytica Chimica Acta 619, 183-191.

Murillo, L.J., Jokiel, P.L. and Atkinson, M.J. (2014) Alkalinity to calcium flux ratios for corals and coral reef communities: variances between isolated and community conditions. PeerJ 2, e249.

Page, H., Andersson, A.J., Courtney, T., De Carlo, E.H., Koester, I., Howins, N., Lebrato, M. and Bahr, K. (2018) Importance of Coral Reef Community Composition and Benthic Metabolism to Seawater Carbonate Chemistry: Implications for Ocean Acidification, 2018 Ocean Sciences Meeting. AGU.

Ringbom, A., Pensar, G. and Wänninen, E. (1958) A complexometric titration method for determining calcium in the presence of magnesium. Analytica Chimica Acta 19, 525-531.

Schönberg, C.H., Fang, J.K., Carreiro-Silva, M., Tribollet, A. and Wisshak, M. (2017) Bioerosion: the other ocean acidification problem. ICES Journal of Marine Science 74, 895-925.

Shiller, A.M. and Gieskes, J.M. (1980) Processes affecting the oceanic distributions of dissolved calcium and alkalinity. Journal of Geophysical Research: Oceans 85, 2719-2727.

Silverman, J., Lazar, B., Cao, L., Caldeira, K. and Erez, J. (2009) Coral reefs may start dissolving when atmospheric CO_2 doubles. Geophysical Research Letters 36, L05606.

Smith, S.R. and Warren, T. (2019) Bermuda and the Sargasso Sea, World Seas: an Environmental Evaluation. Elsevier, pp. 531-547.

Smith, S.V. and Key, G.S. (1975) Carbon dioxide and metabolism in marine environments1. Limnology and Oceanography 20, 493-495.

Smith, S.V. and Kinsey, D.W. (1978) Calcification and organic carbon metabolism as indicated by carbon dioxide, in: Stoddart, D.R., Johannes, R. E. (Ed.), Coral Reefs: research methods. UNESCO Monographs on oceanographic methology, pp. 469-484.

Steiner, Z., Erez, J., Shemesh, A., Yam, R., Katz, A. and Lazar, B. (2014) Basin-scale estimates of pelagic and coral reef calcification in the Red Sea and Western Indian Ocean. Proceedings of the National Academy of Sciences 111, 16303-16308.

Takeshita, Y.T., Cyronak, T., Martz, T.R., Kindeberg, T. and Andersson, A.J. (2018) Coral reef carbonate chemistry variability at different functional scales. Frontiers in Marine Science 5, 175.

Thomas, H., Schiettecatte, L.S., Suykens, K., Koné, Y.J.M., Shadwick, E.H., Prowe, A.E.F., Bozec, Y., de Baar, H.J.W. and Borges, A.V. (2009) Enhanced ocean carbon storage from anaerobic alkalinity generation in coastal sediments. Biogeosciences 6, 267-274.

Venti, A., Andersson, A. and Langdon, C. (2014) Multiple driving factors explain spatial and temporal variability in coral calcification rates on the Bermuda platform. Coral Reefs 33, 979-997.

Venti, A., Kadko, D., Andersson, A., Langdon, C. and Bates, N. (2012) A multi-tracer model approach to estimate reef water residence times. Limnology and Oceanography: Methods 10, 1078-1095.

Wisshak, M., Schönberg, C.H., Form, A. and Freiwald, A. (2012) Ocean acidification accelerates reef bioerosion. PloS one 7, e45124.

Yang, B., Byrne, R.H. and Lindemuth, M. (2015) Contributions of organic alkalinity to total alkalinity in coastal waters: A spectrophotometric approach. Marine Chemistry 176, 199-207.

Yates, K.K. and Halley, R.B. (2006) CO_3^{2-} concentration and pCO_2 thresholds for calcification and dissolution on the Molokai reef flat, Hawaii. Biogeosciences 3, 357-369.

Yeakel, K.L., Andersson, A.J., Bates, N.R., Noyes, T.J., Collins, A. and Garley, R. (2015) Shifts in coral reef biogeochemistry and resulting acidification linked to offshore productivity. Proceedings of the National Academy of Sciences 112, 14512-14517.

CONCLUSIONS

This work and its findings have led to significant insights into the numerous and complex factors controlling biogenic carbonate mineral dissolution in shallow marine environments and its role in a rapidly changing ocean.

Chapter 1

- Dissolution rates of shallow biogenic carbonates observed in the field were orders of magnitude slower than those measured in laboratory settings
- The disparity could be due to several factors including, but not limited to, differences between experimental substrates, varying environmental conditions, the role of metabolic activity and/or the presence of living organisms
- To identify the reasons for this disparity, efforts must be made to make laboratory and field experiments more comparable to one another

Chapter 2

- The same experimental substrates exhibit significantly different sensitivities of dissolution rates to changes in Ω_{Ar} in laboratory versus field settings
- *In situ* dissolution rates in shallow, advective carbonate sediments were found to be primarily controlled by organic matter decomposition (which is absent in the laboratory), but also significantly influenced by the overlying seawater carbonate chemistry and the solubility of the most soluble mineral phase in the sediments
- Shallow carbonate dissolution could be enhanced via ocean acidification, increased respiration, or most likely, a combination of both of these processes

Chapter 3

- Bulk sediment dissolution rates from two different shallow carbonate environments (Bermuda and Heron Island) show no correlation with grain size or mineralogy
- Dissolution rates showed lowered sensitivity to changes in pCO_2 with greater total organic carbon associated with the sediments
- Dissolution rates of bulk carbonate sediments increased by 2-3 times once organic coatings were removed, suggesting that organic coatings on natural sediment grains can override the influence of grain size and mineralogy on dissolution rates by acting as a protective barrier that limits direct interaction of seawater with the mineral surface

Chapter 4

- A multi-annual time-series of Ca and TA measurements across a coral reef platform demonstrated seasonal and inter-annual trends in biogeochemical processes occurring on coral reefs
- Both Ca and TA were depleted inshore relative to offshore during summer and approached or exceeded offshore values during winter
- Ca measurements with a novel spectrophotometric system were challenging and may be best utilized in environments where other processes are thought to significantly influence alkalinity or where significant amounts of Mg-calcites are precipitating and dissolving, but this would require improvements to the instrument